



UNIVERSITÀ DELLA CALABRIA



UNIVERSITA' DELLA CALABRIA

Dipartimento di Biologia, Ecologia e Scienza della Terra (DiBest)

Scuola di Dottorato

LIFE SCIENCES

Indirizzo

BIOLOGIA ANIMALE

Con il contributo di

COMMISSIONE EUROPEA, FONDO SOCIALE EUROPEO E DELLA REGIONE CALABRIA

XXVI CICLO

Heterologous over-expression of the human amino acid transporters LAT1-CD98 and ASCT2

Settore Scientifico Disciplinare: BIO/11 (BIOLOGIA MOLECOLARE)

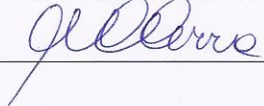
Direttore:

Ch.mo Prof. Marcello Canonaco

Firma 

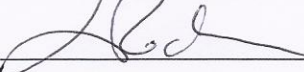
Coordinatore:

Ch.ma Prof.ssa Maria Carmela Cerra


Firma 

Supervisore:

Ch.ma Dott.ssa Lorena Pochini

Firma 

Dottorando: Dott. Piero Pingitore

Firma 

CONTENTS

ABSTRACT	5
RIASSUNTO	8
1. INTRODUCTION	12
1.1 - Biological membranes	12
1.2 - Transport systems	12
1.3 - Amino acid transport	14
1.4 - Mammalian amino acid transporters	15
1.4.1 - Na ⁺ - dependent transporters	16
1.4.2 - Na ⁺ - independent transporters	17
1.5 - The solute carrier (SLC) superfamily	18
1.6 - The SLC1 family	19
1.7 - ASCT2 (SLC1A5)	21
1.8 - SLC7 and SLC3 families	23
1.9 - LAT1 (SLC7A5)	26
1.10 - 4F2hc (SLC3A2)	28
1.11 - hASCT2 and hLAT1 in cancer	29
1.12 - Heterologous protein production	32
1.13 - Heterologous systems	33
1.13.1 - Bacteria	34
1.13.2 - Yeast	34
1.13.3 - Insect cells	35
1.13.4 - Mammalian cells	36
1.14 - <i>Escherichia coli</i> and <i>Pichia pastoris</i>	36
1.15 - Codon bias	40

2. MATERIALS AND METHODS	43
2.1 - Materials	43
2.1.1 - Low Salt LB (Luria-Bertani) medium	43
2.1.2 - YT 2X medium	43
2.1.3 - Yeast Extract Peptone Dextrose Medium (YPD)	43
2.1.4 - Yeast Extract Peptone Dextrose Medium (YPDS)	44
2.1.5 - Buffered Glycerol-complex Medium (BMGY)	44
2.1.6 - Buffered Methanol-complex Medium (BMMY)	44
2.1.7 - Fermentation Basal Salts Medium	45
2.1.8 - Plates	45
2.1.9 - TAE (Tris/Acetate/EDTA) 50 X	46
2.1.10 - IPTG	46
2.1.11 - Protease Inhibitor Cocktail	46
2.1.12 - PMSF	46
2.1.13 - Running buffer for SDS-PAGE 10X	47
2.1.14 - MES running buffer for SDS-PAGE 20X	47
2.1.15 - Coomassie Brilliant Blue	47
2.2 - Experimental procedures	48
2.2.1 - Polymerase chain reaction (PCR)	48
2.2.2 - Agarose gel electrophoresis	49
2.2.3 - Purification of DNA fragments from agarose gel	50
2.2.4 - Cloning	50
2.2.5 - <i>E. coli</i> transformation	51
2.2.6 - DNA extraction by QIAprep Spin Miniprep kit	52
2.2.7 - <i>P. pastoris</i> transformation	52

2.2.8 - Sonication	53
2.2.9 - The French press	54
2.2.10 - Polyacrylamide gel electrophoresis (PAGE)	54
2.2.11 - Western blot	56
2.2.12 - Protein purification by affinity chromatography	57
2.3 - Cloning	58
2.3.1 - Cloning of hASCT2	58
2.3.2 - Cloning of hLAT1	59
2.3.3 - Cloning of hCD98	59
2.4 - Recombinant production	60
2.4.1 - Recombinant production of hASCT2 protein	60
2.4.2 - Recombinant production of hLAT1 protein	61
2.4.3 - Recombinant production of hCD98 protein	62
2.5 - Protein purification	62
2.5.1 - hASCT2 purification	62
2.5.2 - hLAT1 purification	63
2.5.3 - GST-hCD98 Purification	64
3. RESULTS	66
4. CONCLUSION	83
REFERENCES	87
ACKNOWLEDGEMENTS	94
PUBLICATIONS	95

ABSTRACT

Amino acid transport across the plasma membrane in mammalian cells is mediated by different transport systems such as the Na⁺-dependent systems A, ASC and N and the Na⁺-independent system L. Very interestingly some of these transporters such as ASCT2 and LAT1 are over-expressed in many tumors. Cancer cells, in fact, display enhanced need for amino acids and altered amino acid metabolism. Thus, structural and functional studies of these transporters are very important not only for characterization but also for applications in human therapy. Over-expression of the transport proteins is the starting point for obtaining purified transporters. Bacterial and/or yeast cell systems have been employed for this purpose, so far.

LAT1 (SLC7A5) belongs to the system L which catalyze the transport of branched chain and aromatic amino acids. LAT1 is an heterodimer and its counterpart, CD98 (SLC3A2) protein, is probably involved in substrate recognition and membrane localization.

Bacterial over-expression of the hLAT1 transporter has been performed using a screening strategy of *E. coli* strains transformed with several plasmid constructs. The best expression of the hLAT1 protein was achieved after cloning of the cDNA into pH6EX3 vector and transformation of Rosetta(DE3)pLysS cells. The hLAT1 protein was purified by Ni²⁺-chelating chromatography with a yield of about 3.5 mg/L. The cDNA coding for hCD98 was cloned in the pGEX-4T1 vector containing a N-terminal GST tag. Protein expression was obtained using the same bacterial strain above described.

Differently from hLAT1, the GST-CD98 protein was soluble. hCD98 was obtained after thrombin treatment and separation by size exclusion chromatography, with a yield of 2 mg/L.

ASCT2 (SLC1A5) belongs to the system ASC and has high affinity for Ala, Ser, Cys, Gln and Asn. *E. coli* revealed not suitable for expressing this protein. Thus, a different approach using *P. pastoris* was performed to produce the recombinant hASCT2 protein. After codon

optimization for *P. pastoris*, the hASCT2 cDNA was cloned in the pPICZB expression vector carrying a C-terminal 6His-tag. For large protein production, the recombinant *P. pastoris* strain was grown in fermentors. The recombinant proteins was mainly localized to the membrane. After purification using Ni²⁺-NTA resin a yield of at least 10 mg/L was obtained. The procedure described can be now used for producing the three proteins in appropriate amounts for crystallization trials and functional studies.

RIASSUNTO

Il trasporto degli amminoacidi attraverso la membrana plasmatica nelle cellule umane è mediato da differenti sistemi di trasporto come i sistemi Na^+ -dipendenti A, ASC e N, ed il sistema Na^+ -indipendente L. In maniera molto interessante, alcuni di questi trasportatori come ASCT2 e LAT1 sono over-espressi in molti tumori. Le cellule tumorali, infatti, mostrano un aumentato ed alterato trasporto di amminoacidi. Dunque, studi strutturali e funzionali di questi trasportatori sono molto importanti, non solo per la loro caratterizzazione, ma anche per applicazioni utili alle terapie umane.

L'over-espressione di proteine di trasporto è il punto di partenza per ottenere trasportatori purificati. Sistemi cellulari batterici e/o di lievito sono stati utilizzati per questo scopo.

LAT1 (SLC7A5) appartiene al sistema L che catalizza il trasporto di amminoacidi con catena ramificata e aromatici. LAT1 è un etero-dimero e la sua controparte, la proteina CD98 (SLC3A2), è probabilmente coinvolta nel riconoscimento del substrato e nella localizzazione in membrana. L'over-espressione batterica del trasportatore LAT1 è stata ottenuta mediante una strategia che prevedeva lo screening di diversi ceppi cellulari di *E. coli*, trasformati con diversi costrutti plasmidici. Il miglior risultato di espressione della proteina hLAT1 è stato raggiunto dopo clonaggio del cDNA nel vettore pH6EX3 e trasformazione delle cellule Rosetta(DE3)pLysS.

La proteina hLAT1 è stata purificata mediante cromatografia di chelazione al Ni^{2+} con una resa finale di circa 3.5 mg/L.

Il cDNA codificante per hCD98 è stato clonato nel vettore pGEX-4T1 contenente il tag GST nella porzione N-terminale. L'espressione proteica è stata ottenuta utilizzando lo stesso ceppo batterico sopra descritto.

Differentemente da hLAT1, la proteina GST-CD98 era solubile. hCD98 è stata ottenuta dopo taglio con la trombina e separazione tramite cromatografia per esclusione dimensionale, con una resa finale di 2 mg/L.

ASCT2 (SLC1A5) appartiene al sistema ASC ed ha alta affinità per Ala, Ser, Cys, Gln ed Asn. *E. coli* non si è dimostrato adatto per l'espressione di questa proteina. Dunque, un differente approccio utilizzando *P. pastoris* è stato messo a punto per produrre la proteina ricombinante hASCT2. Dopo l'ottimizzazione dei codoni, il cDNA di hASCT2 è stato clonato nel vettore di espressione pPICZB con il tag 6His al C-terminale.

Per la produzione proteica su larga scala, *P. pastoris* ricombinante è stato coltivato nei fermentatori. La proteina ricombinante era localizzata principalmente nelle frazioni di membrana. hASCT2 è stata poi purificata utilizzando la resina Ni²⁺-NTA ottenendo una resa di almeno 10 mg/L. La procedura descritta può essere usata, ora, per la produzione dei tre polipeptidi in quantità sufficiente per test di cristallizzazione e studi funzionali.

Abbreviations and Symbols

AOX	Alcohol Oxidase
ABC	ATP-binding cassette
ASCT	Alanine serine cysteine transporter
BCH	2-aminobicyclo-(2,2,1)-heptane-2-carboxylic acid
C ₁₂ E ₈	Octaethylene glycol monododecyl ether
CAI	Codon adaptation index
DDM	N-Dodecyl β-D-maltopyranoside
DTT	Dithiothreitol
<i>E. coli</i>	<i>Escherichia coli</i>
EDTA	Ethylenediaminetetraacetic acid
GST	Glutathione-S-transferase
IPTG	Isopropyl β-D-1-thiogalactopyranoside
LAT	Large amino acid transporter
LDAO	N,N-Dimethyldodecylamine N-oxide
MPs	Membrane proteins
mTOR	Mammalian target of rapamycin
<i>P. pastoris</i>	<i>Pichia pastoris</i>
PMSF	Phenylmethanesulfonyl fluoride
PTMs	Post translation modifications
PVDF	Polyvinylidene difluoride
<i>S. cerevisiae</i>	<i>Saccharomyces cerevisiae</i>
SLC	Solute carrier
TEMED	Tetramethylethylenediamine
TMD	Transmembrane domain
YNB	Yeast nitrogen base

CHAPTER 1

INTRODUCTION

1.1 - Biological membranes

Biological membranes consist of a continuous lipid bilayer in which many membrane proteins are included. In general, there are three main kind of lipid molecules in the membrane fraction: phospholipids, cholesterol, and glycolipids. Moreover, the lipid compositions of the inner and outer monolayers is different, that is because the two faces of a cell membrane have different functions.

Some proteins, included in the membrane, need specific lipid head groups to work properly; this can explain, in part at least, why eukaryotic biological membranes contain many different kinds of lipid molecules (1).

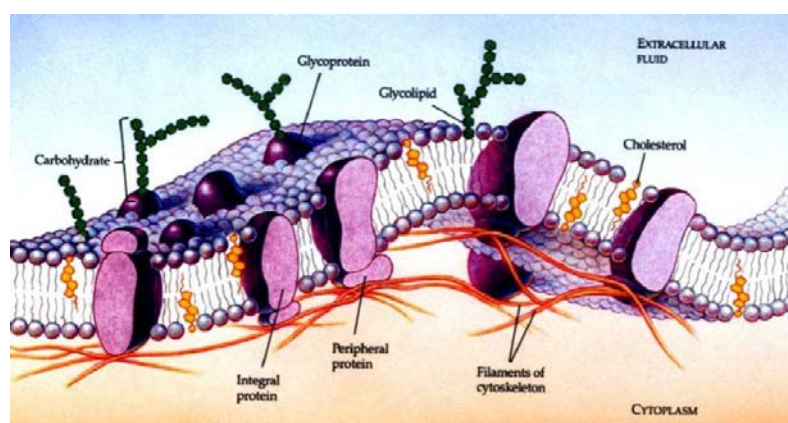


Fig. 1: Schematic drawing showing three-dimensional view of a cell membrane. (Adapted from <http://facstaff.cbu.edu>).

1.2 - Transport systems

In the past, it was believed that many physiological or xenobiotic compounds cross biological membranes by simple diffusion. This observation is not properly correct. Since that time, membrane transporter studies exponentially increased. Transport systems serve the cell in different ways.

They are essential for uptake, elimination, and intracellular trafficking of all nutrients and metabolites; they play a very important role for maintaining and regulating cell homeostasis.

Then, many of these membrane transporter systems are essential for life (2).

These systems allow entry of all essential nutrients into the cytoplasmic compartment, allowing metabolism of exogenous sources of carbon, nitrogen, sulfur, and phosphorus, regulate metabolite concentrations by catalyzing the elimination of end products of metabolic pathways from organelles and cells. These transporters allow elimination of drugs and other toxic compounds from either the cytoplasmic compartment or the plasma membrane. They mediate uptake and efflux of ionic species that must be maintained at different concentrations between internal and external environment. This is really important to maintain a membrane potential, a ion concentration gradients, and appropriate cytoplasmic concentrations of all essential trace minerals that are involved as cofactors in metabolic pathways. Transporters are also directly involved in the elimination of many physiologic molecules such as lipids, proteins, and complex carbohydrates into and beyond the cytoplasmic membrane. All these macromolecules play an important role to protect against environmental insult and predation and also in pathogenesis.

Therefore, it seems clear that integral membrane proteins mediate almost all transmembrane transport processes. Sometimes, they work in conjunction with extra cytoplasmic receptors or with cytoplasmic energy-coupling and regulatory proteins forming protein complex (3).

Transporters can be classified into two main categories: carriers and channels that are fundamentally different.

Carriers bind their substrates with high stereospecificity. They are saturable in the same sense as are enzymes.

Channels are mainly oligomeric complexes of several, often identical, subunits. They show less stereospecificity than carriers and are not saturable.

Transport systems represent a significant fraction of all proteins encoded in the genomes of both simple and complex organisms. There are probably a thousand or more different transporters in the human genome. Only a few hundred transporters from different species have been studied with biochemical and genetic tools, but the three-dimensional structures for only a handful of these have been determined.

Studying many transporters it has been shown sequence similarities among them and in general similar amino acid sequences in proteins reflect similar three-dimensional structures and mechanisms of action. Then, by determining the structure and function of at least one member of each protein family, we could obtain information about structures, substrate specificities and function of other proteins belonging to the same family (4).

1.3 - Amino acid transport

Proteins are introduced with the diet and forms up to 30% of the typical western human diet. After their digestion, the resulting peptides and amino acids are efficiently absorbed by the enterocytes of the small intestine. Enterocytes are specialized cells, where peptides are metabolized, and the resulting amino acids are conveyed by amino acid transporters.

Amino acids are necessary for protein and bioactive molecules synthesis as well as for energy metabolism; they are delivered to all tissues through the blood (5).

The flow of these important nutrients, across the plasma membrane, is mediated and strictly controlled by amino acid transporters. Sometimes, when amino acids act as neurotransmitters or synaptic modulators the transporters allow reuptake from the synaptic cleft.

After the work of Christensen's group, many initial studies with mammalian cells were carried out and different transport systems for amino acids as well as general properties of mammalian amino acid transport were identified.

The main criteria used to classify amino acid transporters on the basis of their function have been, the type of amino acid (acidic, zwitterionic and characteristics of its side chain) and the thermodynamic properties of the transport. To date, this classification is still considered effective, since structural data on higher eukaryote amino acid transporters are incomplete. In the early 1990s, the identification of the first brain GABA transporter and of the first cationic amino acid transporter represent the starting points for the study of mammalian amino acid transporter genes (6).

1.4 - Mammalian amino acid transporters

Christensen and colleagues using radiolabeled amino acids and amino acid analogs studied the functional characteristics, such as substrate specificity, kinetic and regulatory properties, ion dependence and pH sensitivity, to distinguish between specific transporters (7). On the basis of these functional characteristics, the amino acid transporters were classified in different “systems”.

Christensen's work identified system L in which are included amino acid transporters that prefer leucine and other large hydrophobic neutral amino acids, system A (alanine and other small and polar neutral amino acids) and system ASC (alanine, serine, and cysteine).

For amino acid transporters of cationic (system y^+) and anionic amino acids (system X^- ^{AG}) a further nomenclature (x for anionic, y for cationic, z for neutral) has been adopted (5).

In general, amino acid transporters are divided into two categories, **Na⁺-dependent** and **Na⁺-independent**. The Na⁺-dependent amino acid transporters utilize the potential energy present across the membrane established by Na⁺ electrochemical gradient; this gradient is maintained mainly by the Na⁺/K⁺-ATPase, to drive the uptake of amino acids across the membrane against their concentration gradient. On the other hand, Na⁺-independent transporters drive the selective movement of amino acids across the plasma membrane independently of Na⁺. The nomenclature used for mammalian amino acid transporters terms Na⁺-dependent systems in uppercase letters and Na⁺-independent systems in lowercase letters. The only exception is the Na⁺-independent transporter System L which has maintained its uppercase designation for historical purposes (8).

1.4.1 - Na⁺-dependent transporters

System ASC

System ASC includes two Na⁺-dependent antiporters (exchangers) termed ASCT1 and ASCT2 (System ASC amino acid transporters 1 and 2, respectively) (9).

System ASC was initially so termed for three of its preferred substrates (alanine, serine, cysteine) to distinguish it from System A (10).

A transport activity similar to ASC system, was previously described in intestinal and kidney epithelia (11,12); it was known as “neutral brush border” (13), and later named B⁰. Initially, ASC and B⁰ activities could be distinguished by threonine selectivity or the uptake of anionic amino acids at acidic pH values, but more recent studies have not supported this kind of distinction (8).

System N

System N drives Na^+ -coupled influx transport of neutral amino acids, including glutamine, asparagine, and histidine in exchange with H^+ . To date, two human isoforms (SN1/SNAT3/SLC38A3 and SN2/SNAT5/SLC38A5) are known, which have a different tissue localization (14). Kilberg described for the first time System N in rat hepatocytes, demonstrating that transport activity of System N had a substrate specificity for all substrates containing nitrogen in their side chain, such as glutamine, histidine and asparagine (15).

This transport system has served as the focus of several studies in liver and muscle. System N-like activities were also described in skeletal muscle and neurons, and termed Nm and Nb, respectively, to distinguish their transport activities from the liver systems (8).

System A

System A catalyzes transport in almost all cell types, and mediates the symport of most small neutral amino acids, including alanine, serine, and glutamine, with Na^+ ion. There are three different isoforms of system A: ATA1/SNAT1/SLC38A1, ATA2/SNAT2/SLC38A2, and ATA3/SNAT4/SLC38A4 (sodium-coupled neutral amino acid transporters 1,2 and 4, respectively); their main difference is the tissue distribution. (14).

1.4.2 - Na^+ -independent transporters

System L

System L was one of the first transport activities to be identified and was designated as such for its leucine-preferring transport; in particular, this system is involved for entry of large neutral amino acids with bulky side chains such as leucine, isoleucine, and phenylalanine. System L is also involved in glutamine transport, but its rate almost always represents a minority of total uptake (8).

1.5 - The solute carrier (SLC) superfamily

On the basis of functional properties, transporter proteins are divided into two main superfamilies: the solute carrier (SLC) and the ATP-binding cassette (ABC) transporters. In general, SLC members function as influx transporters for nutrients and compounds essential for cell survival, such as sugars, digested peptides, amino acids, nucleosides, and inorganic ions. On the other hand, ABC proteins serve as efflux transporters for unwanted metabolites and toxins, including many anticancer drugs of clinical use (14).

The human SLC superfamily comprises 386 members that catalyze the transport of a broad spectrum of substances. The superfamily transporters are classified into 52 families.

The classification is based on the number of predicted or observed transmembrane α -helices (usually 10–14) and sequence similarity, in which members of each family share sequence identity of at least 20% with at least one other family member. Although their common evolutionary origin, sometimes transporters within an SLC family can have substrates with different physicochemical properties. For example, the SLC22 family includes transporters of organic anions, cations, or zwitterions. On the other hand, SLC families such as the amino acid transporter families SLC1 and SLC7 can be unrelated evolutionarily but still have substrates with very similar physicochemical properties (16).

The members of the SLC families have different biochemical properties. Some of these are coupled transporters or exchangers, often driven by the cellular sodium gradient, and some are passive transporters. Their cellular localization also varies; most of them are localized to the plasma membrane while others are specifically localized in mitochondria, synaptic vesicles or peroxisomes. The SLC family is one of the largest families of membrane proteins in human together with G protein-coupled receptors (GPCRs), voltage gated ion channels and tyrosine kinase receptors. The GPCR family is the largest with about 800 members followed by SLC

family with 386 members, voltage gated ion channels with 143 members and transmembrane protein kinases with 105 members.

The entire SLC content of a single vertebrate genome has not been determined and analyzed completely because phylogenetic relationship between the SLCs is very complex and genes coding for SLC transporters have complex genomic structure, generally with a high number of introns. On the basis of the type of substrate and the number of transmembrane domains, Fredriksson et al. in 2008 identified 10 major classes of substrates that are transported by SLCs as well as classes for orphans (substrate is unknown).

Almost 40% of all SLCs are still orphans. The largest class of substrates is inorganic ions, with in total 58 SLCs. This class constitutes formerly metal and sulfate ion transporters.

The amino acid transport across plasma membrane is strongly regulated, and for this there are over 60 known transporters for amino acids found in different SLC families (SLC4, 6, 7, 16, 25, 36, 38 and 43). In these families, there are also 54 orphan transporters, and many of those could also be amino acid transporters. Therefore, there could be almost 100 SLCs amino acid transporters in the human genome which would account for over 25% of the SLC repertoire (17).

1.6 - The SLC1 family

The solute carrier family 1 (SLC1) includes five high-affinity glutamate transporters, EAAC1/*SLC1A1*, GLT-1/*SLC1A2*, GLAST/*SLC1A3*, EAAT4/*SLC1A6* and EAAT5/*SLC1A7* and the two neutral amino acid transporters, ASCT1/*SLC1A4* and ASCT2/*SLC1A5*.

Each of these transporters exhibits different transport activities despite they have similar predicted structures.

In humans, the five glutamate transporters possess 44–55% amino acid sequence identity with each other, while ASCT1 and ASCT2 exhibit 57% identity with each other (18). In **Table 1**, type and mechanism of transport, substrates, tissue localization and links to disease are summarized:

Human gene name	Protein name	Aliases	Predominant substrates	Transport type/ coupling ions	Tissue distribution and cellular/ subcellular expression	Link to disease	Human gene locus	Sequence accession ID	Splice variants and their specific features
SLC1A1	EAAC1, EAAT3	System X ⁻ _{AG}	L-Glu, α /L-Asp	C/Na ⁺ , H ⁺ and K ⁺	Brain (neurons), intestine, kidney, liver, heart, placenta	Huntington's disease, Epilepsy, Ischemia, Alzheimer's disease, Niemann-Pick disease, Obsessive-compulsive disorder	9p24	NM_004170	
SLC1A2	GLT-1, EAAT2	System X ⁻ _{AG}	L-Glu, α /L-Asp	C/Na ⁺ , H ⁺ and K ⁺	Brain (astrocytes, Bergmann glia, neurons), liver, pancreas	Amyotrophic lateral sclerosis, Alzheimer's disease, Huntington's disease, Epilepsy, Ischemia, Schizophrenia	11p13-p12	NM_004171 NM_001195728 NM_001252652	3 Splice variants differ in their C-terminus
SLC1A3	GLAST, EAAT1	System X ⁻ _{AG}	L-Glu, α /L-Asp	C/Na ⁺ , H ⁺ and K ⁺	Brain (astrocytes, Bergmann glia), heart, skeletal muscle, placenta	Alzheimer's disease, Huntington's disease, Epilepsy, Cerebellar ataxia type 7, Schizophrenia	5p13	NM_004172 NM_001166695 NM_001166696	3 Splice variants differ in their 3' UTR, coding sequences, C-terminus
SLC1A4	ASCT1, SATT	System ASC	L-Ala, L-Ser, L-Cys, L-Thr	C/Na ⁺ , E/ amino acids	Widespread		2p15-p13	NM_003038 NM_001193493	2 Splice variants differ in their 5' UTR, coding sequences, start codon
SLC1A5	ASCT2, AAAT	System ASC	L-Ala, L-Ser, L-Cys, L-Thr, L-Gln, L-Asn	C / Na ⁺ , E/ amino acids	Lung, skeletal muscle, large intestine, kidney, testis, adipose tissue		19q13.3	NM_005628 NM_001145144 NM_001145145	3 Splice variants differ in their 5' UTR, coding sequences, N-terminus
SLC1A6	EAAT4	System X ⁻ _{AG}	L-Glu, α /L-Asp	C/Na ⁺ , H ⁺ and K ⁺	Cerebellum (Purkinje cells)	Spinocerebellar ataxia type 5	19p13.12	NM_005071	
SLC1A7	EAAT5	System X ⁻ _{AG}	L-Glu, α /L-Asp	C/Na ⁺ , H ⁺ and K ⁺	Retina (rod photoreceptors and bipolar cells)		1p32.3	NM_006671	

C: cotransporter, E: exchanger, F: facilitated transporter, O: orphan transporter.

Table 1: SLC1: the high-affinity glutamate and neutral amino acid transporter family. (Adapted from Kanai Y. et al, The SLC1 high-affinity glutamate and neutral amino acid transporter family, 2013)

In **Fig. 2** the phylogenetic tree of SLC1 transporters is shown:

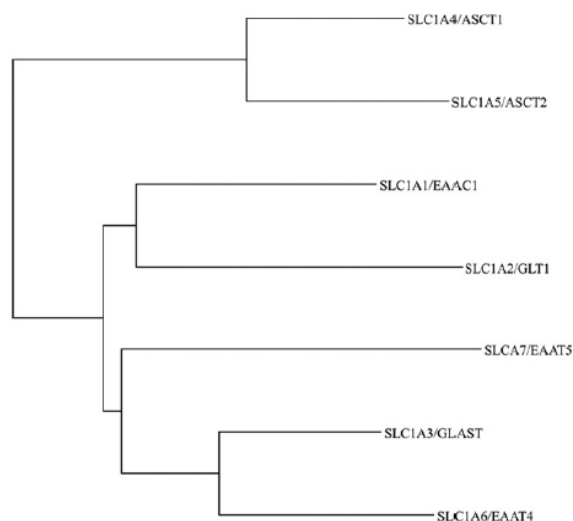


Fig. 2: Phylogenetic tree of the seven human SLC1 family members. (Adapted from Kanai Y. et al, The SLC1 high-affinity glutamate and neutral amino acid transporter family, 2013)

1.7 - ASCT2 (*SLC1A5*)

SLC1A5 gene was located to human chromosome 19q13.3 by chromosomal assignment studies using somatic cell hybrid analysis and fluorescent *in situ* hybridization.

The human SLC1A5 cDNA is 2,885 bp long with an open reading frame of 1,626 bp (including termination codon).

The open reading frame of 1,626 bp encodes a polypeptide of 541 amino acids that has a molecular mass of 57 kDa, called ASCT2 and also known as AAAT or hATB0. Hydrophobicity analysis indicated that the ASCT2 protein contains ten putative transmembrane domains (**Fig. 3**). There are also two potential *N*-glycosylation sites between the transmembrane domains 3 and 4 and two potential sites for protein kinase C-dependent phosphorylation in putative intracellular domains.

```

1  MVADPPRDSK GLAAAEPPT GAWQLASIED QGAAAGGYCG SRDLVRRCLR
51  ANLLVLLTVV AVVAGVALGL GVSAGGALA LGPGALEAFV FPGELLRL
      1 2
101 RMILPLVVC SLIGGAASLD PGALGRLGAW ALLFFLVTTL LASALGVGLA
      3
151 LALQPGAASA AIEASVGAAG SAENAPSKEV LDSFLDLARN IFPSNLVSA
201 FRSYSTTYEE REITGTRVKV PVGOEVEGMN ILGLVVFVIV FGVALRKLGP
      4
251 EGELLIRFFN SFNEATMVLV SWIMWYAPVG IMFLVAGKIV EMEDVGLLFA
      5
301 RLKGYILCCL LGHAIHGLLV LPLIYFLFTR KNPYRFLWGI VTPLATAFGT
      6 7
351 SSSSATLPLM MKCVEENNGV AKHISRFILP IGATVNMDGA ALFQCVAADF
      8
401 IAQLSQQSLD FVKIITILVT ATASSVGAAG IPAGGVITLA IILEAVNLPV
      9
451 DHISLILAVD WLVDRSCTVL NVEGDALGAG LQNYVDRTE SRSTEPELIQ
      10
501 VKSELPLDPL PVPTEGNPL LKHYRGPAGD ATVASEKESV M

```

Fig. 3: Amino acid sequence of hASCT2. Putative trans membrane domains are underlined. Sites for *N*-linked glycosylation (shaded) and protein kinase C-dependent phosphorylation (asterisk) are indicated. (Adapted from Kekuda R. et al., Cloning of the Sodium-dependent, Broad-scope, Neutral Amino Acid Transporter B0 from a Human Placental Choriocarcinoma Cell Line, 1996).

The amino acid sequence of hASCT2 shows 61% identity and 77% similarity to human ASCT1. hASCT2 amino acid sequence shows 40% identity and 65% similarity to human glutamate transporters (19).

hASCT2 transports L-alanine, L-serine, L-cysteine and L-threonine, but also L-glutamine and L-asparagine at high affinity, and some other neutral amino acids with lower affinity. hASCT2 catalyzes also the glutamate transport but with low affinity; this activity is higher at low pH. ASCT2 mediates Na⁺-dependent obligatory exchange of substrate amino acids, and it has been shown to be present in the brush-border membranes of proximal tubule cells (kidney) and enterocytes (intestine). ASCT2 has been found also to be a retrovirus receptor (20). hASCT2 mRNA (2.9 kb) has been shown to be expressed in placenta, lung, kidney,

pancreas, skeletal muscle and human colon carcinoma cell lines (19). Further genomic studies by Northern blot analysis showed its expression in a human kidney proximal tubule cell line and reverse transcriptase-polymerase chain reaction analysis showed its expression in human intestinal epithelia (8,21).

1.8 - SLC7 and SLC3 families

The SLC7 family is divided into two subgroups, the cationic amino acid transporters (CATs, SLC7A1–4 and SLC7A14) and the light chains or catalytic subunits (L-type amino acid transporters (LATs), SLC7A5-13 and SLC7A15) of the heteromeric amino acid transporters (HATs) (**Fig. 4**).

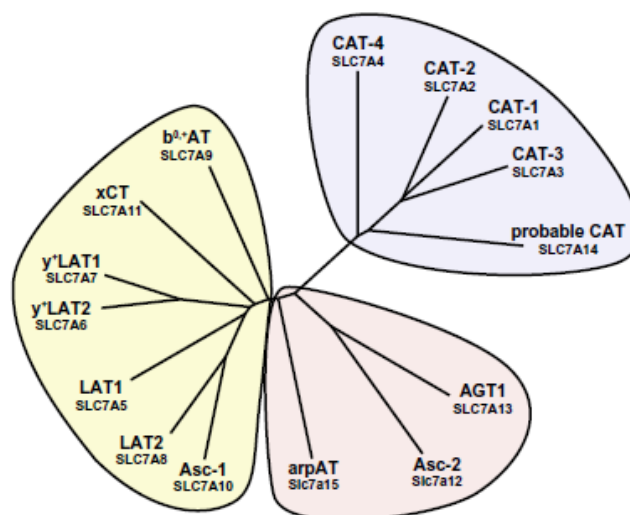


Fig. 4: Phylogenetic tree of SLC7 family members. The SLC7 family is composed of the CATs and the light subunits of HATs. (Adapted from Fotiadis D. et al., The SLC3 and SLC7 families of amino acid transporters, 2013).

LATs are also named glycoprotein-associated amino acid transporters. The SLC3 family, instead, includes the associated heavy subunits (glycoproteins) 4F2hc (SLC3A2) or rBAT (SLC3A1) of HATs.

CATs are facilitated diffusers for cationic amino acids and play an important role in nitric oxide synthesis. These transporters are N-glycosylated and have 14 putative transmembrane domains (TMDs) (22).

On the other hand, LATs are not N-glycosylated and only have 12 TMDs (23). CATs and HATs, originate from an ancestral protein with 12 transmembrane domains and that duplication of the last two domains of this protein, happened about 2.6 billion years ago, is the origin of the CAT structure with 14 domains, according to sequence analyses. Homologous CAT and LAT proteins are also found in prokaryotes, but the cysteine residue of the LATs that is involved in the disulfide bridge with the heavy subunit is not conserved.

The cysteine residue involved in the disulfide bridge between the light chain and the heavy chain is located between TMD III and IV of LATs (**Fig. 5**). HATs are mostly exchangers with a wide spectrum of substrates and they are disulfide-linked heterodimers of SLC3 members and eukaryotic LATs from the SLC7 family.

Six different LATs form heterodimers with 4F2hc (the heavy chain of the 4F2 antigen): LAT1 (SLC7A5), LAT2 (SLC7A8), γ -LAT1 (SLC7A7), γ -LAT1-2 (SLC7A6) and the cystine/glutamate antiporter xCT (SLC7A11) and ASC-1 (SLC7A10).

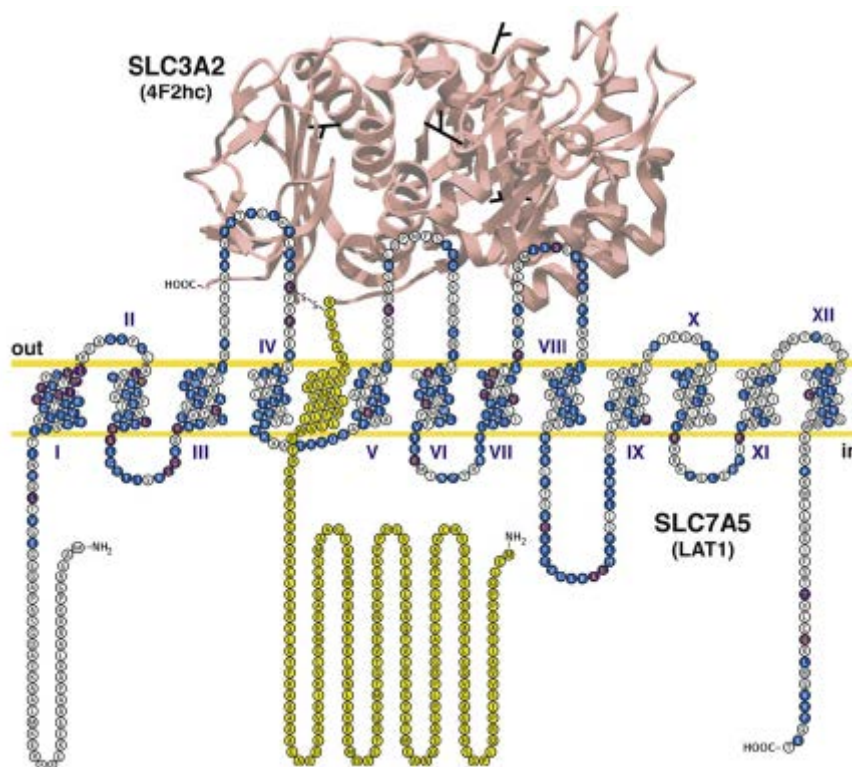


Fig. 5: Model of human heterodimer 4F2hc/LAT1 proteins. (Adapted from Fotiadis D. et al., The SLC3 and SLC7 families of amino acid transporters, 2013).

On the contrary, only the amino acid transporter $b^{0,+}$ AT (SLC7A9) forms heterodimers with rBAT. The two members of the SLC3 family (**Table 2**): rBAT (SLC3A1, also named D2 and NBAT) and 4F2hc (SLC3A2, also named CD98hc and FRP, for fusion regulatory protein) share about 20% identity.

Human gene name	Protein name	Aliases	Predominant substrates	Transport type/coupling ions ⁴	Tissue distribution and cellular/subcellular expression	Link to disease	Human gene locus	Sequence accession ID	Splice variants and their features
SLC3A1	rBAT	NBAT, D2	System $b^{0,+}$ heterodimerizes with light subunit SLC7A9	E (see details in SLC7 table)	Kidney, small intestine, (apical membrane), liver, pancreas	Cystinuria, hypotonia-cystinuria syndrome (HCS) and related Cancer	2p16.3	NM_000341	
SLC3A2	4F2hc	CD98hc, FRP	Systems L, y^+L , x_c^- and asc with light subunits SLC7A5–8 and SLC7A10–11	E (see details in SLC7 table)	Ubiquitous, (basolateral membrane)		11q13	NM_002394 NM_001012661 NM_001012662 NM_001012663 NM_001012664 NM_001013251	6 Splice variants

⁴ C: cotransporter; E: exchanger; F: facilitated transporter; O: orphan transporter.

Table 2: SLC3 – heavy subunits of the heteromeric amino acid transporters. (Adapted from Fotiadis D. et al., The SLC3 and SLC7 families of amino acid transporters, 2013).

4F2hc and rBAT are N-glycosylated and molecular weight for the mature glycosylated forms is ~85 kDa for 4F2hc and ~94 kDa for rBAT. They have an intracellular N-terminus, a single TMD, and a large extracellular C-terminus (50–60 kDa) (24); the ectodomain of human 4F2hc has been solved at 2.1 Å resolution (25). The cysteine involved in the disulfide bridge is four to five amino acids away from the TMD. The main function of the heavy subunit is the trafficking of the transporter to the plasma membrane, but 4F2hc can also be involved into β -integrin signaling, cell fusion and cell proliferation (26).

1.9 - LAT1 (SLC7A5)

LAT1 (SLC7A5) was the first cloned light chain of heteromeric amino acid transporters (27,28). The hLAT1 (NM 003486.5) amino acid transporter consists of 507 amino acids (**Fig. 6**) with a molecular weight of ~55 kDa (28), but its apparent molecular mass in SDS gels is ~40 kDa due to its increased hydrophobicity (5).

```

1 MAVAGAKRRA VAAPATTAAE EERQAREKML EARRGDGADP EGEVTLQRN ITLINGVAII VGTIIGSGIF VTPTGVLKEA
81 GSPGLSLVWV AVCGVFSIVG ALCYAEIGTT ISKSGGDYAY # MLEVYGSLLPA FLKLWIELLI IRPSSQYIVA LVFATYLLKP
161 VFPTCPVPEE AAKLVAQLCV LLLTAVNCYS* VKAATRVQDA FAAAKLLALA LIILLGFIQM GKDIGQGQDAS NLHQKLSFEG
241 TNLVGNIVL ALYSGLFAYG GWNYLNFVTE ENINPYRNLP LAIIISLPV TLVYVLTNLA YFTTLSTNQM LTSEAVAVDF
321 GNYHLGVMSW IIPVFGVLSL FGSVNGSLFT * SSRLEFFVGSR EGHLPISLSM IHPQLLTPVP SLVFTCVMTL MYAFSRDIFS
401 IINFFSFFNW LCVALAIIGM MWLRFKKPEL ERPIKVNLLAL PVFFILACL F LIAVSFWKTP LECGIGFATI LSGLPVYFFG
481 VNNKKNPKWI LQVIFSIVTL CQKLMQVVPQ ET

```

Fig. 6: Amino acid sequence of hLAT1. Potential tyrosine kinase-dependent phosphorylation site and protein kinase C-dependent phosphorylation sites are labeled with # and *, respectively. (Adapted from Kanai Y. et al., Expression Cloning and Characterization of a Transporter for Large Neutral Amino Acids Activated by the Heavy Chain of 4F2 Antigen (CD98), 1998).

Heteromeric transporter 4F2hc/LAT1 drives the sodium-independent obligatory exchange with 1:1 stoichiometry of large neutral amino acids such as leucine, isoleucine, valine, phenylalanine, tyrosine, tryptophan, methionine, and histidine. The LAT1 affinity for large neutral and aromatic amino acids is up to 100-fold higher on the cytosolic side of the transporter compared to the extracellular side. LAT1 transfers one amino acid out of the cell and at the same time another amino acid molecule is transported into the cell and is sensitive to 2-aminobicyclo-(2,2,1)-heptane-2-carboxylic acid (BCH), a specific inhibitor of the system L (24). LAT1 is involved in the transport of several drugs such as L-DOPA, melphalan, baclofen, 3-*O*-methyldopa, alpha-methyltyrosine, gabapentin, alphamethyldopa, thyroid hormones, pregabalin and gabapentin (29). Its activity also not influenced by extracellular pH (30).

SLC7A5 gene coding for hLAT1 is expressed in the placenta > the brain > the spleen > the testes and the colon (27). Experiments using anti-LAT1 antibodies demonstrated that LAT1 is mainly expressed in microvessels of the central nervous system, where it is involved in the transport of L-3,4-dihydroxyphenylalanine (L-DOPA) across the blood–brain barrier (31), in the inner blood-retinal barrier, where it plays an important role in maintaining large neutral amino acids and neurotransmitters (32), as well as in placental membranes feeding with thyroid hormones and amino acids the fetus and the placenta (24).

No splice variants of LAT1 transporter have been identified. However, 352 single nucleotide polymorphisms (SNPs) have been described in the SLC7A5 gene. Only five SNPs are in the coding region; three are synonymous SNPs and two non-synonymous (rs1060250 and rs17853937). The non-synonymous SNP rs1060250 (N230K) didn't show any functional implication (33) while is still not clear the relationship between rs17853937 (D223V) polymorphism and the protein activity. In 2006, an amino acidic substitution in position 41

(G41D) of the LAT1 gene has been described in a phenylketonuric patient population. This mutation could be involved in the exceptionally mild clinical course of the disease in some patients (30).

1.10 - 4F2hc (SLC3A2)

The 4F2 heavy chain (4F2hc, also called CD98 in mice) gene has been identified on chromosome 11 and seems to be more ubiquitously expressed than other human heavy chain rBAT (6). The 4F2hc glycoprotein can bind with many light chains to form different transporters, and its main role is the trafficking of the complex to the membrane. The 4F2hc protein is comprised of 630 amino acid residues, it is heavily glycosylated, resulting in an apparent molecular mass of ~85 kDa. The light subunits are connected to the 4F2hc heavy subunit by a disulfide bridge (27).

The two cysteines involved in the disulfide bridge, are located just outside the plasma membrane of the 4F2hc protein and in the extracellular loop between transmembrane helix 3 and 4 of all light subunits (**Fig. 7**) (34).

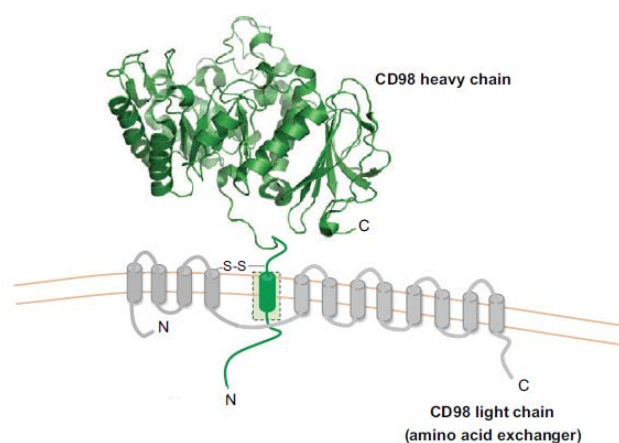


Fig. 7: schematic representation of CD98/light chain. (Adapted from Cantor J.M. et al., CD98 at the crossroads of adaptive immunity and cancer, 2012).

1.11 - hASCT2 and hLAT1 in cancer

A constant nutrients supply is required by tumors to support their characteristic unabated growth. In fact, tumor cells can consume more nutrients than required for their own metabolic needs, and exhibit different metabolic profiles compared to normal cells. These differences provide the overarching theme in the “tumor metabolome” definition. The nutrients supply of tumors occurs through the collective processes of angiogenesis and the portentous increased expression of nutrient transporters in the plasma membranes of constituent cells. Compared to normal cells or tissues, cancer cells display improved and altered amino acids channeling. Amino acids are the primary source of cellular nitrogen, used for a wide range of cellular biosynthesis mechanisms such as nucleotide, glutathione and protein synthesis. In addition to their metabolic utility, amino acids also play a regulatory role in modulate growth, mainly through signaling to the energy, nutrient and growth factor integrating kinase mammalian target-of-rapamycin (mTOR). Given their metabolic importance, it is not surprising that amino acids are taken up at accelerated rates by growing tumors (9).

In 1990, before amino acid transporter isolation, Christensen proposed that specific amino acid carriers could be upregulated to support the high levels of protein synthesis necessary for growth and proliferation of cancer cells (35).

In 2005, Fuchs B.C. and Bode B.P., using the “cDNA Virtual Northern” tool of the Cancer Genome Anatomy Project (CGAP) website (<http://cgap.nci.nih.gov>), found ASCT2 and LAT1 expression levels upregulated three-fold (collectively) in a variety of cancerous tissues where their expression pattern is almost identical (**Table 3**).

Tissue	ASCT2			LAT1		
	Normal	Cancerous	<i>P</i> -value	Normal	Cancerous	<i>P</i> -value
Brain	2/212500	36/160667	<0.01	9	37	<0.01
Colon	1/16386	76/159312	0.01	0	90	<0.01
Eye	4/75629	26/44354	<0.01	10	16	0.01
Head and neck	1/43747	2/67260	0.45	0	7	0.06
Kidney	4/59845	24/74443	<0.01	0	11	0.01
Liver	5/58771	16/72408	0.04	0	4	0.14
Lung	7/102295	30/169681	0.01	1	25	<0.01
Lymph node	0/80715	12/47425	<0.01	7	40	<0.01
Mammary gland	3/45920	30/82268	<0.01	9	14	0.40
Muscle	1/72119	14/37001	<0.01	0	10	<0.01
Ovary	1/9206	42/84150	0.06	0	20	0.13
Pancreas	0/7181	22/73165	0.13	1	50	0.05
Placenta	13/197318	28/38969	<0.01	18	12	<0.01
Skin	1/43036	35/121727	<0.01	19	120	<0.01
Stomach	0/19104	39/115697	0.01	1	36	0.03

Table 3: expression level of ASCT2 and LAT1 mRNA (ESTs) in normal and cancerous specific human tissues. (Adapted from Fuchs B.C. et al., Amino acid transporters ASCT2 and LAT1 in cancer: Partners in crime?, 2005).

Based on the available data, both LAT1 and ASCT2 are portentously expressed in primary human cancers and several cancer cell lines, where they have been shown to be a key role in growth and survival. To date it is still unknown why these amino acid transporters are craved by tumors cells. Fuchs B.C. and Bode B.P. hypothesized that LAT1 is so important to the transformed cells because it provides the essential amino acids to enhance growth in cancer cells via mTOR-stimulated translation, whereas ASCT2 is a key role player in maintaining the cytoplasmic amino acid pool and it is required to drive LAT1 function, suppresses apoptosis, and supplies energetic fuel via glutamine delivery (**Fig. 8**).

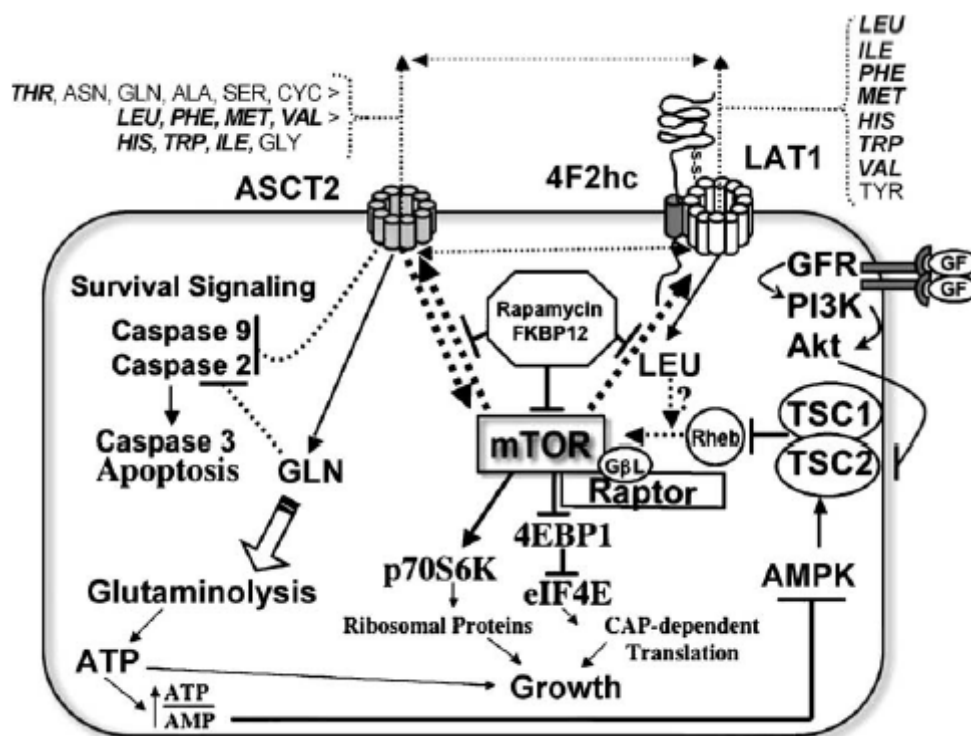


Fig. 8: relationship of ASCT2, LAT1 and mTOR in the growth and survival of cancer cells. (Adapted from Fuchs B.C. et al., Amino acid transporters ASCT2 and LAT1 in cancer: Partners in crime?, 2005).

Among the ASCT2 high affinity substrates, represented by small neutral amino acid, there is glutamine which is highly consumed by tumor cells. Both glutamine and ASCT2 have been shown to inhibit apoptosis through independent but overlapping pathways. While, among intermediate affinity ASCT2 substrates, a lot of LAT1 essential amino acids are included (**in bold; Fig. 9**). LAT1 functions as a heterodimer with 4F2hc delivering mostly essential amino acids to the cytoplasm. Both ASCT2 and LAT1 are obligate exchangers, and may share substrates for import/export in a transport cycle (double headed dashed arrows) necessary to equilibrate cytoplasmic amino acid pools. The mTOR kinase integrates signaling from growth factors, energy metabolism, and nutrients (especially LAT1 amino acids), to regulate translation via phosphorylation of key regulatory proteins (9). Recent data suggest reciprocal stimulatory links between ASCT2, LAT1 and mTOR. Loss of ASCT2 expression or

deprivation of LAT1 essential amino acids inhibit mTOR signaling; reciprocally, rapamycin inhibits mTOR activity and down-regulates ASCT2 and LAT1 expression.

Target-of-rapamycin (TOR) is a member of the phosphatidylinositol-3-kinase-related kinase (PIKK) family and represents a serine/threonine kinase, evolutionarily high conserved, that integrates signaling from growth factors, energy status and nutrients, especially amino acids (36). Rapamycin is an immunosuppressant that blocks T-cell proliferation by arresting cells in G1 phase. When complexed with the prolyl isomerase *FK506* binding protein (FKBP12), rapamycin binds to mammalian TOR (mTOR) inhibiting its activity. In mammalian cells, mTOR senses intracellular amino acid status through an unknown mechanism, and regulates translation by phosphorylating key regulatory proteins. Both mTOR-mediated phosphorylation events stimulate the translation of specific classes of mRNA into growth-related proteins. Thus, mTOR main function is to regulate growth in cells. Because of its role in growth, rapamycin and related analogs able to inhibit mTOR, are being developed as potential cancer therapies. However, recent evidence suggests that not all mTOR-regulated functions are rapamycin-sensitive, including the trafficking of 4F2hc-associated amino acid transporters to the plasma membrane (9).

1.12 - Heterologous protein production

Heterologous protein production is a particular approach used to amplify the yield of a desired protein target. To date, this is not a well established process, because an optimal protein production experiment is based on different parameters and many of these are still poorly understood. This kind of experiment is much more challenging for eukaryotic proteins and membrane proteins. Many eukaryotic membrane proteins are targets for different drugs and they are implicated in diseases as cancer, cystic fibrosis, epilepsy, hyperinsulinism, heart

failure, hypertension and Alzheimer's disease. All this makes them potential target for structural and functional characterization. For this purpose, large amounts of pure protein, and hence high production levels in a particular host, are required (37).

To understand how membrane proteins function and how their activity can be modulate by specific drugs, experiments on their structures and function are essential prerequisites.

The pharmaceutical industry is directly involved in this kind of study, to produce new drugs that can bind membrane proteins modulating their activity.

To date, high-resolution structures are available for a wide spectrum of soluble proteins, but three-dimensional structures have been described for only 34 membrane proteins, and most of them have prokaryotic origin, with only five being mammalian membrane proteins. These particular MPs were crystallized for their natural abundance, avoiding all the difficulties associated with heterologous overexpression. Furthermore, the most of medically and pharmaceutically relevant MPs are present in natural tissues at very low concentration, making heterologous overexpression in host cells an important prerequisite for large-scale production and structural studies. In general, mammalian MPs are more difficult to purify in large scale compared to prokaryotic MPs, due to the need to produce them in heterologous systems to achieve large amounts of protein (38).

1.13 - Heterologous systems

Studying the structure and the function of membrane proteins, the first aspect to clarify is which heterologous system should be used for the production of the protein target (39). There are many heterologous systems used for the production of eukaryotic integral membrane proteins; commonly one is the prokaryotic system (bacteria) and three are eukaryotic systems

(yeast, insect cells, and mammalian cells). The choice of the best expression system for the protein target remains highly empirical (40).

1.13.1 - Bacteria

Often prokaryotic homologous proteins can be expressed in bacteria in large amount, thus they have been most amenable for obtaining structural data on membrane proteins. However, this approach can not easily be applied to mammalian proteins, since these proteins are mainly expressed in inclusion bodies, from which they need to be purified under denaturing conditions.

For this reason, derivatives of *E. coli* BL21(DE3) strain, CD41(DE3) and CD43(DE3), selected to grow to high cell density and to overproduce proteins without any toxic effect for the host cell, have been successfully exploited for mitochondrial MPs production (38).

In general, among many systems available for heterologous protein production, the Gram-negative bacterium *Escherichia coli* is one of the most used. *E. coli* can grow rapidly and at high density on inexpensive media, has well-characterized genetics and an large number of cloning plasmids and mutant host strains are available. A lot of work has been directed at improving the performance and versatility of this system, despite there is no guarantee that a recombinant protein product will be found in *E. coli* at high level in a full-length and active form (41).

1.13.2 - Yeast

The two yeast systems most commonly used for protein production are *Saccharomyces cerevisiae* and *Pichia pastoris*. A lot of work has been done in *S. cerevisiae* to understand the

parameters necessary for membrane protein expression, and a greater variety of different strains is available. On the other hand, *P. pastoris* offers a tightly regulated inducible expression system. In general, yeast has several advantages as host system for the eukaryotic protein expression compared to prokaryotic system. Like bacteria, yeast can be genetically manipulated, its genome is very well characterized, can be easily cultured, and can be grown at very high density. On the other hand, yeast is an eukaryotic host and have protein processing and post-translational modification mechanisms related to those found in mammalian cells (40).

S. cerevisiae has been successfully used to functionally produce and purify several mammalian membrane proteins. The methylotrophic yeast, *P. pastoris*, has been used for the production of more than 300 heterologous proteins and as a tool for large-scale recombinant soluble protein production (42). In high cell density cultures, ethanol (a product of *S. cerevisiae* fermentation) becomes toxic and limits further growth and foreign protein production. *P. pastoris*, can be cultured at very high densities (500 OD₆₀₀ U/mL) in the controlled environment of a fermenter thanks to its preference for respiratory growth. Furthermore, using *P. pastoris*, foreign genes are stably integrated in single or multiple copy behind the *AOX1* (alcohol oxidase 1) promoter, one of the strongest, most regulated promoters known (38).

1.13.3 - Insect cells

The baculovirus expression system (BVES) was found studying insect pests. To date, this system is commonly used as a method for protein expression in insect cells, while agricultural applications are limited. The advent of serum-free media and the use of intermediate-scale

shaker suspension systems have made BVES a very accessible system, despite it is more expensive than yeast.

However, insect cells are simpler to grow compared to mammalian cells and at the same time, they offer a membrane composition and post translation modifications closer to those of mammalian cells than yeast (40).

1.13.4 - Mammalian cells

Mammalian, and mainly human, cells offer the most native cellular environment for the production of membrane proteins that are associated with human physiology and disease.

In the past, their use in structural studies had been limited by the high costs and experimental approaches of culturing and transfecting.

Traditionally, mammalian expression systems are based on the isolation of stable transformants and on the use of viral vectors to transfect the host cells (40).

1.14 - Escherichia coli and Pichia pastoris

To date, two different heterologous systems are particularly well represented in the scientific literature reporting on recombinant protein production.

Escherichia coli was the first host to be used for this purpose almost 40 years ago. Within the past 15 years, *Pichia pastoris* has successfully entered the scene and is now the second most-used host for recombinant protein production. On the basis of the PubMed citation database, the use of *P. pastoris* as an heterologous system has increased from 4% to 17%, from 1995 to 2009. Within the same time period, the usage of *E. coli* as an expression host remained constant, with approximately 60% of the recombinant genes reported. Eukaryotic proteins

tend to form in *E. coli* inclusion bodies and the protein yield is low. This because of the rate of gene translation in *E. coli* is 4- to 10-fold higher than in eukaryotes. *E. coli* should not be used as heterologous system if posttranslational modifications (PTMs) are important for the study because these microorganisms are unable to incorporate PTMs, such as N-linked glycan chains (43).

Many important elements are essential in the design of recombinant expression systems. Heterologous expression is normally induced from a plasmid with some genetic elements: origin of replication (*ori*), an antibiotic resistance marker, transcriptional promoters, translation initiation regions (TIRs) as well as transcriptional and translational terminators.

A strong transcriptional promoter to control gene expression is required for protein production in a heterologous system. Promoter can be activated thermal or chemical and the most common inducer is the sugar molecule isopropyl-beta-D-thiogalactopyranoside (IPTG) (**Fig. 9**).

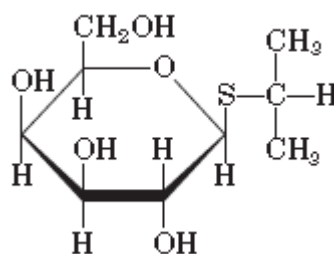


Fig. 9: isopropyl-beta-D-thiogalactopyranoside (IPTG).

One of the most used expression system in *E. coli* is the pET expression system. More than 40 different pET plasmids are available. The system consists of hybrid promoters, multiple cloning sites for the incorporation of different fusion tags and protease cleavage sites. Protein production of the target requires a host strain lysogenized by a DE3 phage fragment, encoding the T7 RNA polymerase, under the control of the IPTG inducible *lacUV5* promoter (**Fig. 10**). LacI represses the *lacUV5* promoter and the T7/lac hybrid promoter on the expression

plasmid. T7 RNA polymerase is transcribed when IPTG binds and triggers the release of tetrameric LacI from the *lac* operator. Transcription of the target gene from the T7/*lac* hybrid promoter (repressed by LacI as well) is, at this point, started by T7 RNA polymerase (**Fig. 10**) (44).

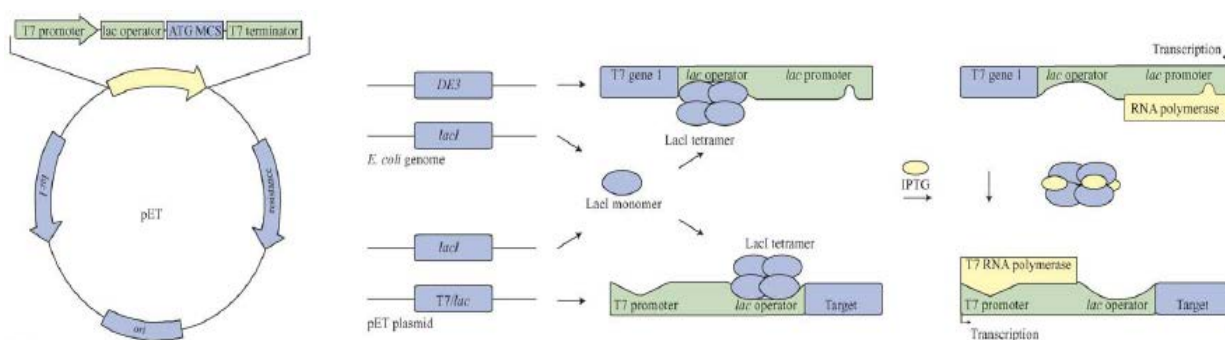


Fig. 10: The pET expression system. A general pET plasmid configuration is shown on the left. The macromolecular situations prior to and after induction are on the right. (Adapted from Sørensen H. P. et al., Advanced genetic strategies for recombinant protein expression in *Escherichia coli*, 2004).

E. coli has a wide spectrum of advantages and many of these are also offered by *P. pastoris*, a methylotropic yeast that can metabolize methanol and use it as its only carbon source. On the other hand, *P. pastoris* folds most eukaryotic proteins more efficiently and forms disulfide bonds correctly.

Pichia pastoris is an eukaryotic system and it has many of the advantages of higher eukaryotic expression systems such as protein processing, folding, and posttranslational modification; at the same time it is easy to manipulate as *Escherichia coli* or *Saccharomyces cerevisiae* and generally gives higher expression levels. All these properties make *Pichia* very useful as a protein expression system.

When *P. pastoris* grows in methanol-containing medium the promoter of the alcohol oxidase I (AOX1) gene is upregulated. This strong and tightly regulated promoter is incorporated into the majority of vectors used for expression of recombinant genes in *P. pastoris* (43).

The metabolism of methanol starts with the oxidation of methanol to formaldehyde using molecular oxygen by the enzyme alcohol oxidase. This first reaction generates also hydrogen peroxide. This compound is toxic, and for this reason, methanol metabolism takes place within a specialized cell organelle, named peroxisome. Alcohol oxidase enzyme has low affinity for O₂, and *Pichia pastoris* compensates by producing large amounts of the enzyme. The promoter involved in alcohol oxidase production is the one used to drive heterologous protein expression in *Pichia*.

In particular, two genes in *Pichia pastoris* code for alcohol oxidase, and they are called *AOX1* and *AOX2*. The alcohol oxidase activity is mainly due to the product of the *AOX1* gene and its production is tightly regulated and induced by methanol. The *AOX1* gene has been isolated and a plasmid with *AOX1* promoter is used to drive expression of the gene target. *AOX2* gene is about 97% homologous to *AOX1*, and when only *AOX2* is expressed growth on methanol is much slower than with *AOX1*.

Linear DNA obtained after plasmid digestion, can generate very stable transformants of *Pichia pastoris* via homologous recombination between the plasmid DNA and regions of homology within the genome. Multiple insertion events occur spontaneously during the homologous recombination and the **Fig. 11** shows the insertion mechanism into the genome and the result of multiple insertions to the *AOX1* locus (45).

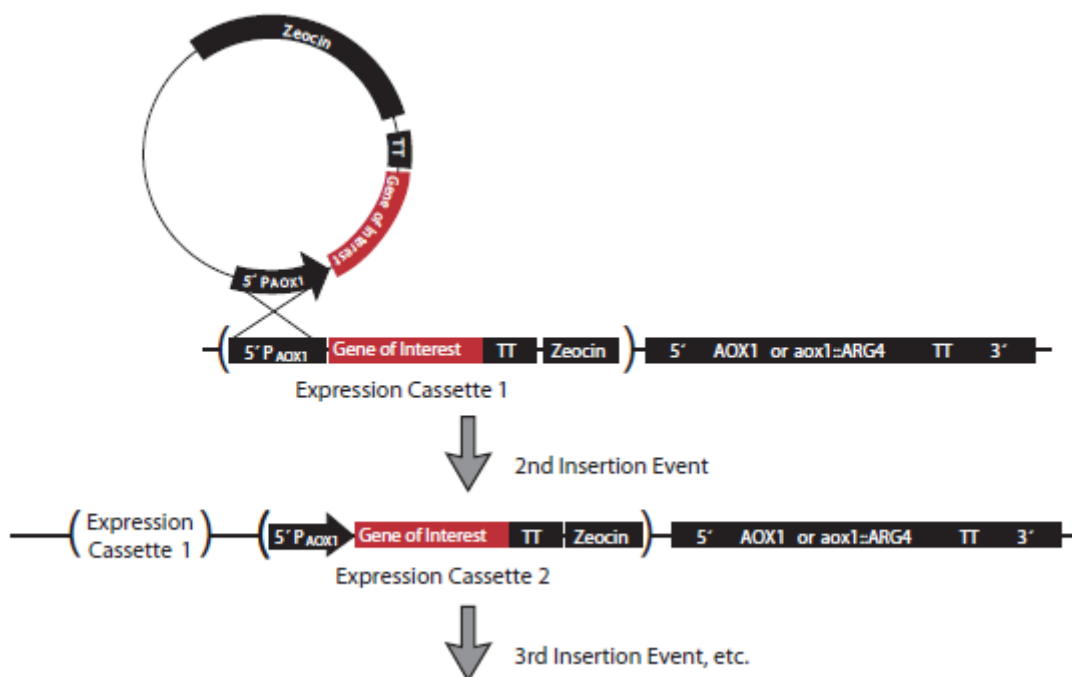


Fig. 11: Recombination and integration in *Pichia pastoris* genome. (Adapted from Invitrogen EasySelect *Pichia* Expression Kit, 2010).

1.15 - Codon bias

The genetic code uses 61 nucleotide triplets (codons) to encode 20 amino acids and three codons to terminate translation (STOP codons); it means that each amino acid could be encoded by more than one different but synonymous codons (methionine and tryptophan being the only exception). These codons are ‘read’ in the ribosome by complementary tRNAs that have been charged with the appropriate amino acid. The ability of the genetic code to encode the same amino acid with different codons is defined as “degeneracy of the genetic code”. The degeneration of the genetic code allows the same protein to be encoded by alternative nucleic acid sequences (46). Although the same amino acid could be encoded by different codons, each organism has its own preferred codon for each individual amino acid (37). This is called codon bias.

There is a high variability in the frequencies with which different codons are used between different organisms, between proteins expressed at high or low levels within the same organism, and sometimes even within the same operon (47).

Andersson and coworkers have hypothesized that codon biases reduce the diversity of isoacceptor tRNAs reducing the metabolic load. This results in a benefit for the organisms that spend part of their lives under rapid growth conditions (48). The reasons for codon bias are still unknown, but it has become increasingly clear that codon biases can have a profound impact on the heterologous expression of proteins (46).

In fact, more efficient translation can be obtained when adapting a gene sequence using the preferred codons of the host organism. Basically, there are two different ways to increase the final protein yield: optimize the consensus sequence around the starting ATG to ensure efficient translation initiation as well as optimize all the codons of the gene target to be host specific (37).

The gene expression levels are modulate and influenced by a wide variety of factors. The native gene coding for the protein target, during heterologous expression, contains tandem rare codons that can reduce the efficiency of translation or block the translational machinery. For this reason, to improve the heterologous protein production, can be useful obtaining and using the optimezed gene to be host specific, that can achieve the highest possible level of production. During codon optimization many parameters are considered such as codon usage, GC content, inhibition of splicing and prevention of stable mRNA secondary structures.

CHAPTER 2

MATERIALS AND METHODS

2.1 - Materials

2.1.1 - Low Salt LB (Luria-Bertani) medium

- 1% Tryptone
- 0.5% Yeast extract
- 0.5% NaCl

These compounds were dissolved in water and the pH of the solution was adjusted to 7.5 with 1 N NaOH.

2.1.2 - YT 2X medium

- 1.6% Tryptone
- 1% Yeast extract
- 0.5% NaCl

These compounds were dissolved in water, the pH of the solution was adjusted to 7.5 with 1 N NaOH and autoclaved for 20 minutes on liquid cycle.

2.1.3 - Yeast Extract Peptone Dextrose Medium (YPD)

1% Yeast extract

2% Peptone from meat

2% Dextrose (glucose)

These compounds were dissolved in water and autoclaved for 20 minutes on liquid cycle.

2.1.4 - Yeast Extract Peptone Dextrose Medium (YPDS)

1% Yeast extract

2% Peptone from meat

2% Dextrose (glucose)

1 M Sorbitol

These compounds were dissolved in water and autoclaved for 20 minutes on liquid cycle.

2.1.5 - Buffered Glycerol-complex Medium (BMGY)

1% Yeast extract

2% Peptone from meat

100 mM Potassium phosphate, pH 6.0

1.34% YNB (Yeast nitrogen base)

4×10^{-5} % Biotin

1% Glycerol

Dissolve peptone from meat and yeast extract in water. Autoclave 20 minutes on liquid cycle.

Cool to room temperature, then add YNB (filter sterilized), biotin (filter sterilized), glycerol (autoclaved), potassium phosphate (autoclaved) and mix well.

2.1.6 Buffered Methanol-complex Medium (BMMY)

1% Yeast extract

2% Peptone from meat

100 mM Potassium phosphate, pH 6.0

1.34% YNB (Yeast nitrogen base)

$4 \times 10^{-5}\%$ Biotin

0.5% Methanol

Dissolve peptone from meat and yeast extract in water. Autoclave 20 minutes on liquid cycle.

Cool to room temperature, then add YNB (filter sterilized), biotin (filter sterilized), methanol (filter sterilized), potassium phosphate (autoclaved) and mix well.

2.1.7 - Fermentation Basal Salts Medium

Phosphoric acid, 85%	26.7 mL
Calcium sulfate	0.93 grams
Potassium sulfate	18.2 grams
Magnesium sulfate-7H ₂ O	14.9 grams
Potassium hydroxide	4.13 grams
Glycerol	40 grams
Water	to 1 L

These compounds were dissolved in water, added to fermentor and autoclaved for 20 minutes on liquid cycle.

2.1.8 - Plates

To make LB, YPD or YPDS plates 2% agar was added. When the temperature is about 60°C the specific antibiotic was added and plates were stored at 4°C.

2.1.9 - TAE (Tris/Acetate/EDTA) 50 X

- 242 grams Tris base
- 18.6 grams EDTA (Ethylenediaminetetraacetic acid)
- 60 mL Glacial acetic acid

Use acetic acid to adjust pH 8 and bring up the volume to 1 liter with water.

2.1.10 - IPTG

The isopropyl β -D-1-thiogalactopyranoside (IPTG) was resuspended in sterile water and used in a concentration range between 0.1 mM and 1 mM.

2.1.11 - Protease Inhibitor Cocktail

Inhibits serine, cysteine, aspartic and thermolysin-like proteases, and aminopeptidases.

One mL of cocktail was used for the inhibition of proteases extracted from 20 g of *Escherichia coli* cells.

2.1.12 - PMSF

The PMSF (Phenylmethanesulfonyl fluoride) inhibits serine proteases such as trypsin, chymotrypsin and cysteine proteases. Its effective concentration is between 0.1-1 mM. It was used in *Pichia pastoris* lysate at a final concentration of 0.5 mM.

2.1.13 - Running buffer for SDS-PAGE 10X

- 250 mM Tris base
- 14,4% glycine
- 1% SDS

These compounds were dissolved in water and the pH was adjusted to 8.3. The 1X buffer was used during the running.

2.1.14 - MES running buffer for SDS-PAGE 20X

- 1M MES (2-*N*-morpholino ethanesulfonic acid)
- 1M Tris base
- 20 mM EDTA
- 2% SDS

These compounds were dissolved in water and the pH should be 7.3. The 1X buffer was used during the running.

2.1.15 - Coomassie Brilliant Blue

- 0.25 g Coomassie Brilliant Blue
- 45 mL Methanol
- 45 mL Distilled H₂O
- 10 mL Acetic acid

2.2 - Experimental procedures

2.2.1 - Polymerase chain reaction (PCR)

The polymerase chain reaction (PCR) is a biochemical technology used in many fields to amplify a single or a few copies of a piece of DNA, generating thousands to millions of copies of a particular DNA fragment. Short DNA fragments called primers, containing sequences complementary to the start and end of the DNA target, along with a DNA polymerase are key components to enable selective and repeated amplification. As PCR progresses, the DNA generated is itself used as a template for replication in which the DNA template is amplified. To perform a PCR reaction, the DNA template that contains the target sequence is mixed with primers, free nucleotides, and an enzyme called DNA polymerase. The thermocycler, a particular machine, increases and decreases the temperature of the sample automatically. In the first step, the mixture is heated to separate the double-stranded DNA template into single strands. The mixture is then cooled so that the primers can bind to the DNA template. At this point, the DNA polymerase begins to synthesize new strands of DNA starting from the primers. Following synthesis and at the end of the first cycle, each double-stranded DNA molecule consists of one new and one old DNA strand. PCR then continues with additional cycles (usually 25-35 cycles) that repeat the previous steps. The reaction mixture consists of:

- 10 μL buffer 5 X (containing MgCl_2 1.5 mM);
- 1 μL dNTP mix (0.2 mM dATP, 0.2 mM dCTP, 0.2 mM dGTP, 0.2 mM dTTP);
- 0.3 μM Forward primer;
- 0.3 μM Reverse primer;
- 0.1-0.75 μg template DNA;

- 0.6 μL di Phusion High Fidelity Finnzymes 2 u/ μL
- H_2O nuclease-free to 50 μL

Typical thermal cycling conditions :

Initial denaturation	Denaturation	Annealing	Extension	Final extension	
96 °C	96 °C	45-65 °C	72 °C	72 °C	4 °C
5'	30"	30"	90"	10'	∞
30-40 Cicli					

2.2.2 - Agarose gel electrophoresis

Agarose gel electrophoresis is a method used in molecular biology, to separate a population of DNA in a matrix of agarose. The DNA can be separated by length applying an electric field to move the negatively charged molecules through an agarose matrix. Most agarose concentration used is between 0.7% (gives good separation or resolution of large 5–10kb DNA fragments) and 2% (gives good resolution for small 0.2–1 kb fragments). Agarose is dissolved in a suitable electrophoresis buffer such as Tris/Acetate/EDTA (TAE) or Tris/Borate/EDTA (TBE).

Agarose gels are normally stained with ethidium bromide, which intercalates into the major grooves of the DNA and fluoresces under UV light. Other safer methods of staining are SYBR Green or methylene blue. The gel stained with ethidium bromide is viewed with an

ultraviolet (UV) transilluminator while SYBR Green requires the use of a blue-light transilluminator.

2.2.3 - Purification of DNA fragments from agarose gel

The DNA fragments separated by agarose gel were isolated and purified using the gel extraction kits Wizard SV Gel and PCR Clean-Up System (Promega). These quick protocol are simple to perform, and the PCR products are purified from contaminants, including primer dimers, PCR additives and amplification primers. Protocols included in these kits generally call for the dissolution of the gel-slice in 3 volumes of chaotropic agent at 50-60°C to dissolve the agarose, freeing the DNA for binding to the silica membrane. Then, the solution is applied to a spin-column (DNA remains in the column). Washing with ethanol 70% (the DNA remains in the column, salt and impurities are washed out), and elution of the DNA in a small volume (20 µL) of nuclease-free water or elution buffer free of salt or macromolecular contaminants, are performed. These kits can also be used to purify DNA from enzymatic reactions such as restriction digestion and alkaline phosphatase treatment.

2.2.4 - Cloning

DNA for cloning experiments can be obtained from RNA using reverse transcriptase (cDNA), or in the form of synthetic DNA. The DNA is treated with restriction enzymes to generate fragments with ends capable of being linked to those of the vector. DNA and vector, treated with same enzymes, are simply mixed together at appropriate concentrations (a molar ratio of 1:3 vector to insert) and exposed to DNA Ligase (T4 DNA ligase in our case) that covalently links the ends together. This reaction is termed ligation.

A typical ligation protocol is shown below:

COMPONENT	VOLUMES
Vector DNA (3 kb)	50 ng
Insert DNA (1 kb)	50 ng
Buffer T4 DNA Ligase 10X	2 μ L
T4 DNA Ligase	1 μ L
Nuclease-free water	to 20 μ L

2.2.5 - *E. coli* transformation

Transformation is the process of getting the recombinant vector or empty vector into host cells. To enable the cells to take up circular vector DNA they have to be made competent. The method for the preparation of competent cells depends on the transformation method.

E. coli cells were grown in 100 mL LB medium overnight at 37°C to OD₆₀₀~ 0.4-0.6. The cells were centrifuged at 4000 rpm for 15 minutes at 4°C and the pellet resuspended with 50 mL ice cold CaCl₂ 50 mM and stored on ice for 30 minutes. At this point, the resuspension was again centrifuged and the pellet resuspended with 2 mL of CaCl₂ 50 mM.

170 μ L of competent cells were mixed with ligation mix (10 μ L) or plasmidic DNA (100 ng) and incubated for 30 minutes on ice. The mixture was heat shocked at 42°C for 90 seconds and returned on ice for 2 minutes. At this point, 170 μ L LB medium were added and the mixture was incubated for 1 hour at 37°C with shaking. The cells were plated on LB agar plates containing appropriate antibiotics.

2.2.6 - DNA extraction by QIAprep Spin Miniprep kit

The QIAprep miniprep procedure (Qiagen) is based on alkaline lysis of bacterial cells followed by adsorption of DNA onto silica membrane in the presence of high concentration of chaotropic salt. Bacteria are lysed under alkaline conditions, and the lysate is subsequently neutralized and adjusted to high-salt binding conditions. After lysate clearing, the sample is ready for purification on the QIAprep silica membrane. The protocol is designed for purification of up to 20 µg of high-copy plasmid DNA from 1–5 mL overnight cultures of *E. coli* in LB medium. The bacterial cells pellet is resuspended in 250 µL Buffer P1 and transfer to a microcentrifuge tube. 250 µL Buffer P2 were added and mixed by inverting the tube 4–6 times. Then, 350 µL Buffer N3 were added and mixed immediately by inverting the tube 4–6 times. The mixture was centrifuged for 10 min at 13,000 rpm in a table-top microcentrifuge. The supernatant was loaded to the QIAprep spin column by pipetting and centrifuged for 60 seconds. The column was first washed by adding 0.5 mL Buffer PB and centrifuged for 60 seconds and then washed by adding 0.75 mL Buffer PE and centrifuged for 60 seconds. The column was centrifuged at full speed for an additional 1 min to remove residual wash buffer containing ethanol. The DNA was eluted adding 50 µL Buffer EB or nuclease-free water to column and centrifuging for 3 minutes.

2.2.7 - P. pastoris transformation

P. pastoris cells were transformed by electroporation. To prepare cells for transformation, *Pichia pastoris* X33 strain was grown in 10 mL YPD at 30°C overnight. This culture was used to inoculate 250 mL of fresh YPD medium and grown to an $OD_{600} = 1.3$ – 1.5 . The cells were centrifuged at $1,500 \times g$ for 5 minutes at 4°C and the pellet resuspended with 250 mL of

ice-cold sterile water. The cells were centrifuged as in previously step and resuspended with 125 mL of ice-cold sterile water. At this point, the cells were centrifuged at $1,500 \times g$ for 5 minutes at 4°C and the pellet was resuspended with 10 mL of ice-cold sterile 1M sorbitol. The cells were centrifuged again and resuspended with 400 μL of ice-cold sterile 1M sorbitol. The competent cells were kept on ice and used the same day.

80 μL of the cells were mixed with 5–10 μg of linearized DNA (in 5–10 μL sterile water) and transferred to an ice-cold 0.2 cm electroporation cuvette. The cuvette was incubated with the cells on ice for 5 minutes. The cells were pulsed using 2.2 kV, 25 μF and 200 ohm by electroporator and immediately 1 mL of ice-cold 1 M sorbitol was added to the cuvette. The cuvette content was transferred to a sterile 15-mL tube and incubated at 30°C without shaking for 1 to 2 hours.

50, 100, 200 and 450 μL each were spread on separate, labeled YPDS plates containing 100 $\mu\text{g}/\text{mL}$ ZeocinTM and incubated 3 days at 30°C until colonies form. A total of 52 transformants were screened for growth on YPDS plates containing a high concentration of ZeocinTM (2000 $\mu\text{g}/\text{mL}$) and analyzed after 2 days.

2.2.8 - Sonication

Sonication is the process of converting an electrical signal into a physical vibration. Sonication is usually performed to break apart compounds or cells for further examination. The vibration has a very powerful effect on solutions, causing their molecules to break apart and cells to rupture. The laboratory method for cell disruption applies ultrasound (typically 20–50 kHz) to the sample. In principle, the high-frequency is generated electronically and the mechanical energy is transmitted to the sample via a metal probe that oscillates with high frequency. The sonication probe transmits the vibration to the sample. This probe is a

carefully constructed tip that moves in time with the vibration, transmitting it into the solution. The high-frequency oscillation causes a localized high pressure region resulting in cavitation and impaction, ultimately breaking open the cells.

In general, a sonication device consists of an ultrasonic electric generator, a transducer that converts the electric signal to mechanical vibration by using piezoelectric crystals and a sonication probe.

2.2.9 - The French press

The **French press**, or **French pressure cell press**, is an apparatus used in biological experimentation to break the plasma membrane by passing the cells through a narrow valve under high pressure. A French press is commonly used to break the plasma membrane and cell wall of yeast, bacteria and other microorganisms for isolation of proteins and other cellular components.

The press uses an external pump to drive a piston within a larger cylinder that contains the liquid sample. The motor-driven piston develops pressures up to 40,000 psi.

The highly pressurized sample is then pressed past a small valve. As the sample passes through the valve, the shear stress and decompression of the sample, cause cellular disruption.

The major components of a French press are made of stainless steel to prevent sample contamination.

2.2.10 - Polyacrylamide gel electrophoresis (PAGE)

Polyacrylamide gel electrophoresis (PAGE), is a technique widely used to separate biological macromolecules, such as proteins, according to their mobility. Mobility is a function of the molecular weight, conformation and charge of the molecule.

Molecules can be run in their native state, preserving the original molecular structure, or a chemical denaturant can be added to remove this structure and turn the molecule into an unstructured linear chain whose mobility depends only on its length and mass.

For proteins, sodium dodecyl sulfate (SDS) is the most common anionic detergent applied to protein samples to linearize them and to impart a negative charge. This kind of separation is called SDS-PAGE.

The polyacrylamide gels typically consist of acrylamide, bisacrylamide, the denaturant (SDS), and a buffer with an adjusted pH. A source of free radicals and a stabilizer, such as ammonium persulfate and TEMED are added to initiate polymerization.

Polymerization is initiated by ammonium persulfate and TEMED (tetramethylethylenediamine): TEMED accelerates the rate of formation of free radicals from persulfate and these in turn catalyze polymerization. The polymerization reaction creates a gel because of the bisacrylamide, which can form cross-links between two polyacrylamide molecules. The acrylamide concentration of the gel can also be varied, generally in the range from 5% to 25%. In our case, the concentration was 12% or with a gradient from 4% to 12%. Lower percentage gels are better to separate higher molecular weight molecules, while much higher percentages are needed to resolve smaller proteins.

The protein samples were solubilized with (0.2 M Tris Base, 7.5% SDS, 3% glycerol, 100 mM dithiothreitol, and 0.01% bromophenol blu) or (NuPAGE® LDS Sample Buffer by Invitrogen).

The running buffer contained (25 mM Tris Base, 1.4% glycine and 0.1% SDS) or MES buffer (1M MES, 1M Tris Base, 20 mM EDTA and 2% SDS). The gels were stained using Coomassie staining (0.25 g Coomassie Brilliant Blue, 45 mL water, 45 mL methanol and 10 mL acetic acid), Silver staining (40% methanol/10% acetic acid for 20', 10% glutaraldehyde for 15', water for 15', 0.16 mM DTE for 15', 0.1% silver nitrate for 20' and 30 mM sodium carbonate plus 0.03% formaldehyde) or SimplyBlue SafeStain (Invitrogen).

2.2.11 - Western blot

The **western blot** (also called immunoblot) is a widely used technique used to detect specific proteins in the sample of tissue extract or homogenate. In the first step, it uses SDS-PAGE to separate proteins. The proteins are then transferred to a membrane (typically nitrocellulose or PVDF), where they are stained using specific antibodies that bind target proteins. The proteins moved from the gel onto the membrane maintain the organization they had within the gel. Samples were taken from cell cultures after breaking by sonication (*E. coli*) or French press (*P. pastoris*) or sometimes after affinity chromatography (purified proteins).

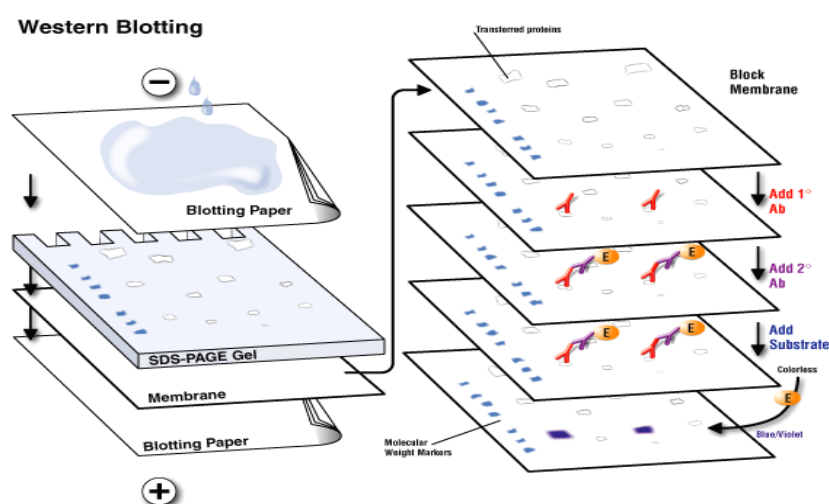


Fig. X: Schematic representation of western blotting technique (Adapted from www.komabiotech.co.kr)

To prevent the interactions between the membrane and the antibodies used for detection of the target protein, blocking of non-specific binding is achieved by placing the membrane in a dilute solution of protein; in our case 3% Bovine serum albumin (BSA) or dry milk, and with a minute percentage (0.1%) of detergent such as Tween 20. During the detection process the membrane is "probed" for the protein of interest with a modified antibody which is linked to a reporter enzyme. This enzyme can drive a colourimetric reaction (peroxidase) and produces a color or a chemiluminescent reaction and produce light (the light is then detected by CCD cameras).

2.2.12 - Protein purification by affinity chromatography

Affinity chromatography is a separation method based on a specific binding interaction between an immobilized ligand and its binding partner.

The most common use of affinity chromatography is for the purification of recombinant proteins. Recombinant proteins have been genetically modified so as to allow them to be selected for affinity binding; they are called tagged protein. In our case, tags include glutathione-S-transferase (GST) or hexahistidine (6His). Histidine tags have an affinity for nickel or cobalt ions which have been immobilized by forming coordinate covalent bonds with a chelator incorporated in the stationary phase. For elution, an excess amount of a compound able to act as a metal ion ligand, such as imidazole was used. GST has an affinity for glutathione which is commercially available immobilized as glutathione agarose. During elution, excess glutathione is used to displace the tagged protein.

2.3 - Cloning

2.3.1 - Cloning of hASCT2

The wild type gene was isolated from total RNA of primary human fibroblasts by reverse transcription. Initially, the 1623 bp cDNA encoding hASCT2 (GenBank NM_005628.2, SLC1A5) was amplified using the forward primer NdeI-hASCT2: 5'-GGAATTCCATATGGTGGCCGATCCTCCTCG-3' and the reverse primer HindIII-hASCT2: 5'-CCCAAGCTTTTACATGAC TGATTCCTTCTC-3', respectively. The amplified cDNA sequence was verified by sequencing using the ABI 310 automated sequencer Applied Biosystems. For subsequent cloning to *P. pastoris*, the full length cDNA coding for hASCT2 was amplified using the forward primer EcoRI-hASCT2: 5'-ATACCGGAATTCAAATGG TTGCCGATCCTCCTCGAGACTCC-3' and the reverse primer XbaI-ASCT2: 5'-ATACTAGTCTAGATCAATGATGATGATGATGATGCATGACTGATTCCTTCTCAGAGGC-3', coding a C-terminal His6 tag.

The hASCT2 gene was codon optimized for *P. pastoris* by GenScript and the artificial cDNA included a 5' EcoRI restriction site plus the Kozak consensus sequence and a 3' XbaI restriction site plus a C-terminal His6 fusion tag. In the optimized gene, the Codon Adaptation Index (CAI) was upgraded from 0.51 (wild type) to 0.82 (optimized) and the GC content was decreased from 63.01% to 45.43%. For cloning in *P. pastoris* both the wild type gene (wt-hASCT2) and the optimized gene (Opt-hASCT2) were inserted in the EcoRI/XbaI sites of the pPICZB expression vector, resulting in two different recombinant constructs, defined as pPICZB-(wt)hASCT2-His6 and pPICZB-(Opt)hASCT2-His6. Both constructs were verified by sequencing.

2.3.2 - Cloning of hLAT1

The hLAT1 cDNA (1,521 bp) (GenBank NM_003486, SLC7A5) was amplified from total reverse-transcribed mRNA extracted from HEK293 cells. Primers used for amplification were 5'-ATGGCGGGTGCGGGCCCCGAAGCGGCGCGCTAGC-3' (forward) and 5'-TGTCTCCTG GGGGACCACCTGCATGAGCTTCTGAC-3' (reverse). The sequence of the cDNA was analysed by an automated sequencer (ABI 310 Applied Biosystems) and corresponded to the hLAT1 coding sequence in three different determinations.

The hLAT1 cDNA was then amplified using the primers 5'-CGCGGATCCATGGCGGGTG CGGGCCCCGAAG-3' (forward) and 5'-CCGCTCGAGCTATGTCTCCTGGGGGACCAC-3' (reverse).

Each primer carries the recognition sites of BamHI and XhoI restriction enzymes. The cDNA containing the restriction sites was cloned in the pH6EX3 and pET-41a(+) expression vectors. The resulting recombinant plasmids, defined pH6EX3-hLAT1 and pET-41a(+)-hLAT1, encoded the hLAT1 protein carrying the extra N-terminal 6His tag or a GST tag, plus a S tag, respectively.

2.3.3 - Cloning of hCD98

The 1,890 bp cDNA encoding for SLC3A2, acquired from LifeSciences (IRAU p969D0814D), was amplified by 5'-CCGGAATTCCATGGAGCTACAGCCTCCTG A-3' (forward) and 5'-CCGCTCGAGTCAGGCCGCGTAGGGGAAGC-3' (reverse) primers, then sub-cloned in the pH6EX3 or pGEX-4T1 vectors. The recombinant plasmids pH6EX3-hCD98 or pGEX-4T1-hCD98, code for fusion proteins corresponding to the mature form of

hCD98 carrying the N-terminal amino acid sequence M-S-P-I-H-H-H-H-H-L-V-P-R-G-S-E-A-S-N-S- or the glutathione-S-transferase, respectively.

2.4 - Recombinant production

2.4.1- Recombinant production of hASCT2 protein

To obtain the recombinant hASCT2-His₆ protein, the resulting plasmids were linearized with PmeI and the transformation into the *P. pastoris* wild type strain X-33 was performed by electroporation (see 2.2.7). To select putative multi-copy recombinants a total of 52 transformants for each construct were tested for growth on YPDS plates containing 2000 µg/mL Zeocin and analyzed after 3 days. For large scale protein production, *P. pastoris* strains producing recombinant hASCT2 (X33/pPICZB-(wt)hASCT2-His₆ and X33/pPICZB-(Opt)hASCT2-His₆) were grown at 30°C in a 3 L fermentor (Infors HT) having an Initial Fermentation Volume (IFV) of 1.5 L basal salt medium containing 6.53 mL PTM1 trace salts. An overnight pre-culture of 75 mL in BMGY having an OD₆₀₀ of about 4 was used to inoculate the fermentor.

The initial glycerol volume was consumed after approximately 24 h and the culture was fed with 150 mL 50% glycerol (v/v) for 24 h to increase biomass. To induce production of recombinant hASCT2, the culture was fed with 150 mL methanol for 48 h. To obtain the membrane fraction, *P. pastoris* cells overproducing hASCT2 were resuspended in buffer A (50 mM Tris, pH 7.4, 150 mM NaCl, 6 mM β-mercaptoethanol and 0.5 mM PMSF) at a concentration of about 1 g/mL. Droplets of the cell suspension were frozen in liquid nitrogen and cells were broken by an French press (four passages). The suspension was centrifuged at 6000 g for 30 min and the supernatant containing membrane and cytosolic fractions (crude

extract) was collected. This supernatant was ultracentrifuged in a Ti45 rotor at 140,000 g for 1 h. The resulting membrane pellet was washed with urea buffer (5 mM Tris pH 7.4, 2 mM EDTA, 2 mM EGTA and 4 M urea) and then again ultracentrifuged as above. The washed membrane fractions (pellet) containing (wt)hASCT2 or (Opt)hASCT2 were resuspended in buffer B (25 mM Tris, pH 7.4, 250 mM NaCl, 6 mM β -mercaptoethanol and 10% glycerol) at a final concentration of about 300 mg/mL and homogenized using a handheld electric homogenizer. Aliquots of 6 mL of the membrane fraction were stored at -80°C . Various stages from the protein purification procedure were analyzed by SDS-PAGE and immunoblot.

2.4.2 - Recombinant production of hLAT1 protein

To produce the GST-hLAT1 recombinant protein, *E. coli* Rosetta(DE3)pLysS cells, treated with calcium chloride, were transformed with the pET-41a(+)-hLAT1 while to produce the 6His-hLAT1 the cells were transformed with pH6EX3-hLAT1. Selection of transformed colonies was performed on LB-agar plates in which 30 $\mu\text{g}/\text{mL}$ kanamycin plus 34 $\mu\text{g}/\text{mL}$ chloramphenicol or 100 $\mu\text{g}/\text{mL}$ ampicillin plus 34 $\mu\text{g}/\text{mL}$ chloramphenicol were present, respectively. Colonies were inoculated in 100 mL of a medium (2X YT at pH 7.0) containing Bacto peptone (1.6 %), Bacto yeast extract (1 %) and NaCl (0.5 %). Also this medium contained antibiotics at the same concentrations as above. Cell cultures were grown overnight (37°C) under rotary shaking (about 200 rpm). Fifty mL aliquot of the cell culture was transferred to 0.5 L of a medium (2X YT) prepared with the components above described. When the optical density of the cell cultures, measured at 600 nm wavelength, was 0.5–0.7, different IPTG concentrations (from 0.1 to 1 mM) were tested for inducing the expression of the protein coded by the cDNA inserted in the recombinant plasmid. Two 0.25 L aliquots of the cell suspension were differently treated: one aliquot was grown at 28°C while the other at

37°C. Every 2 h, 50 mL from each aliquot were collected and centrifuged (3,000g, 4°C, 10 min); pellets (aliquots of 0.2 g wet weight) were stored at -20°C. A bacterial pellet aliquot, after thawing was dissolved in 2 mL medium (20 mM hepes/tris pH 7.5 plus 20 µL of protease inhibitor cocktail and 0.5 mM PMSF). The suspension was treated by sonication (10 min/ 1 s sonication/1 s intermission, 4°C; SONICS sonifier, Vibracell VCX-130). The insoluble cell fraction was separated by centrifugation (12,000g, 4°C, 30 min). Proteins were separated on SDS-PAGE.

2.4.3 - Recombinant production of hCD98 protein

pH6EX3-hCD98 (6His-CD98) and pGEX4T1-hCD98 (GST-hCD98) were used for transforming *E. coli* Rosetta(DE3)pLysS. Selection of transformed colonies was performed on LB-agar plates in which 100 µg/mL ampicillin plus 34 µg/mL chloramphenicol were present, respectively. Colonies were inoculated in 100 mL of LB medium containing Bacto peptone (1%), Bacto yeast extract (0.5%) and NaCl (0.5%). Also this medium contained antibiotics at the same concentrations as above. Expression, pellet storing, cell breaking and protein separation were performed as described above (Sect. 2.4.2).

2.5 - Protein purification

2.5.1 - hASCT2 purification

For large-scale solubilization and purification (Opt)-hASCT2, about 1.5 g of washed membranes (300 mg/mL) was resuspended in buffer B containing 1% C₁₂E₈ (w/w) to a concentration of 150 mg/mL and gently mixed by agitation for 3 h at 4°C. After solubilization, the solubilized material was centrifuged at 120,000 g for 1 h, imidazole (50

mM) was added to the supernatant which was mixed with 3 mL Ni-nitrilotriacetic acid (NTA) agarose resin equilibrated with the equilibration buffer (20 mM Tris pH 7.4, 300 mM NaCl, 10% glycerol, 6 mM β -mercaptoethanol, 0.03% $C_{12}E_8$, and 50 mM imidazole) and incubated by gentle agitation for 3 h at 4 °C. The Ni-NTA resin was subsequently packed into a plastic 1 mL column. The resin was washed with 30 mL of the equilibration buffer. Then, 4 mL of the same buffer containing 300 mM imidazole and 2 mL of the same buffer containing 500 mM imidazole (referred as elution buffers) were added. Fractions of 1 mL were collected; fractions 2–4 were pooled and desalted on a PD-10 desalting column pre-equilibrated with desalting buffer (20 mM Tris pH 7.4, 100 mM NaCl, 10% glycerol, 6 mM β -mercaptoethanol and 0.03% $C_{12}E_8$), from which 3.5 mL was collected. Desalted protein was concentrated to 250 μ L by vacuum Vivaspin 30 K spin concentrator and loaded onto a Superdex 200 10/300 GL column pre-equilibrated with desalting buffer, and eluted with the same buffer using the ÄKTA FPLC system. Fractions of 500 μ L were collected and analyzed by SDS-PAGE. The total protein concentration of each fraction was determined by Bradford protein assay using bovine serum albumin (BSA) as a standard (Bio-Rad DC Protein assay). Protein samples were analyzed by precasted SDS-PAGE on NuPAGE® 4–12% Bis-Tris Gels under reducing conditions with 20 mM DTT. The gel was stained with SimplyBlue™ SafeStain (Invitrogen). Immunoblotting analysis was performed using anti-His6 antibody 1:5000. To verify the identity of the recombinant protein the purified fraction was analyzed by SDS-PAGE, the band of interest excises and analyzed by mass spectrometry.

2.5.2 - hLAT1 purification

In order to purify 6His-LAT1 protein the pellet was used. After washing by 0.1 M Tris/HCl pH 8.0, the pellet was dissolved in 100 mM DTE, 0.8% sarkosyl, 3.5 M urea, 10% glycerol,

200 mM NaCl and buffered at pH 8.0 with 10 mM Tris/HCl. After centrifugation (12,000g, 10 min, 4°C) the supernatant was recovered and applied on a His select Ni²⁺ affinity gel column (0.5 X 2.5 cm) equilibrated with 8 mL buffer (0.1% sarkosyl, 10% glycerol, 200 mM NaCl, 10 mM Tris/HCl pH 8.0). 5 mL washing buffer (0.1% Triton X-100/200 mM NaCl/10% glycerol/5 mM DTE/10 mM Tris/HCl pH 8.4), 3 mL washing buffer plus 10 mM imidazole, 3 mL washing buffer plus 50 mM imidazole were used for eluting proteins in 12 fractions (1 mL). Purified hLAT1 was present in the tenth fraction.

2.5.3 - GST-hCD98 Purification

To purify the GST-hCD98 protein, the soluble fraction (supernatant) (1.5 mL), obtained after lysate centrifugation (12,000g, 4°C, 30 min), was mixed with 500 µL of glutathione Sepharose 4B preconditioned with PBS buffer at pH 7.4 and kept for 30 min in a Stuart agitator. After 120 min the resin was washed three times with the buffer PBS pH 7.4 and, then added with 1.5 mL of 10 mM GSH/20 mM TrisHCl pH 8.2. After 2 min the suspension was subjected to short spin centrifugation and the supernatant was collected (1.5 mL of purified GST-hCD98). The purified GST-hCD98 was concentrated in Amicon centrifugal filters to a volume of 200 µL and incubated 12 h at 25°C, 500 rpm with 1.5 unit of thrombin and, then, loaded on G-200 chromatography column (0.7 cm diameter, 15 cm height) preconditioned with PBS pH 7.4 and eluted with the same buffer.

Purified hCD98 was collected in fraction three (80 µg protein in 500 µL) and GST in fractions 6-7 (1 mL).

CHAPTER 3

RESULTS

The wild type gene coding for hASCT2 was isolated from total RNA of primary human fibroblasts by reverse transcription. Initially, the 1623 bp cDNA was cloned in many *E. coli* expression vectors. Thus, plasmids with and without fusion tags were employed, such as pMWT7, pH6EX3, pET-21a(+), etc. and different *E. coli* strains were used. Although, a lot of different conditions were screened for hASCT2 protein production, we didn't get any appreciable expression.

For this reason, the 1623 bp cDNA encoding for hASCT2 and the optimized gene for *P. pastoris* were cloned into pPICZ B vector (**Fig. 12**):

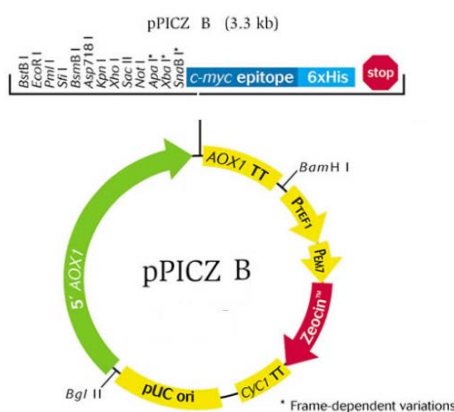


Fig. 12: Schematic representation of pPICZ B vector used for *P. pastoris* expression.

Into the cDNA optimized by Genescript several codons were changed according to the codon usage of *Pichia pastoris*, as shown below. The CAI (Codon adaptation index), a measurement of codon bias, was upgraded from 0.52 to 0.82.

Optimized	GCCGACCCTCCTAGAGACAGTAAGGGACTTGCTGCCGCCGAACCTACCGCTAATGGTGGGA
Original	GCCGATCCTCCTCGAGACTCCAAGGGGCTCGCAGCGGCGGAGCCCACCGCCAACGGGGGC
Optimized	TTGGCTTTGGCTTCTATCGAAGATCAGGGTGCTGCCGCAGGTGGATACGTGGATCCAGA
Original	CTGGCGCTGGCCTCCATCGAGGACCAAGGCGCGGCAGCAGGCGGCTACTGCGGTTCCCGG
Optimized	GATCAAGTCAGAAGATGCTTGAGAGCTAAC TTGCTTGTTTGTCTTACTGTTGTCGCCGTT
Original	GACCAGGTGCGCCGCTGCCTTCGAGCCAACTGCTTGTGCTGCTGACAGTGGTGGCCGTG
Optimized	GTGCGAGGTGTTGCTCTTGGTTTGGGAGTCTCCGGTGCAGGTGGAGCACTTGCAATTGGGA
Original	GTGGCCGCGTGGCGCTGGGACTGGGGGTGTCGGGGGCCGGGGTGCCTGGCGTTGGGC

Optimized	CTGAAAGATTGTCAGCATTTGTTTCCAGGAGAGTTGCTTTTGAGACTTTTGAGAATG
Original	CCGGAGCGCTTGAGCGCCTTCGTCTTCCCGGGCGAGCTGCTGCTGCGTCTGCTGCGGATG
Optimized	ATTATCCTTCCTTTGGTTGTCTGTAGTTTGATTGGTGGAGCTGCCTCTTTGGACCAGGT
Original	ATCATCTTGCCGCTGGTGGTGTGCAGCTTGATCGGCGGCGCCGACCTGGACCCCGGC
Optimized	GCTTTGGGAAGACTTGGTGTCTGGGCCCTTTGTTTTTCTTGGTCACTACACTTTTGCCA
Original	GCGCTCGGCCGTCTGGGCGCCTGGGCGCTGCTCTTTTTCTGGTCAACACGCTGCTGGCG
Optimized	TCCGCTTTGGGTGTTGGACTTGCCTGGCACTTCAACCTGGTGCAGCTTCA GCCGCAATT
Original	TCGGCGCTCGGAGTGGGCTTGGCGCTGGTCTGTCAGCCGGGCGCCGCTCCGCCGCATC
Optimized	AACGCTAGTGTGGAGCTGCCGGTTCTGCCGAAATGCACCTTCCAAGGAGTTTTTGAT
Original	AACGCTCCGTGGGAGCCGCGGCAGTGCCGAAATGCCCCAGCAAGGAGGTGCTCGAT
Optimized	TCATTTTTGGACCTTGCTAGAAACATTTCCATCTAATTTGGTTTCCGCAGCTTTTAGA
Original	TCGTTCTTGATCTTGCAGAAATATCTTCCCTTCCAACCTGGTGTGTCAGCAGCCTTTCGC
Optimized	TCATACAGTACCCTTATGAAGAGAGAAACATCACAGGTACCAGAGTTAAGTCCAGTT
Original	TCATACTTACCACCTATGAAGAGAGAAATATCACCGAACAGGGTGAAGGTGCCCGT
Optimized	GGACAGGAAGTTGAGGGTATGAATATTTGGGACTTGTGTCTTTGCCATCGTCTTCGGA
Original	GGGCAGGAGGTGGAGGGGATGAACATCTGGGCTTGGTAGTGTTTGCCATCGTCTTTGGT
Optimized	GTTGCATTGAGAAAACCTGGACCTGAA GGAGAGCTTTTGATCAGATTTTCAACTCCTTT
Original	GTGGCGCTGCGGAAGCTGGGCGCTGAAGGGGAGCTGCTTATCCGCTTCTCAACTCCTTC
Optimized	AATGAAGCTACAATGGTCTTGGTTTCA TGGATTATGTGGTACGCTCCAGTTGGTATCATG
Original	AATGAGGCCACCATGGTCTTGGTCTCTGGATCATGTGGTACGCCCTGTGGGCATCATG
Optimized	TTTTTGGTTCGCCGAAAGATTGTTGAAATGGAGGATGTCGGTCTTTGTTTCGCTAGATTG
Original	TTCTTGGTGGCTGGCAAGATCGTGGAGATGGAGGATGTGGGTTACTCTTTGCCCGCCTT
Optimized	GGAAAATATATCCTTTGTGCTTTTGGGTCATGCCATTACGGACTTTTGGTTTTGCCT
Original	GGCAAGTACATTTCTGTGCTGCTGCTGGGTCACGCCATCCATGGGCTCCTGGTACTGCC
Optimized	CTTATCTACTTTTTGTTCACTAGAAAGAACCTTATAGATTTTTGTGGGGTATTGTTACC
Original	CTCATCTACTTCTCTTCAACCGCAAAAACCCCTACCGCTTCTGTGGGGCATCGTGACC
Optimized	CCATTGGCTACTGCC TTCGGAACATCTTCTCAAGTGCTACATTGCCTCTTATGATGAAG
Original	CCGCTGGCCACTGCCTTTGGGACCTCTTCCAGTTCCGCCACGCTGCCGCTGATGATGAAG
Optimized	TGTGTTGAA GAGAACAATGGTGTGCA AAGCATATCTCCAGATTCA TTTTGCCAATCGGT
Original	TGCGTGGAGGAGAATAATGGCGTGGCCAAGCACATCAGCCGTTTCATCTGCCCATCGGC
Optimized	GCTACTGTTAATATG GATGGAGCCGCATTGTTTCAA TGCCTGCTGCCGTTTTCATTGCT
Original	GCCACCGTCAACATGGACGGTGC CGCGCTCTTCCAGTGCCTGGCCGAGTTCATTGCA
Optimized	CAGTTGTCACAACAGAGTTTGGACTTCGTTAAGATCATCACAACTTTGGTCACTGCAACA
Original	CAGCTCAGCCAGCAGTCTTGGACTTCGTAAAGATCATCACCATCTGGTCAACGGCCACA
Optimized	GCTTCTTCCGTTGGA GCA GCTGGTATCCCTGCTGGTGGAGTTTGGACCCTTGCAATTATC
Original	GCGTCCAGCGTGGGGGACGCGGCATCCCTGCTGGAGGTGTCCTCACTCTGGCCATCATC
Optimized	TTGGAAGCTGTCAACTTGCCAGTTGATCATATTAGTTTGATCCTTGCTGTCGATTGGTTG
Original	CTCGAAGCAGTCAACCTCCCGGTGACCATATCTCCTTGATCCTGGCTGTGGACTGGCTA
Optimized	GTTGACAGATCTTGTACCGTCTTGAACGTTGAAGGAGATGCTTTGGGTGCCGGA CTTTTG
Original	GTCGACCGGTCTGTACCGTCTCAATGTAGAAGGTGACGCTCTGGGGGACGACTCCTC
Optimized	CAAAATTACGTTGACAGAACCGAATCCAGATCCACTGAACTGAGTTGATTGAGTTAAG
Original	CAAAATTACGTGGACCGTACGGAGTGCAGAAGCACAGAGCCTGAGTTGATACAAGTGAAG

Optimized	TCTGAGTTGCCACTTGACCCATTGCCCTGTCCA ACTGAAGAGGGTAATCCTCTTTTGAAA
Original	AGTGAGCTGCCCCCTGGATCCGCTGCCAGTCCCCACTGAGGAAGGAAACCCCTCCTCAA
Optimized	CACTATAGAGGACCAGCTGGAGACGCAACTGTCGCCTCTGAAAAAGAA TCCGTTATGCAC
Original	CACTATCGGGGGCCCGCAGGGGATGCCACGGTTCGCCTCTGAGAAGGAATCAGTCATGCAT
Optimized	CACCATCATCACCCTAA
Original	CATCATCATCATCATTGA

Moreover, GC content and unfavorable peaks have been optimized to prolong the half-life of the mRNA as shown in **Fig. 13**.

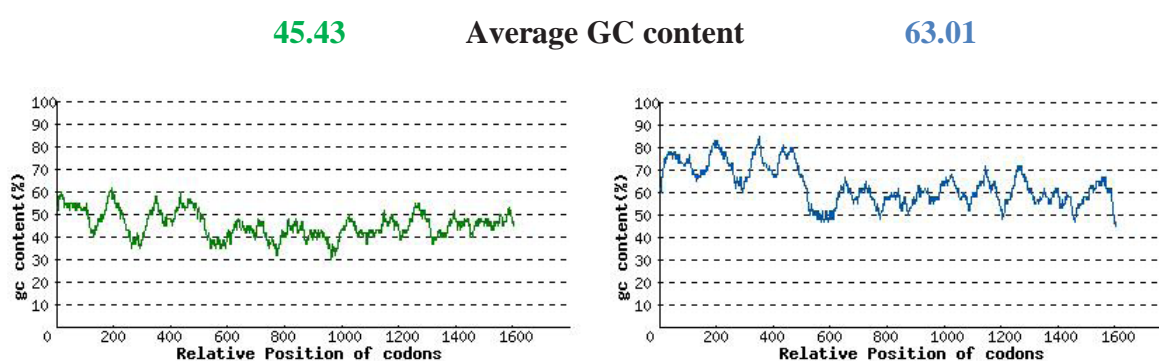


Fig. 13: The ideal percentage range of GC content in the cDNA is between 30-70 %. Peaks of %GC content in a 60 bp window have been removed.

To identify high producing *P. pastoris* clones, a high zeocin screen was performed followed by a small scale production test in 25 mL cultures to verify proper membrane localization of recombinant hASCT2. From these tests, the positive clones for the following large scale production were obtained. To achieve higher production levels of wild type (wt)hASCT2 and optimized (Opt)hASCT2 (obtained by the cDNA optimized for *P. pastoris*, coding the same hASCT2 protein as the wt cDNA), the growth was scaled up in a 3 L fermentor to supply the high oxygen demand of *P. pastoris*. Cultivating X-33/(wt)hASCT2 and X-33/(Opt)hASCT2 under tightly controlled regimes resulted in a total cell mass of 350 g wet weight. Under this culture condition, high yields of an over-produced protein with an apparent molecular mass of

about 50 kDa were observed both in the X-33/(wt)hASCT2 and X-33/(Opt)hASCT2 (**Fig. 14A**).

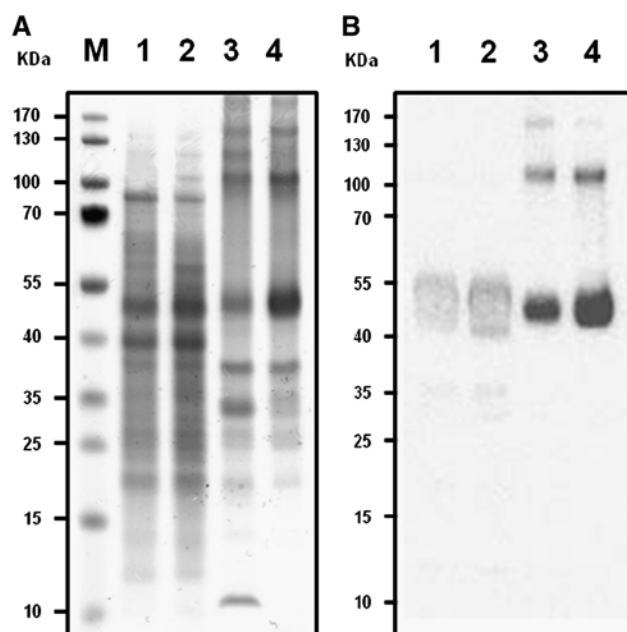


Fig. 14: Production of (wt)hASCT2 and (Opt)hASCT2 using fermentor growth. (A) SDS-PAGE (4–12%) gel electrophoresis analysis of the hASCT2 production stained as described in Materials and methods. M: protein markers; lanes 1–2, crude extract from *P. pastoris* cells producing (wt)hASCT2 (lane 1) or (Opt)hASCT2 (lane 2) in the fermentor; lanes 3–4: membrane fraction from *P. pastoris* cells producing (wt)hASCT2 (lane 3) or (Opt)hASCT2 (lane 4) in the fermentor. In each lane 10 μ g total protein was loaded. (B) Immunoblot using an anti-His antibody showing hASCT2 production of the same protein fractions as in (A). In lanes 1 and 2, 50 μ g total protein was loaded, in lanes 3 and 4, 1 μ g total protein was loaded.

The protein was identified as the hASCT2 in crude extract and membrane fractions by immunoblotting using an anti-His antibody (**Fig. 14B**). The yield of (Opt)hASCT2 was more than two-fold as compared to the (wt) hASCT2. Thus, in all the experiments hASCT2 from X-33/(Opt)hASCT2 was used. One or two higher molecular mass bands were detected by the immunostaining, corresponding to double and triple apparent molecular masses of the hASCT2 monomer (**Fig. 14B**). Before purification, a solubilization trial was carried out on the membrane fraction to find a suitable detergent. Nine different detergents (Cholate, LDAO,

Brij35, DDM, CHAPS, Fos-choline-12, C₁₂E₈, Triton X-100) were tested (**Fig. 15**). DDM, LDAO, Fos-choline-12 and C₁₂E₈ showed the best efficiency in solubilizing hASCT2, although only C₁₂E₈ revealed to be suitable for protein reconstitution in liposomes.

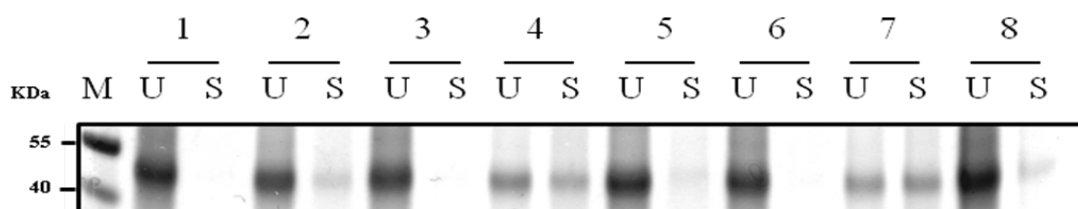


Fig. 15: Solubilization trials for hASCT2. Total membrane fraction was solubilized and analyzed by SDS-PAGE (U: unsoluble fraction; S: soluble fraction). Detergents tested were: (1) Cholate 5%, (2) LDAO 0.5%, (3) Brij35 2%, (4) Fos-choline-12 1%, (5) DDM 1.5%, (6) CHAPS 2%, (7) C₁₂E₈ 1%, (8) Triton X-100 2%.

For large scale purification, urea washed membranes extracted from the X33/(Opt)hASCT2 were solubilized with 1% C₁₂E₈. The solubilized protein (**Fig. 16A lane 1**) was incubated with the Ni-NTA agarose resin.

After washing, virtually all the unbound proteins were removed and most of the protein was found in fractions 2–4 after elution (1 ml each) in 300 mM imidazole (**Fig. 16A lanes 3–5**). The addition of the same elution buffer containing 500 mM imidazole led to a further recovery of small amounts of hASCT2 as observed in fractions 5–6 (**Fig. 16A, lanes 6–7**). The purified fractions contained a 50 kDa protein besides the two higher molecular mass bands corresponding to dimeric and trimeric forms of the protein which were verified by the immunoblot (**Fig. 16B**).

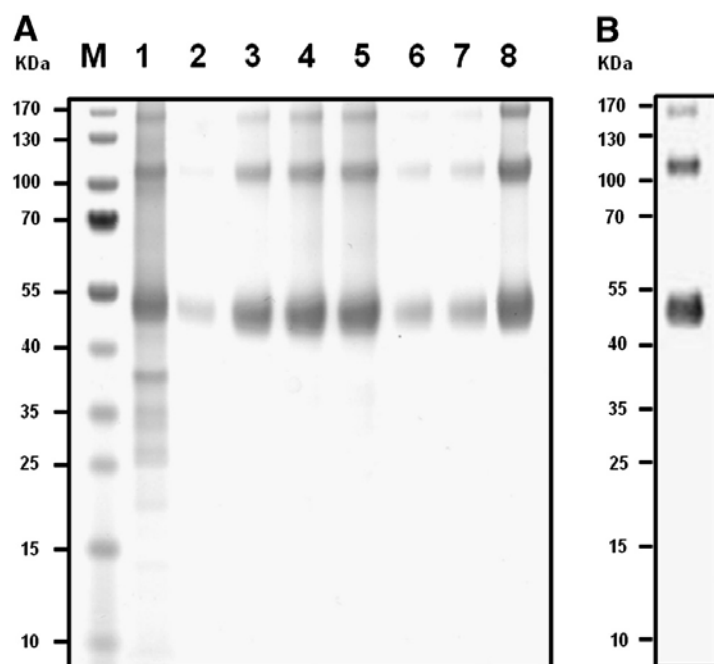


Fig. 16: Purification of (Opt)hASCT2. (A) SDS-PAGE (4–12%) gel electrophoresis analysis of the (Opt)hASCT2 purification stained as described in Materials and methods. M: protein markers; lane 1: membrane fraction from *P. pastoris* cells producing (Opt)hASCT2 in the fermentor (10 μ g) solubilized with 1% $C_{12}E_8$; lanes 2–5: fractions 1–4 from Ni-NTA affinity chromatography eluted with 300 mM imidazole elution buffer; lanes 6–7: fractions 5–6 from Ni-NTA affinity chromatography eluted with 500 mM imidazole elution buffer; lane 8: pooled purified fractions 2–4 after desalting on PD10 column. (B) Immunoblot of purified protein on lane 8 using an anti-His antibody.

To confirm the correspondence of the purified bands with the hASCT2 protein, mass spectrometry analysis was also performed. Only peptides containing the hASCT2 sequence (**Table 4**) were recognized after trypsin treatment of the 50 kDa and the other higher molecular mass bands present in the purified fraction.

Peptide mass (Da)	Sequence position	Peptide sequence
801.39	1-7	mVADPPR ^{1,2,3}
984.51	2-10	VADPPRDSK ^{1,2,3}
1062.49	363-372	CVEENNGVAK ¹
1096.64	248-257	LGPEGELLIR ^{1,2}
1102.54	526-537	GPAGDATVASEK ^{1,2,3}
1131.55	1-10	mVADPPRDSK ^{1,2,3}
1133.52	363-372	cVEENNGVAK ^{1,2,3}
1135.49	203-211	SYSTTYEER ^{1,2,3}
1143.62	493-502	STEPELIQVK ^{1,2,3}
1277.67	179-189	EVLDSFLDLAR ¹

1: peptides of monomer

2: peptides of dimer

3: peptides of trimer

m: oxidation

c: propionamide

Table 4: Mass values and amino acid sequences obtained by mass spectrometry analysis of the tryptic peptides of recombinant hASCT2.

These higher molecular mass bands of hASCT2 are probably formed by monomers tightly interacting or covalently cross-linked and could not be dissolved by SDS. Protein fractions with apparent monomeric molecular mass on SDS-PAGE could be isolated from the higher molecular mass products by size exclusion chromatography using a Superdex 200 column (**Fig. 17**).

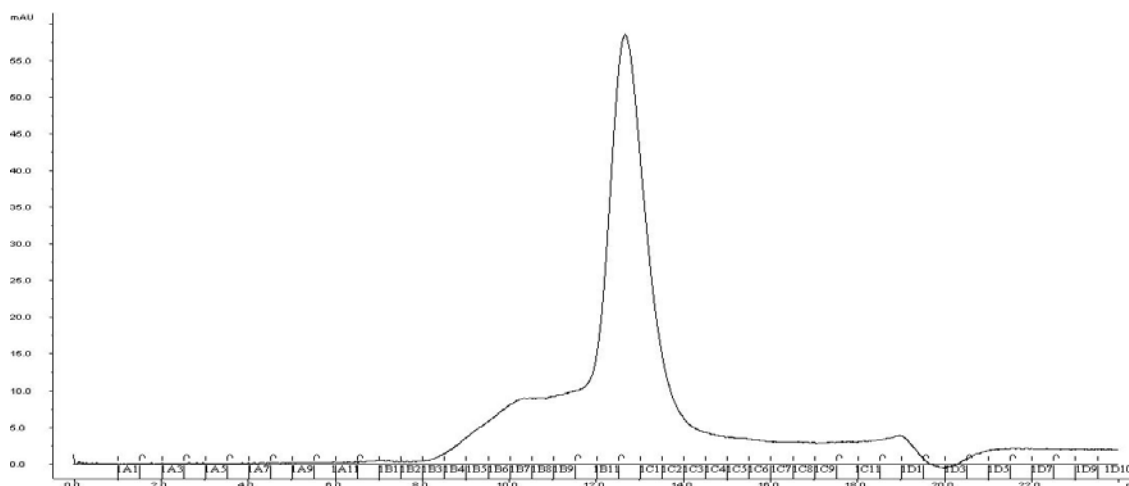


Fig. 17: FPLC analysis of purified (Opt)hASCT2. The purified protein by affinity chromatography was applied to a Superdex 200 size exclusion column. (Opt)hASCT2 was eluted as one peak, which likely represent the trimeric form.

However, most of the oligomeric forms of hASCT2 were eluted in the fractions corresponding to the void volume (**Fig. 18 lanes 1–3**) of the column or to very high molecular masses (**lanes 4–7**), indicating that these protein forms were mostly super-aggregated. While, most of the protein with apparent molecular mass of 50 kDa on SDS-PAGE (**Fig. 18 lanes 8–11**) eluted in the fractions corresponding to about 150 kDa, as also shown in **Fig. 17**, indicating that the non-aggregated protein was most likely in a trimeric form before SDS treatment. The final protein yield after the purification procedure was estimated to be 10 mg per liter of cell culture.

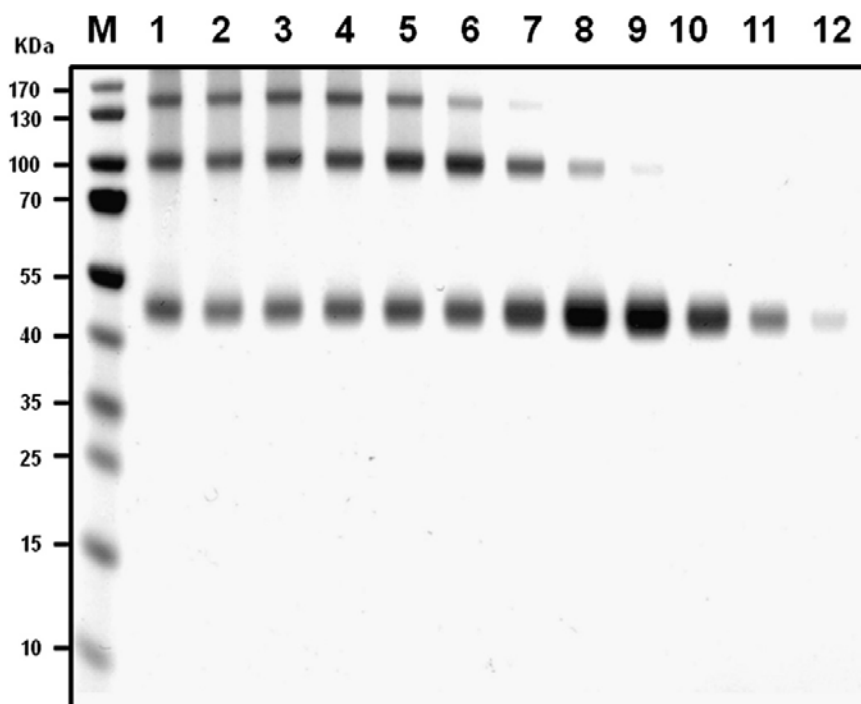


Fig. 18: SDS-PAGE analysis of (Opt)hASCT2 size exclusion chromatography. A total of 250 μ L of desalted purified hASCT2 was loaded onto a Superdex 200 size exclusion column and eluted with 20 mM Tris pH 7.4, 100 mM NaCl, 10% glycerol, 6 mM β -mercaptoethanol and 0.03% $C_{12}E_8$. Fractions of 0.5 mL were collected and analyzed by SDS-PAGE (4–12%). M: protein markers; lanes 1–12 protein fractions from 8 mL to 14 mL volume column. Fractions 8–11 correspond to a molecular mass of about 150 kDa according to standard calibration of the column manufacturer.

The 1,521 bp hLAT1 cDNA was amplified from HEK 293 cells using primers constructed on hLAT1 cDNA ends (NM_003486 of GenBank). The cDNA apparent size was about 1,500 bp estimated on agarose gel. The amplified cDNA did not contain mutations with respect to the hLAT1 coding sequence (GeneBank, not shown). Different vectors were employed to express hLAT1. To improve the solubility of the hydrophobic hLAT1 protein, the cDNA was firstly cloned in the vector pET41-a(+) (**Fig. 19**) containing a N-terminal GST-tag.

However, the protein was collected only in the insoluble fractions of cell lysate. Thus, plasmids without GST or other tags were also employed to test the expression of hLAT1, such as pET-28a(+), pMWT7, pH6EX3 (**Fig. 21**) and pET-21a(+). All the constructs were used to transfect *E. coli* Rosetta(DE3)pLysS cells. Only in the case of pH6EX3-hLAT1 a significant amount of over-expressed protein was revealed in cell lysate insoluble fractions.

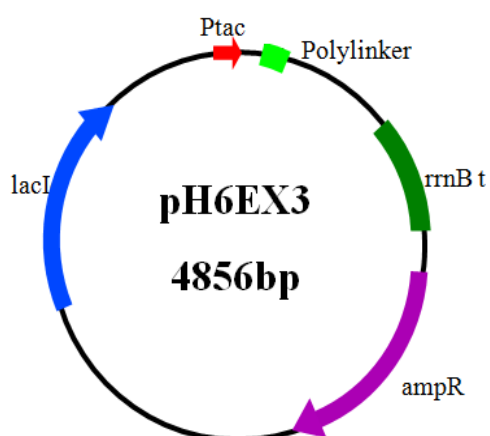


Fig. 21: Map of pH6EX3 vector used for protein production in *E. coli*.

On the basis of previous experience with membrane transporter expression the growth temperature was kept at 28°C. **Figure 22** shows the protein patterns of cell lysates at increasing time after induction with IPTG.

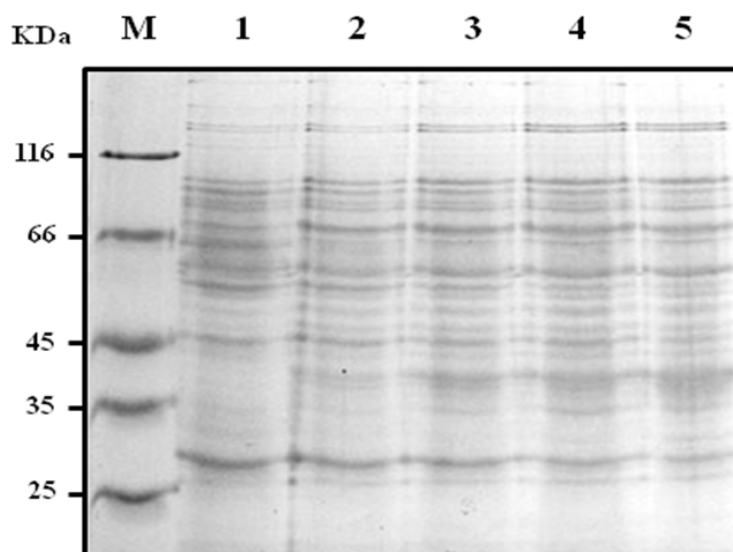


Fig. 22: Recombinant 6His-hLAT1 expression. Proteins were separated by SDS-PAGE and stained using coomassie staining. Lane M: molecular mass standards; lane 1, uninduced cell lysate (80 μ g), lanes 2–5: pellets of the insoluble fraction of cell lysate (80 μ g), after 1, 2, 4 and 8 h of IPTG-induction, respectively.

A protein (**Fig. 22 lanes 2–5**), with apparent molecular mass of about 40 kDa was present after induction by 0.4 mM IPTG, which was absent in the non induced cell lysate (**Fig. 22 lane 1**). This protein band was accompanied by a second protein with slightly lower (39 kDa) apparent molecular mass. The amount of the 40 kDa protein increased with the time with optimal conditions at 8 h after 0.4 mM IPTG induction (**Fig. 22 lane 5**). The effect of changing the growth temperature was investigated. After 8 h of induction, the amount of over-expressed protein at 37°C (**Fig. 23 lane 3**) was comparable to that obtained at 28°C (**Fig. 23 lane 6**). On the contrary, even after overnight growth, at 20°C the expression of hLAT1 protein (**Fig. 23 lane 8**) was much lower than at 28°C. The hLAT1 obtained using the pH6EX3 vector contained an N-terminus 6His-tag which was useful to purify the protein under denaturing condition on Ni²⁺-chelating affinity resin.

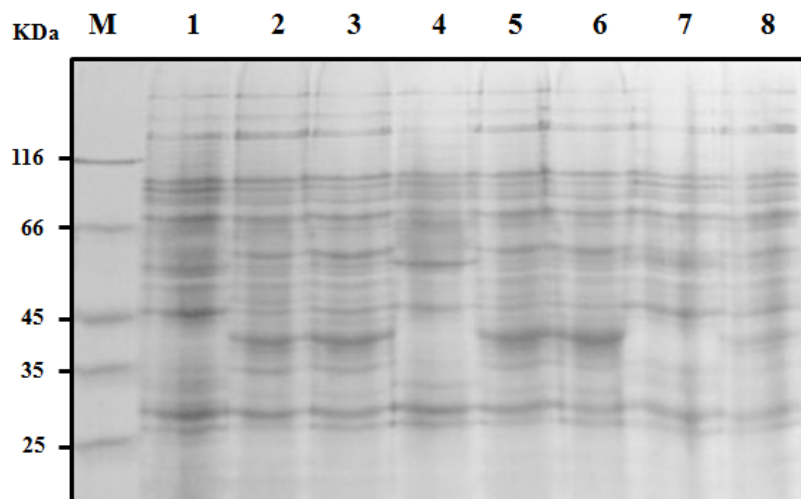


Fig. 23: Effect of temperature on the expression of recombinant pH6EX3-hLAT1 in *E. coli* Rosetta(DE3)pLysS. Proteins were separated by SDS-PAGE and stained using coomassie staining. Lane M: molecular mass standards; lane 1, uninduced cell lysate (80 μ g) cultured at 37°C, lanes 2, 3: pellets of the insoluble fraction of cell lysate (80 μ g), cultured at 37°C after 4 and 8 h of IPTG-induction, respectively; lane 4, uninduced cell lysate (80 μ g) cultured at 28°C, lanes 5, 6 pellets of the insoluble fraction of cell lysate (80 μ g), cultured at 28°C after 4 and 8 h of IPTG-induction, respectively; lane 7, uninduced cell lysate (80 μ g) cultured at 20°C, lane 8, pellet of induced cell lysate (80 μ g), cultured over night at 20°C.

Deoxycholate, and the non ionic Triton X-100, C₁₂E₈ or n-dodecyl-b-D-maltoside at concentrations up to 5% were not suitable for solubilising hLAT1. Only sodium dodecylsulphate and sarkosyl were effective in solubilising the expressed protein. Therefore, hLAT1 was solubilized in sarkosyl, which is a milder ionic detergent than sodium dodecylsulphate. A concentration of 0.8% was enough to solubilize the expressed protein. Sarkosyl was used to solubilize the protein pellet (**Fig. 22 lane 5**) together with 3.5 M urea and 5 mM DTE. A Ni²⁺-chelating column was then used for purification of recombinant hLAT1. After loading the solubilized protein on the column, most of the contaminating proteins were eluted by the washing buffer.

The 6His-hLAT1 was specifically eluted in the presence of imidazole (50 mM); the corresponding eluted fraction contained a purified protein which was separated on SDS-

PAGE (**Fig. 24A, lane 2**). The protein was enriched of about 30 folds compared to the total protein content in the bacterial lysate. The recombinant hLAT1 was identified by an anti-His antibody: an immunostained band was detected both in the bacterial lysate obtained after IPTG induction as well as in the purified protein fraction (**Fig. 24B lanes 1, 2**). The purification procedure led to a yield of hLAT1 protein of about 3.5 mg/L of cultured cells or 3.5 mg purified protein per 4 g cells (wet weight).

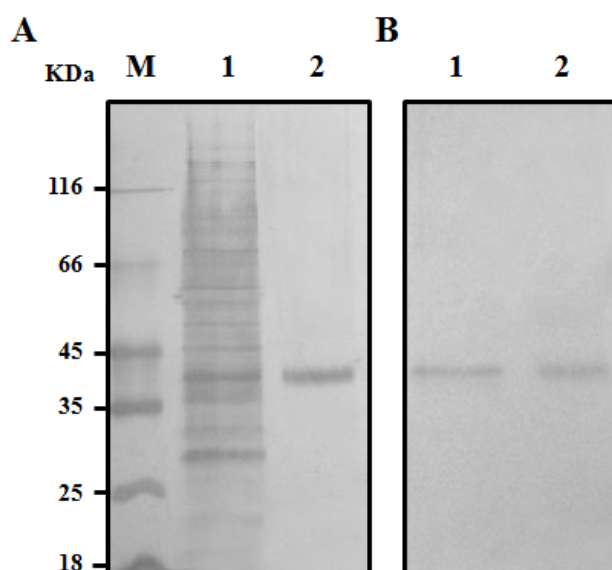


Fig. 24: hLAT1 purification. Proteins were separated by SDS-PAGE and stained using coomassie staining. Lane M molecular mass standards. Lane 1 pellet of the insoluble fraction of cell lysate (80 μ g), cultured at 28°C after 8 h of IPTG-induction, lane 2 purified hLAT1 protein (2.5 μ g). (B) Immunodecorated proteins recognized by anti-His antiserum (1:1,000) after Western blotting on PVDF membrane. 3,3'-diaminobenzidine staining of the same protein fractions of lanes 1 and 2 of (A).

The 1,521 bp hCD98 cDNA was amplified from Image plasmid using primers constructed on the basis of the hCD98 cDNA (BC001061.2, GenBank). The cDNA showed a 1,500 bp apparent size on agarose gel. No mutations were present in the cDNA with respect to the hCD98 sequence (GeneBank). The pH6EX3 vector was firstly used for hCD98. However, a low amount of soluble protein was obtained with this plasmid in Rosetta(DE3)pLysS and

other *E. coli* strains. Thus, to increase the efficiency of expression the use of a tag was adopted. The hCD98 cDNA was cloned in pGEX-4T1 carrying an N-terminal GST-tag. *E. coli* Rosetta (DE3)pLysS cells were transfected with this construct and the dependence of the expression pattern on the IPTG concentration and time of induction were tested at 28°C. As shown in **Fig. 25** an abundant protein band was detected in the soluble fractions of cell lysates under different conditions (**lanes 2–10**) and without detergent, indicating that the construct was soluble in agreement with the predominance of hydrophilic amino acids with respect to LAT1; this band was not present in non induced cells (**lane 1**). The highest amount of the construct was obtained 4 h after induction with 0.4 mM IPTG (**lane 6**). The molecular mass of the protein, 116 kDa, was not far from the sum of the theoretical molecular masses of hCD98 plus GST, i.e. 94.6 kDa.

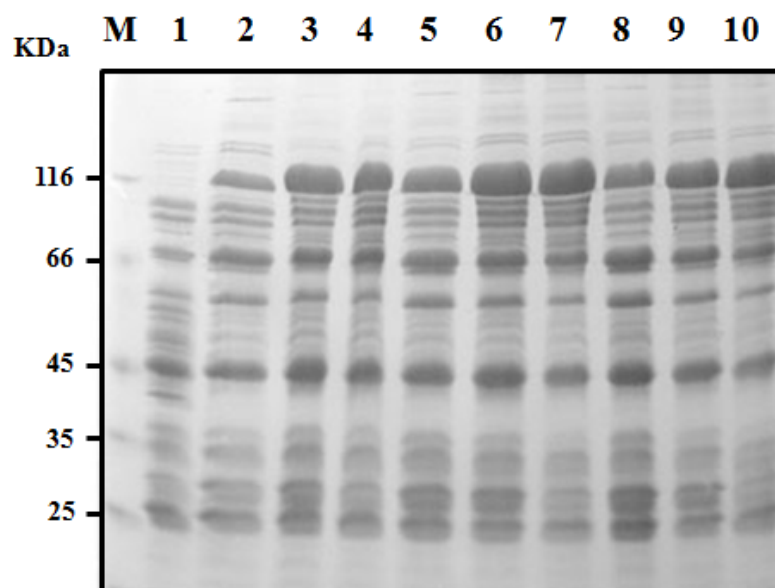


Fig. 25: Expression of recombinant pGEX-4T1-hCD98 in *E. coli* Rosetta(DE3)pLysS. Proteins were separated by SDS-PAGE and stained using coomassie staining. Lane M molecular mass standards; lane 1 uninduced cell lysate (80 µg), lanes 2–4 soluble fraction of cell lysate (90 µg), after 2 h of 0.1, 0.4, 1 mM IPTG induction, respectively; lanes 5–7 soluble fraction of cell lysate (110 µg), after 4 h of 0.1, 0.4, 1 mM IPTG induction, respectively; lanes 8–10 soluble fraction of cell lysate (110 µg), after 6 h of 0.1, 0.4, 1 mM IPTG induction, respectively.

The construct GST-hCD98 carried a thrombin cleavage site between the two proteins. To find optimal conditions for separating the hCD98 from the GST tag, the dependence of the thrombin cleavage on the time of incubation was studied in the soluble fraction of cell lysate. After 12 h incubation virtually all the protein construct had been cleaved with appearance of two protein bands with apparent molecular masses of 62 and 27 kDa, close to the molecular mass of hCD98 and GST, respectively. The entire protein construct was subjected to purification on a GST-Sepharose resin prior to thrombin treatment according to the optimal conditions found. After 12 h of thrombin treatment the construct was completely hydrolyzed in the two fragments, i.e., the GST and the hCD98 (**Fig. 26 lane 2**). After the cleavage the two proteins were separated by Sephadex G-200 chromatography and the hCD98 was obtained in a 99% pure form (**Fig. 26 lane 3**). The apparent molecular mass of hCD98, 62 kDa fitted with the theoretical mass of the protein, 68 kDa. The yield of the purification was about 2 mg/L of cell culture.

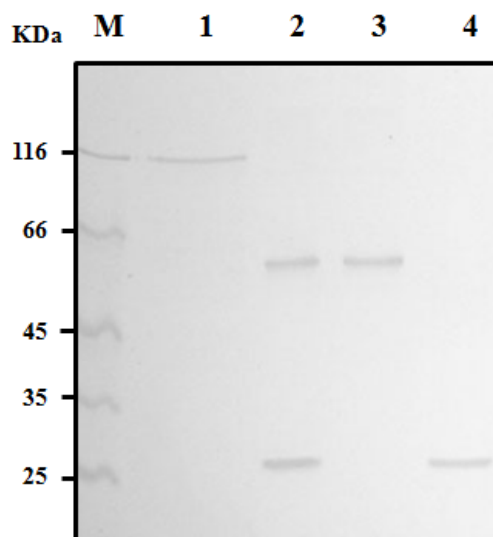


Fig. 26: CD98 purification. Proteins were separated by SDS-PAGE and stained using coomassie staining. Lane M molecular mass markers; lane 1 purified GST-hCD98 (10 μ g); lane 2 protein of lane 1 after 12 h of thrombin treatment; lane 3 purified hCD98 after G-200 gel filtration chromatography (2.5 μ g); lane 4 purified GST after G-200 gel filtration chromatography (2 μ g).

CHAPTER 4

CONCLUSION

One of the major challenges concerning the study of mammalian and especially human transporters is to obtain sufficient amount of purified proteins for both structural and functional characterization. Moreover, the availability of suitable methods for transport assay is essential to characterize recombinant proteins obtained by heterologous production. Only in recent years, the number of successful over-production trials of mammalian and human transporters has slightly increased. Over-production has been achieved using *Escherichia coli* as host, both as entire organism (2,49) or in cell free systems (50). However, while we described the first case of high level expression of the human amino acid transporter LAT1 in *E. coli*, in several cases it was not possible to obtain significant levels of human proteins in bacteria, thus suggesting another host for production. This was the case for hASCT2 which was toxic to several bacterial strains screened for expression trials. Using the yeast *P. pastoris* we succeeded in obtaining high levels of recombinant hASCT2, similar to the recently expressed hLAT2 transporter (26). hLAT2 and hASCT2 represent the only mammalian amino acid transporters produced in yeast, so far.

An important step for increasing the yield of recombinant hASCT2 protein was the optimization of the codons to the yeast translation machinery. Noteworthy, the over-produced hASCT2 was associated to the yeast membrane fraction indicating proper folding of recombinant hASCT2. The preferred detergent for solubilization, C₁₂E₈, was proven by the functional characterization and correlated well with previous studies conducted on the rat(r)ASCT2 solubilized in its active form from rat kidney membranes (51). Moreover, the purified hASCT2 was eluted from Superdex 200 chromatography as a 150 kDa oligomeric form suggesting that the protein tends to form trimers. This observation is in agreement with the data obtained on the GlTPh transporter of *P. horikoshii* (52) and to the homology structural model of rASCT2 (53).

Thus, the main novelty of this work consists, besides in obtaining over-expressed hASCT2 and hLAT1, also in the successful use of yeast and bacterial systems for production of two human plasma membrane amino acids transporters.

Indeed, this system revealed suitable for the expression of hLAT1, which was not expressed in appreciable amount by *P. pastoris*. Several plasmids and *E. coli* strains have been tested to achieve appreciable expression of the protein. The over-expressed cell lysate contained an abundant protein band accompanied by a faint band with a slightly lower apparent molecular mass; these proteins were not present in the cell lysate obtained in absence of IPTG induction. The slightly higher electrophoretic mobility of the lower band was probably due to a more compact form of the protein induced by partial oxidation and formation of disulphides among some of the 12 Cys in hLAT1 amino acidic sequence.

The concentration of the lower band decreased, respect to the main band, with increasing the time of induction and was virtually absent in the purified fraction.

Probably the presence of DTE in the purification buffer prevented the formation of the oxidized form of the protein. While hLAT1 was obtained in high yield in pH6EX3 plasmid, in the case of hCD98 a GST tag at the N-terminus of the protein had to be introduced for expression the hCD98 at appreciable level.

After thrombin treatment, GST and hCD98 were efficiently separated by size exclusion chromatography with a high yield of purified protein.

Further important advances of this methodology is the availability of hLAT1 purified protein, highly hydrophobic, in a soluble state in non-ionic detergent. This protein, indeed, was not solubilized from the cell lysate using non-ionic detergents while it became soluble after the Ni²⁺-affinity chromatography procedure. This was due to a slow process of on-column substitution of the ionic detergent with the non ionic Triton X-100. The electrophoretic

mobility of the protein was higher than expected, i.e., the apparent molecular mass was lower than the theoretical mass, 55,010 Da, as calculated using Compute pI/ Mw tool available at http://web.expasy.org/compute_pi/.

This discrepancy was observed for several transport proteins (2,54,55) and is due to the higher degree of hydrophobicity of the membrane proteins respect to the molecular mass markers.

The availability of the hASCT2 and hLAT1 proteins in a soluble state is of great importance for functional and kinetic characterization using proteoliposome reconstitution and further structural analysis, since proteins in this form can be treated by chromatography and concentrative steps previous to crystallization.

In fact, only X-ray diffraction analysis of hASCT2 and hLAT1 crystals could definitively give information on the three dimensional structure of the transporters. The high level of production of the functional protein in a homogeneous purified fraction allows crystallographic screening for this purpose. The homology structure and, when available, the high-resolution structure will in addition be used in docking strategies for fast analysis of transporter-inhibitor interactions, which could be validated in proteoliposomes.

The importance of the study of hASCT2 and hLAT1 resides in the finding that the expression of these transporters is increased in several human cancers (56).

Then, hASCT2 and hLAT1 represent potential targets for cancer therapy (see Introduction). For example, ASCT2 over-expression has been linked to the tumor suppressor pRb/E2F pathway (57).

In this context, the reconstituted hASCT2 and hLAT1 will be very helpful for testing drugs and xenobiotics of relevance for human health. This could allow the identification of possible specific inhibitors of transport activity, in order to elicit apoptosis in cancer cells. The

availability of recombinant proteins also allows site-directed mutagenesis on the human proteins.

Applying such methods will shed further light in the involvement of hASCT2 in pathophysiology as well as in defining molecular mechanisms of transport and structural details such as the actual oligomeric form of the protein.

Therefore, the results described in this work constitutes the basis for in vitro screening of molecules, including drugs and biologically active compounds, which specifically interact with the transporter inhibiting its function. This has a great impact in human health offering important perspectives in cancer therapy, as previously postulated on the basis of studies performed with intact cells (58).

REFERENCES

1. Alberts B., Bray D., Lewis J., et al., *Molecular Biology of the Cell*, Third edition.
2. Indiveri C., Galluccio M., Scalise M., Pochini L., *Strategies of Bacterial Over Expression of Membrane Transporters Relevant in Human Health: The Successful Case of the Three Members of OCTN Subfamily*, *Mol Biotechnol* 54:724–736 (2013).
3. Milton H. Saier, JR., *A Functional-Phylogenetic Classification System for Transmembrane Solute Transporters*, *Microbiology and molecular biology reviews*, 354–411, (2000).
4. Nelson D.L., Cox M.M., *Lehninger Principles of Biochemistry*, Fourth Edition.
5. Bröer S., *Amino Acid Transport Across Mammalian Intestinal and Renal Epithelia*, *Physiol Rev* 88: 249–286, (2008).
6. Palacin M., Estevez R., Bertran J., Zorzano A., *Molecular biology of mammalian plasma membrane amino acid transporters*, *Physiol. Rev.* 78 969–1054, (1998).
7. Christensen, H.N., *Role of amino acid transport and counter-transport in nutrition and metabolism*. *Physiol. Rev.* 70: 43–77, (1990).
8. Bobe B.P., *Recent Molecular Advances in Mammalian Glutamine Transport*, *The Journal of Nutrition*, 2475S-2485S, (2001).
9. Fuchs B.C., Bobe B.P., *Amino acid transporters ASCT2 and LAT1 in cancer: partners in crime?* *Semin. Cancer Biol.* 15 254–266, (2005).
10. Christensen H.N., Liang M., Archer E.G., *A distinct Na⁺-requiring transport system for alanine, serine, cysteine, and similar amino acids*. *J. Biol. Chem.* 242: 5237–5246 (1967).

11. Doyle F.A., McGivan J.D., The bovine renal epithelial cell line NBL-1 expresses a broad specificity Na⁺-dependent neutral amino acid transport system (System B0) similar to that in bovine renal brush border membrane vesicles. *Biochim. Biophys. Acta* 1104: 55–62, (1992).
12. Souba W.W., Pan M., Stevens B.R., Kinetics of the sodium dependent glutamine transporter in human intestinal cell confluent monolayers. *Biochem. Biophys. Res. Commun.* 188: 746–753, (1992).
13. Stevens B.R., Ross H.J., Wright E.M., Multiple transport pathways for neutral amino acids in rabbit jejunal brush border vesicles. *J. Membr. Biol.* 66: 213–225, (1982).
14. Nakanishi T., Tamai I., Solute Carrier Transporters as Targets for Drug Delivery and Pharmacological Intervention for Chemotherapy, *Journal of Pharmaceutical Sciences*, Vol. 100, No. 9, (2011).
15. Kilberg M.S., Handlogten M.E., Christensen H.N., Characteristics of an amino acid transport system in rat liver for glutamine, asparagine, histidine, and closely related analogs. *J. Biol. Chem.* 255: 4011–4019, (1980).
16. Schlessinger A., Yee S.W., Sali A., Giacomini K.M., SLC Classification: An Update, *Clinical pharmacology & Therapeutics*, Volume 94 Number 1, (2013).
17. Fredriksson R., Nordström K.J.V., Stephansson O., Hägglund M.G.A., Schiöth H.B., The solute carrier (SLC) complement of the human genome: Phylogenetic classification reveals four major families, *FEBS Letters* 582 3811–3816, (2008).
18. Kanai Y., Cléménçon B., Simonin A., Leuenberger M., Lochner M., Weisstanner M., Hediger M.A. The SLC1 high-affinity glutamate and neutral amino acid transporter family, *Molecular Aspects of Medicine* 34 108–120, (2013).

19. Kekuda R., Prasad P.D., Fei Y.J., Torres-Zamorano V., Sinha S., Yang-Feng T.L., Leibach F.H., Ganapathy V., Cloning of the Sodium-dependent, Broad-scope, Neutral Amino Acid Transporter Bo from a Human Placental Choriocarcinoma Cell Line, *The Journal of Biological Chemistry* Vol. 271, No. 31, 18657–18661, (1996).
20. Kanai Y., Hediger M.A., The glutamate/neutral amino acid transporter family SLC1: molecular, physiological and pharmacological aspects *Eur J Physiol* 447: 469-479, (2004).
21. Kekuda R., Torres-Zamorano V., Fei Y. J., Prasad P.D., Li H.W., Mader L.D., Leibach F.H., Ganapathy V., Molecular and functional characterization of intestinal Na⁺-dependent neutral amino acid transporter B0, *Am. J. Physiol.* 272: G1463–G1472 (1997).
22. Closs E.I., Boissel J.P., Habermeier A., Rotmann A., Structure and function of cationic amino acid transporters (CATs). *J. Membr. Biol.* 213 (2), 67–77, (2006).
23. Gasol E., Jimenez-Vidal M., Chillaron J., Zorzano A., Palacin M., Membrane topology of system xc⁻ light subunit reveals a re-entrant loop with substrate-restricted accessibility. *J. Biol. Chem.* 279 (30), 31228–31236, (2004).
24. Fotiadis D., Kanai Y., Palacín M., The SLC3 and SLC7 families of amino acid transporters, *Molecular Aspects of Medicine* 34 139–158, (2013).
25. Fort J., de la Ballina L.R., Burghardt H.E., Ferrer-Costa C., Turnay J., Ferrer-Orta C., Uson I., Zorzano A., Fernandez-Recio J., Orozco M., Lizarbe M.A., Fita I., Palacin M., The structure of human 4F2hc ectodomain provides a model for homodimerization and electrostatic interaction with plasma membrane. *J. Biol. Chem.* 282 (43), 31444–31452, (2007).

26. Costa M., Rosell A., Álvarez-Marimon E., Zorzano A., Fotiadis D., Palacín M., Expression of human heteromeric amino acid transporters in the yeast *Pichia pastoris*, *Protein Expression and Purification* 87 35–40, (2013).
27. Kanai Y., Segawa H., Miyamoto K., Uchino H., Takeda E., Endou H., Expression cloning and characterization of a transporter for large neutral amino acids activated by the heavy chain of 4F2 antigen (CD98). *J. Biol. Chem.* 273 (37), 23629–23632, (1998).
28. Mastroberardino L., Spindler B., Pfeiffer R., Skelly P.J., Loffing J., Shoemaker C.B., Verrey F., Amino-acid transport by heterodimers of 4F2hc/CD98 and members of a permease family. *Nature* 395 (6699), 288–291, (1998).
29. Su T.Z., Feng M.R., Weber M.L., Mediation of highly concentrative uptake of pregabalin by L-type amino acid transport in chinese hamster ovary and caco-2 cells. *J. Pharmacol. Exp. Ther.* 313, 1406–1415, (2005).
30. del Amo E.M., Urtti A., Yliperttula M., Pharmacokinetic role of L-type amino acid transporters LAT1 and LAT2, *European Journal of Pharmaceutical Sciences* 35 161–174, (2008).
31. Kageyama T., Nakamura M., Matsuo A., Yamasaki Y., Takakura Y., Hashida M., Kanai Y., Naito M., Tsuruo T., Minato N., Shimohama S., The 4F2hc/LAT1 complex transports L-DOPA across the blood-brain barrier. *Brain Res.* 879 (1–2), 115–121, (2000).
32. Tomi M., Mori M., Tachikawa M., Katayama K., Terasaki T., Hosoya K., L-type amino acid transporter 1-mediated L-leucine transport at the inner blood-retinal barrier. *Invest. Ophthalmol. Vis. Sci.* 46 (7), 2522–2530, (2005).

33. Boado R.J., Li J.Y., Wise P., Pardridge W.M., Human LAT1 single nucleotide polymorphism N230K does not alter phenylalanine transport. *Mol. Genet. Metab.* 83, 306–311, (2004).
34. Cantor J.M., Ginsberg M.H., CD98 at the crossroads of adaptive immunity and cancer, *Journal of Cell Science* 125, 1373–1382, (2012).
35. Christensen HN. Role of amino acid transport and countertransport in nutrition and metabolism. *Physiol Rev*;70:43–77, (1990).
36. Fingar DC, Blenis J. Target of rapamycin (TOR): an integrator of nutrient and growth factor signals and coordinator of cell growth and cell cycle progression. *Oncogene*;23:3151–71, (2004).
37. Hedfalk K., Codon optimisation for heterologous gene expression in yeast, *Methods Mol Biol.*, 866:47-55, (2012).
38. Mus-Veteau I., Heterologous expression and purification systems for structural proteomics of mammalian membrane proteins. *Comp Funct Genom*; 3: 511–517, (2002).
39. Tate C.G., Haase J., Baker C., Boorsma M., Magnani F., Vallis Y., Williams D.C., Comparison of seven different heterologous protein expression systems for the production of the serotonin transporter, *Biochim Biophys Acta*;1610(1):141-53, (2002).
40. Midgett C.R., Madden D.R., Breaking the bottleneck: Eukaryotic membrane protein expression for high-resolution structural studies, *Journal of Structural Biology* 160 265–274,(2007).
41. Baneyx F., Recombinant protein expression in *Escherichia coli*, *Current Opinion in Biotechnology*, 10:411-421, (1999).

42. Cereghino J.L., Cregg J.M., Heterologous protein expression in the methylotrophic yeast *Pichia pastoris*. FEMS Microbiol Rev 24: 45–66, (2000).
43. Sørensen H.P., Towards universal systems for recombinant gene expression, Microbial Cell Factories 2010, 9:27, (2010).
44. Sørensen H.P., Mortensen K.K., Advanced genetic strategies for recombinant protein expression in *Escherichia coli*. Journal of Biotechnology 115, 113–128, (2005).
45. EasySelect *Pichia* Expression Kit, For Expression of Recombinant Proteins Using pPICZ and pPICZ α in *Pichia pastoris*, Manual part no. 25-0172, Invitrogen, (2010).
46. Gustafsson C., Govindarajan S. and Minshull J., Codon bias and heterologous protein expression. Trends in Biotechnology Vol.22 No.7, (2004).
47. Gouy M., Gautier C., Codon usage in bacteria: correlation with gene expressivity. Nucleic Acids Res. 10, 7055–7074 (1982).
48. Andersson G.E., Kurland C.G., An extreme codon preference strategy: codon reassignment. Mol. Biol. Evol. 8, 530–544 (1991).
49. Quick M., Wright E.M., Employing *Escherichia coli* to functionally express, purify, and characterize a human transporter, Proc. Natl. Acad. Sci. U. S. A. 99 8597–8601 (2002).
50. Keller T., Schwarz D., Bernhard F., Dotsch V., Hunte C., Gorboulev V., Koepsell H., Cell free expression and functional reconstitution of eukaryotic drug transporters, Biochemistry 47 4552–4564 (2008).
51. Oppedisano F., Pochini L., Galluccio M., Cavarelli M., Indiveri C., Reconstitution into liposomes of the glutamine/amino acid transporter from renal cell plasma membrane: functional characterization, kinetics and activation by nucleotides, Biochim. Biophys. Acta 1667 122–131 (2004).

-
52. Forrest L.R., Kramer R., Ziegler C., The structural basis of secondary active transport mechanisms, *Biochim. Biophys. Acta* 1807 167–188 (2011).
53. Oppedisano F., Galluccio M., Indiveri C., Inactivation by Hg²⁺ and methylmercury of the glutamine/amino acid transporter (ASCT2) reconstituted in liposomes: prediction of the involvement of a CXXC motif by homology modelling, *Biochem. Pharmacol.* 80 1266–1273 (2010).
54. Galluccio M., Pochini L., Amelio L., Accardi R., Tommasino M., Indiveri C., Over-expression in *E. coli* and purification of the human OCTN1 transport protein, *Protein Exp Purif* 68:215–220 (2009).
55. Palacin M., Nunes V., Font-Llitjos M., Jimenez-Vidal M., Fort J., Gasol E., Pineda M., Feliubadalo L., Chillaron J., Zorzano A., The genetics of heteromeric amino acid transporters, *Physiology (Bethesda)*, 20:112–124 (2005).
56. Ganapathy V., Thangaraju M., Prasad P.D., Nutrient transporters in cancer: relevance to Warburg hypothesis and beyond, *Pharmacol Ther* 121:29–40 (2009).
57. Reynolds M.R., Lane A.N., Robertson B., Kemp S., Liu Y., Hill B.G., Dean D.C., Clem B.F., Control of glutamine metabolism by the tumor suppressor Rb, *Oncogene*, (2013).
58. Fan X., Ross D.D., Arakawa H., Ganapathy V., Tamai I., Nakanishi T., Impact of system L amino acid transporter 1 (LAT1) on proliferation of human ovarian cancer cells: a possible target for combination therapy with anti-proliferative aminopeptidase inhibitors, *Biochem Pharmacol* 80:811–818 (2010).

ACKNOWLEDGEMENTS

"La presente tesi è cofinanziata con il sostegno della Commissione Europea, Fondo Sociale Europeo e della Regione Calabria. L'autore è il solo responsabile di questa tesi e la Commissione Europea e la Regione Calabria declinano ogni responsabilità sull'uso che potrà essere fatto delle informazioni in essa contenute".

PUBLICATIONS



Large scale production of the active human ASCT2 (SLC1A5) transporter in *Pichia pastoris* – functional and kinetic asymmetry revealed in proteoliposomes[☆]



Piero Pingitore^{a,b}, Lorena Pochini^a, Mariafrancesca Scalise^a, Michele Galluccio^a,
Kristina Hedfalk^b, Cesare Indiveri^{a,*}

^a Department BEST (Biologia, Ecologia, Scienze della Terra) Unit of Biochemistry and Molecular Biotechnology, University of Calabria, Via P. Bucci 4c, 87036 Arcavacata di Rende, Italy

^b Department of Chemistry and Molecular Biology, University of Gothenburg, PO Box 462, SE-405 30 Göteborg, Sweden

ARTICLE INFO

Article history:

Received 13 April 2013

Received in revised form 28 May 2013

Accepted 31 May 2013

Available online 10 June 2013

Keywords:

Transport

Over-expression

Purification

Liposomes

ABSTRACT

The human glutamine/neutral amino acid transporter ASCT2 (hASCT2) was over-expressed in *Pichia pastoris* and purified by Ni²⁺-chelating and gel filtration chromatography. The purified protein was reconstituted in liposomes by detergent removal with a batch-wise procedure. Time dependent [³H]glutamine/glutamine antiport was measured in proteoliposomes which was active only in the presence of external Na⁺. Internal Na⁺ slightly stimulated the antiport. Optimal activity was found at pH 7.0. A substantial inhibition of the transport was observed by Cys, Thr, Ser, Ala, Asn and Met (≥ 70%) and by mercurials and methanethiosulfonates (≥ 80%). Heterologous antiport of [³H]glutamine with other neutral amino acids was also studied. The transporter showed asymmetric specificity for amino acids: Ala, Cys, Val, Met were only inwardly transported, while Gln, Ser, Asn, and Thr were transported bi-directionally. From kinetic analysis of [³H]glutamine/glutamine antiport Km values of 0.097 and 1.8 mM were measured on the external and internal sides of proteoliposomes, respectively. The Km for Na⁺ on the external side was 32 mM. The homology structural model of the hASCT2 protein was built using the GltPh of *Pyrococcus horikoshii* as template. Cys395 was the only Cys residue externally exposed, thus being the potential target of SH reagents inhibition and, hence, potentially involved in the transport mechanism.

© 2013 The Authors. Published by Elsevier B.V. All rights reserved.

1. Introduction

Amino acid transport systems play the pivotal role of maintaining the amino acid homeostasis in mammalian cells. Among many transporters involved in this function there is a group which shares specificity for glutamine, thus playing the role of mediating glutamine trafficking in different tissues and intestinal and renal (re)absorption [1–3]. A lot of functional data have been obtained by studying the

transporters in cell systems such as cancer cell lines or *Xenopus laevis* oocytes. Thus the glutamine-specific transporters have been firstly classified on the functional basis. More recently the various transporters have been assigned to different protein families (SLC) on the basis of gene and primary structure analysis. Taking into account both types of classifications, the glutamine-specific transporters can be divided in sodium-dependent systems: system ASC/ATB0 (SLC1), system B^{0,+} (SLC6), system y + L (SLC7), system N and A (SLC38) and sodium-independent systems: system L (SLC7) and system b^{0,+} (SLC6). Some transporters can be further distinguished in tolerant (N and y + L) or not tolerant (ASCT2) for the substitution of Na⁺ by Li⁺ or sensitivity towards inhibitors such as MeAIB (system A) or BCH (System L, LAT1) [1–3]. However, several functional properties of the amino acid transporters remain unknown or controversial, due to some limitations of the cell experimental models given by the contemporary presence of similar transport systems and/or enzymes which could affect the transport assays and by the difficult access to the internal side. Most of these problems can be overcome using simpler models for studying transport, such as the proteoliposome experimental system which revealed suitable for studying functional and kinetic properties of transporters [4,5]. Concerning the structure of mammalian amino acid transporters no crystallographic data is available so far. High resolution structures have only been achieved for some

Abbreviations: MeAIB, a-(methylamino)isobutyric acid; BCH, 2-aminobicyclo-(2,2,1)-heptane-2-carboxylic acid; C₁₂E₈, octaethylene glycol monododecyl ether; YPDS, Yeast Extract Peptone Dextrose Sorbitol; BMGY, Buffered Glycerol-complex Medium; DDM, n-dodecyl-beta-D-maltoside; LDAO, n-dodecyl-N,N-dimethylamine-N-oxide; CHAPS, 3-((3-cholamidopropyl)dimethylammonium)-1-propanesulfonate; p-OHMB, p-hydroxymercuribenzoate; MTSET, 2-(trimethylammonium)ethyl methanethiosulfonate, Bromide; MTSEA, 2-aminoethyl methanethiosulfonate hydrobromide; NEM, N-ethylmaleimide; PEM, N-phenylmaleimide; PLP, pyridoxal-5-phosphate; DEPC, diethyl pyrocarbonate

[☆] This is an open-access article distributed under the terms of the Creative Commons Attribution-NonCommercial-No Derivative Works License, which permits non-commercial use, distribution, and reproduction in any medium, provided the original author and source are credited.

* Corresponding author. Tel.: +39 0984 492939; fax: +39 0984 492911.

E-mail addresses: piero.pingitore@alice.it (P. Pingitore), lorena.pochini@unical.it (L. Pochini), mariafrancesca.scalise@unical.it (M. Scalise), michele.galluccio@unical.it (M. Galluccio), kristina.hedfalk@chem.gu.se (K. Hedfalk), cesare.indiveri@unical.it (C. Indiveri).

bacterial homologues of amino acid transporters [6,7]. On the basis of these structures, homology models have been obtained for mammalian amino acid transporters, some of which have been in part validated by chemical targeting [8–10]. Very interestingly the expression of some of the transporters responsible for glutamine trafficking is up-regulated in tumors [2]. Cancer cells, in fact, require high amounts of glutamine for energy and growth purposes [2,11]. In this scenario it becomes clear that the study of glutamine transporters is a hot research topic and strategies for over-expressing the transporters in large scale and studying their structure/function relationships are very welcome. Among the most interesting transporters in human physiology and pathology there is the Na⁺-dependent glutamine/neutral amino acid transporter ASCT2 (SLC1A5) previously known in humans as ATB0. This transport system has been identified in human cell systems even though the kinetic properties and substrate specificity are not fully understood [2,3,12] while the rodent isoform, besides being studied in cell systems [13–16], has been also functionally and kinetically characterized in proteoliposomes [9,17,18]. Basic functional and kinetic parameters of the kidney rat protein determined in both experimental models correlated well. Novel functional properties such as the ATP regulation, the internal side Km, the reaction mechanism, and the pH dependence of glutamate transport were revealed using proteoliposomes [17,18]. Due to its over-expression in cancer cells, ASCT2 has been proposed as a potential target for antitumor drugs [2]. Very recently, a molecular screening of ditiiazoles, potent inhibitors of the rat ASCT2, has been carried out in proteoliposomes [19]. These results highlighted the importance of obtaining the recombinant human ASCT2 for performing structural, functional and inhibition studies. In this work, the high level production of the human ASCT2 in *Pichia pastoris* is described. The function of the transporter extracted from yeast membranes has been assayed in proteoliposomes where the protein has been inserted in a right-side-out orientation (see Discussion) with respect to the cell membrane, thus constituting a suitable tool for unequivocal functional characterization and interaction studies with potential drugs.

2. Materials and methods

2.1. Materials

The *P. pastoris* wild type strain (X-33), the pPICZB vector, NuPAGE® 4–12% Bis-Tris Gels were purchased from Invitrogen; restriction endonucleases and other cloning reagents from Fermentas; PD-10 columns, Superdex 200 10/300 GL, ÄKTA FPLC system, ECL plus, Hybond ECL membranes and L-[³H]glutamine from GE Healthcare; Ni-NTA agarose and polypropylene columns from QIAGEN, anti His₆ antibody from Clontech; the anti mouse IgG HRP conjugate from Promega; C₁₂E₈ from Anatrace; Amberlite XAD-4, egg yolk phospholipids (3-sn-phosphatidylcholine from egg yolk), Sephadex G-75, L- glutamine and all the other reagents were from Sigma-Aldrich.

2.2. Cloning of hASCT2

The wild type gene was isolated from total RNA of primary human fibroblasts by reverse transcription. Initially, the 1623 bp cDNA encoding hASCT2 (GenBank NM_005628.2, SLC1A5) was amplified using the forward primer *NdeI*-hASCT2: 5'-G GAA TTC CAT ATG GTG GCC GAT CCT CCT CG-3' and the reverse primer *HindIII*-hASCT2: 5'-CCC AAG CTT TTA CAT GAC TGA TTC CTT CTC-3', respectively. The amplified cDNA sequence was verified by sequencing using the ABI 310 automated sequencer Applied Biosystems. For subsequent cloning to *P. pastoris*, the full length cDNA coding for hASCT2 was amplified using the forward primer *EcoRI*-hASCT2: 5'-ATA CCG GAA TTC AAA ATG GTT GCC GAT CCT CCT CGA GAC TCC-3' and the reverse primer *XbaI*-hASCT2: 5'-A TAC TAG TCT AGA TCA ATG ATG ATG ATG ATG CAT GAC TGA TTC CTT CTC AGA GGC-3', coding a C-terminal His₆ tag.

Restriction sites are underlined and the Kozak consensus sequence is shown in bold.

The hASCT2 gene was codon optimized for *P. pastoris* by GenScript and the artificial cDNA included a 5' *EcoRI* restriction site plus the Kozak consensus sequence and a 3' *XbaI* restriction site plus a C-terminal His₆ fusion tag. In the optimized gene, the Codon Adaptation Index (CAI) [20] was upgraded from 0.51 (wild type) to 0.82 (optimized) and the GC content was decreased from 63.01% to 45.43%. For cloning in *P. pastoris* both the wild type gene (wt-hASCT2) and the optimized gene (Opt-hASCT2) were inserted in the *EcoRI/XbaI* sites of the pPICZB expression vector, resulting in two different recombinant constructs, defined as pPICZB-(wt)hASCT2-His₆ and pPICZB-(Opt)hASCT2-His₆. Both constructs were verified by sequencing.

2.3. Recombinant production of hASCT2

To obtain the recombinant hASCT2-His₆ protein, the resulting plasmids were linearized with *PmeI* and the transformation into the *P. pastoris* wild type strain X-33 was performed by electroporation [21]. To select putative multi-copy recombinants a total of 52 transformants for each construct were tested for growth on YPDS plates containing 2000 µg/mL Zeocin and analyzed after 3 days. Small-scale production was performed in triplicates in shake flask cultures as previously described [22]. For large scale protein production, *P. pastoris* strains producing recombinant hASCT2 (X33/pPICZB-(wt)hASCT2-His₆ and X33/pPICZB-(Opt)hASCT2-His₆) were grown at 30 °C in a 3 L fermentor (Infors HT) having an Initial Fermentation Volume (IFV) of 1.5 L basal salt medium [23] containing 6.53 mL PTM1 trace salts [24]. An overnight pre-culture of 75 mL in BMGY having an OD₆₀₀ of about 4 was used to inoculate the fermentor. The initial glycerol volume was consumed after approximately 24 h and the culture was fed with 150 mL 50% glycerol (v/v) for 24 h to increase biomass. To induce production of recombinant hASCT2, the culture was fed with 150 mL methanol for 48 h. To obtain the membrane fraction, *P. pastoris* cells overproducing hASCT2 were resuspended in buffer A (50 mM Tris, pH 7.4, 150 mM NaCl, 6 mM β-mercaptoethanol and 0.5 mM PMSF) at a concentration of about 1 g/mL. Droplets of the cell suspension were frozen in liquid nitrogen and cells were broken by an X-Press (four passages). The suspension was centrifuged at 6000 g for 30 min and the supernatant containing membrane and cytosolic fractions (crude extract) was collected. This supernatant was ultracentrifuged in a Ti45 rotor at 140,000 g for 1 h. The resulting membrane pellet was washed with urea buffer (5 mM Tris pH 7.4, 2 mM EDTA, 2 mM EGTA and 4 M urea) and then again ultracentrifuged as above. The washed membrane fractions (pellet) containing (wt)hASCT2 or (Opt)hASCT2 were resuspended in buffer B (25 mM Tris, pH 7.4, 250 mM NaCl, 6 mM β-mercaptoethanol and 10% glycerol) at a final concentration of about 300 mg/mL and homogenized using a handheld electric homogenizer. Aliquots of 6 mL of the membrane fraction were stored at –80 °C. Various stages from the protein purification procedure were analyzed by SDS-PAGE and immunoblot.

2.4. Solubilization and purification of hASCT2

For large-scale solubilization and purification (Opt)-hASCT2, about 1.5 g of washed membranes (300 mg/mL) was resuspended in buffer B containing 1% C₁₂E₈ (w/w) to a concentration of 150 mg/mL and gently mixed by agitation for 3 h at 4 °C. After solubilization, the solubilized material was centrifuged at 120,000 g for 1 h, imidazole (50 mM) was added to the supernatant which was mixed with 3 mL Ni-nitrilotriacetic acid (NTA) agarose resin equilibrated with the equilibration buffer (20 mM Tris pH 7.4, 300 mM NaCl, 10% glycerol, 6 mM β-mercaptoethanol, 0.03% C₁₂E₈, and 50 mM imidazole) and incubated by gentle agitation for 3 h at 4 °C. The Ni-NTA resin was subsequently packed into a plastic 1 mL column. The resin was washed with 30 mL of the equilibration buffer. Then, 4 mL of the

same buffer containing 300 mM imidazole and 2 mL of the same buffer containing 500 mM imidazole (referred as elution buffers) were added. Fractions of 1 mL were collected; fractions 2–4 were pooled and desalted on a PD-10 desalting column pre-equilibrated with desalting buffer (20 mM Tris pH 7.4, 100 mM NaCl, 10% glycerol, 6 mM β -mercaptoethanol and 0.03% $C_{12}E_8$), from which 3.5 mL was collected. Desalted protein was concentrated to 250 μ L by vacuum Vivaspin 30 K spin concentrator and loaded onto a Superdex 200 10/300 GL column pre-equilibrated with desalting buffer, and eluted with the same buffer using the ÄKTA FPLC system. Fractions of 500 μ L were collected and analyzed by SDS-PAGE. The total protein concentration of each fraction was determined by Bradford protein assay using bovine serum albumin (BSA) as a standard (Bio-Rad DC Protein assay). Protein samples were analyzed by precasted SDS-PAGE on NuPAGE® 4–12% Bis-Tris Gels under reducing conditions with 20 mM DTT. The gel was stained with SimplyBlue™ SafeStain (Invitrogen). Immunoblotting analysis was performed using anti-His₆ antibody 1:5000. To verify the identity of the recombinant protein the purified fraction was analyzed by SDS-PAGE, the band of interest excised and analyzed by mass spectrometry as previously described [25].

2.5. Reconstitution of the hASCT2 into liposomes

The purified hASCT2 was reconstituted by removing the detergent using the batch-wise method. In this procedure, the mixed micelles containing detergent, protein and phospholipids were incubated with 0.5 g Amberlite XAD-4 resin under rotatory stirring (1400 rev/min) at room temperature (25 °C) for 40 min [26]. The composition of the initial mixture used for reconstitution was: 100 μ L of the solubilized protein (5 μ g protein), 120 μ L of 10% $C_{12}E_8$, 100 μ L of 10% egg yolk phospholipids (w/v) in the form of sonicated liposomes prepared as previously described [5], 10 mM L-glutamine, and 20 mM Tris/HCl pH 7.0 (except where differently specified) in a final volume of 700 μ L. All the operations were performed at 4 °C.

2.6. Transport measurements

To remove the external substrate for uptake experiments, 600 μ L of proteoliposomes was passed through a Sephadex G-75 column (0.7 cm diameter \times 15 cm height) pre-equilibrated with 20 mM Tris/HCl pH 7.0 and sucrose at an appropriate concentration to balance the internal osmolarity. Transport (uptake) measurement was started by adding 50 μ M [³H]glutamine and 50 mM Na-gluconate (except where differently specified) to the proteoliposomes. For efflux measurements, proteoliposomes (600 μ L), containing 10 mM glutamine, were preloaded with radioactivity by transporter-mediated exchange equilibration [27] by incubation with 50 μ M [³H]glutamine at high specific radioactivity (2 μ Ci/nmol) and 50 mM Na-gluconate for 120 min at 25 °C. External compounds were removed by another passage of the proteoliposomes through Sephadex G-75 as described above. Transport (efflux) measurement was started by adding non radioactive substrates to the preloaded proteoliposomes. In both uptake and efflux assays, transport was stopped by adding 10 μ M mersalyl at the desired time interval. In control samples, the inhibitor was added at time zero according to the inhibitor stop method [28]. The assay temperature was 25 °C. At the end of the transport assay, each sample of proteoliposomes (100 μ L) was passed through a Sephadex G-75 column (0.6 cm diameter \times 8 cm height) to separate the external from the internal radioactivity. Liposomes were eluted with 1 mL 50 mM NaCl and collected in 4 mL of scintillation mixture, vortexed and counted. For the determination of [³H]glutamine uptake, the experimental values were corrected by subtracting the respective controls (samples inhibited at time zero); the initial rate of transport was measured by stopping the reaction after 10 min, i.e., within the initial linear range of [³H]glutamine uptake into the proteoliposomes. For the determination of [³H]glutamine efflux the experimental values at each time were subtracted from the radioactivity initially present in the proteoliposomes

at time zero. Fitting of experimental data in a first order rate equation to obtain rate constants was performed using the non linear regression analysis Grafit software (version 5.0.13).

To measure the specific activity of hASCT2, the amount of reconstituted recombinant protein was estimated from Coomassie blue stained SDS-PAGE gels by using the Chemidoc imaging system equipped with Quantity One software (Bio-Rad) as previously described [29].

2.7. Homology modeling of hASCT2

The homology structural model of the hASCT2 was built using the glutamate transporter homologue from *Pyrococcus horikoshii* crystal structure (1XFH) as template. The amino acid sequence of the rat ASCT2 (NP_786934) and the glutamate transporter (NP_143181) was aligned manually using ClustalW as described in Ref. [6] and adjusted for hASCT2, belonging to the same family of glutamate and neutral amino acid transporters as rASCT2. The optimized alignment was used to run the program Modeller 9.11 [30].

3. Results

3.1. Over-production and purification of hASCT2

To identify high producing *P. pastoris* clones, a high zeocin screen was performed followed by a small scale production test in 25 mL cultures to verify proper membrane localization of recombinant hASCT2 (data not shown). From these tests, the positive clones for the following large scale production were obtained. To achieve higher production levels of (wt)hASCT2 and (Opt)hASCT2 (obtained by the cDNA optimized for *P. pastoris*, coding the same hASCT2 protein as the wt cDNA), the growth was scaled up in a 3 L fermentor to supply the high oxygen demand of *P. pastoris*. Cultivating X-33/(wt)hASCT2 and X-33/(Opt)hASCT2 under tightly controlled regimes resulted in a total cell mass of 350 g wet weight.

Under this culture condition high yields of an over-produced protein with an apparent molecular mass of about 50 kDa were observed both in the X-33/(wt)hASCT2 and X-33/(Opt)hASCT2 (Fig. 1A). The protein was identified as the hASCT2 in crude extract and membrane fractions by immunoblotting using an anti-His antibody (Fig. 1B). The yield of (Opt)hASCT2 was more than two-fold as compared to the (wt) hASCT2. Thus, in all the experiments hASCT2 from X-33/(Opt)hASCT2 was used. One or two higher molecular mass bands were detected by the immunostaining, corresponding to double and triple apparent molecular mass of the hASCT2 monomer (Fig. 1B).

Before purification, a solubilization trial was carried out on the membrane fraction to find a suitable detergent. Nine different detergents (Cholate, DDM, Brij35, LDAO, β -octylglucoside, CHAPS, Fos-choline-12, Triton X-100, $C_{12}E_8$) were tested. DDM, LDAO, Fos-choline-12 and $C_{12}E_8$ showed the best efficiency in solubilizing hASCT2 (not shown), although only $C_{12}E_8$ revealed to be suitable for protein reconstitution in liposomes (see below). For large scale purification, urea washed membranes extracted from the X33/(Opt)hASCT2 were solubilized with 1% $C_{12}E_8$. The solubilized protein (Fig. 2A lane 1) was incubated with the Ni-NTA agarose resin. After washing, virtually all the unbound proteins were removed and most of the protein was found in fractions 2–4 after elution (1 mL each) in 300 mM imidazole (Fig. 2A lanes 3–5). The addition of the same elution buffer containing 500 mM imidazole led to a further recovery of small amounts of hASCT2 as observed in fractions 5–6 (Fig. 2A, lanes 6–7). The purified fractions contained a 50 kDa protein besides the two higher molecular mass bands corresponding to dimeric and trimeric forms of the protein which were verified by the immunoblot (Fig. 2B). To confirm the correspondence of the purified bands with the hASCT2 protein, mass spectrometry analysis was also performed. Only peptides containing the hASCT2 sequence (Table 1) were recognized after trypsin treatment of

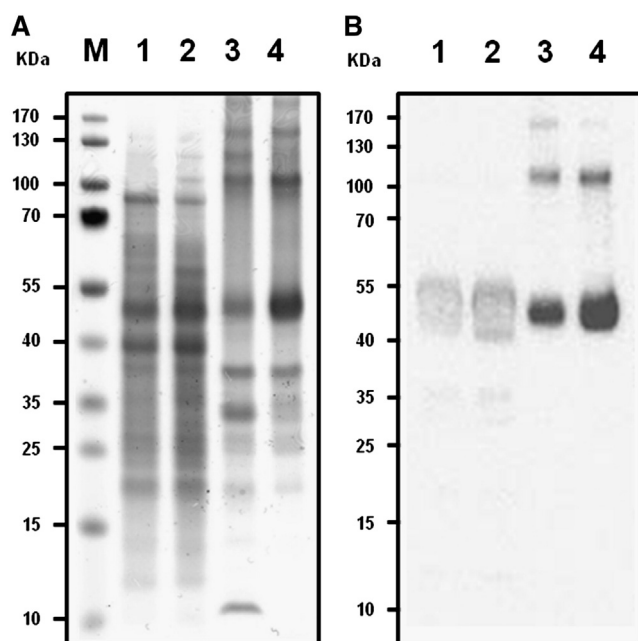


Fig. 1. Production of (wt)hASCT2 and (Opt)hASCT2 using fermentor growth. (A) SDS-PAGE (4–12%) gel electrophoresis analysis of the hASCT2 production stained as described in **Materials and methods**. M: protein markers; lanes 1–2, crude extract from *P. pastoris* cells producing (wt)hASCT2 (lane 1) or (Opt)hASCT2 (lane 2) in the fermentor; lanes 3–4: membrane fraction from *P. pastoris* cells producing (wt)hASCT2 (lane 3) or (Opt)hASCT2 (lane 4) in the fermentor. In each lane 10 μg total protein was loaded. (B) Immunoblot using an anti-His antibody showing hASCT2 production of the same protein fractions as in (A). In lanes 1 and 2, 50 μg total protein was loaded, in lanes 3 and 4, 1 μg total protein was loaded.

the 50 kDa and the other higher molecular mass bands present in the purified fraction (Fig. 2). These higher molecular mass bands of hASCT2 are probably formed by monomers tightly interacting or covalently cross-linked and could not be dissolved by SDS. Protein fractions

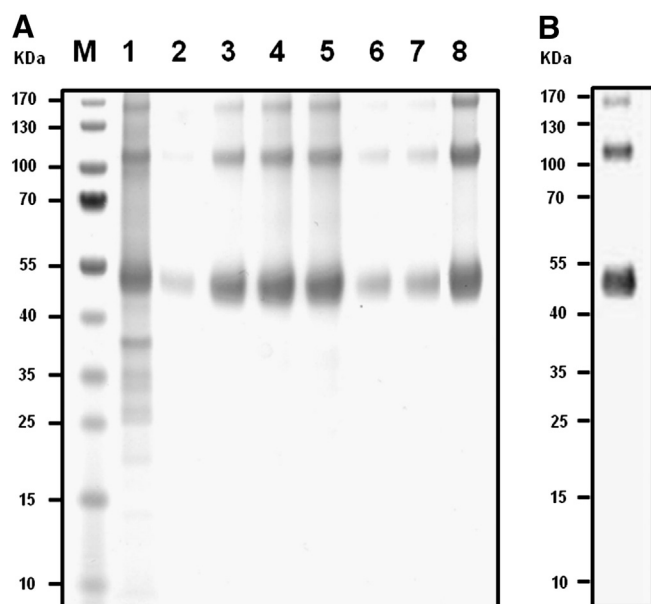


Fig. 2. Purification of (Opt)hASCT2. (A) SDS-PAGE (4–12%) gel electrophoresis analysis of the (Opt)hASCT2 purification stained as described in **Materials and methods**. M: protein markers; lane 1: membrane fraction from *P. pastoris* cells producing (Opt)hASCT2 in the fermentor (10 μg) solubilized with 1% C_{12}E_8 ; lanes 2–5: fractions 1–4 from Ni-NTA affinity chromatography eluted with 300 mM imidazole elution buffer; lanes 6–7: fractions 5–6 from Ni-NTA affinity chromatography eluted with 500 mM imidazole elution buffer; lane 8: pooled purified fractions 2–4 after desalting on PD10 column. (B) Immunoblot of purified protein on lane 8 using an anti-His antibody.

Table 1

Mass values and amino acid sequence obtained by mass spectrometry analysis of the tryptic peptides of recombinant hASCT2.

Peptide mass (Da)	Sequence position	Peptide sequence
984.51	2–10	VADPPRDSK ^{a-c}
1277.67	179–189	EVLDSFLDLAR ^a
1135.49	203–211	SYSTTYEER ^{a-c}
1096.64	248–257	LGPEGELLIR ^{a,b}
1062.49	363–372	CVEENNGVAK ^a
1143.62	493–502	STEPELIQVK ^{a-c}
1102.54	526–537	GPAGDATVASEK ^{a-c}
1133.52	363–372	cVEENNGVAK ^{a-c}
801.39	1–7	mVADPPR ^{a-c}
1131.55	1–10	mVADPPRDSK ^{a-c}

m: oxidation.

c: propionamide.

^a Peptides from monomer.

^b Peptides from dimer.

^c Peptides from trimer.

with apparent monomeric molecular mass on SDS-PAGE could be isolated from the higher molecular mass products by size exclusion chromatography using a Superdex 200 column (Fig. 3). However, most of the oligomeric forms of hASCT2 were eluted in the fractions corresponding to the void volume (lanes 1–3) of the column or to very high molecular masses (lanes 4–7), indicating that these protein forms were mostly super-aggregated. While, most of the protein with apparent molecular mass of 50 kDa on SDS-PAGE (Fig. 3 lanes 8–11) eluted in the fractions corresponding to about 150 kDa, indicating that the non-aggregated protein was most likely in a trimeric form before SDS treatment. The final protein yield after the purification procedure was estimated to be 10 mg per liter of cell culture.

3.2. Optimization of the reconstitution

The reconstitution procedure previously established for the rASCT2 [17] was not effective as it is, for reconstituting the hASCT2. The procedure of detergent removal had to be changed from cyclic column passages to batch-wise procedure to prolong the time of incubation of the reconstitution mixture with the hydrophobic resin. Moreover, some parameters which are known to be critical for the detergent removal reconstitution method had to be modified. The detergent/lipid ratio was increased from 0.95 (w/w), used for the rat protein, to 1.2 (w/w); while the amount of protein in the reconstitution mixture was reduced from 30 to 5 μg .

3.3. Functional characterization

The time dependence of the transport activity was measured as 50 μM [^3H]glutamine uptake in proteoliposomes, under different conditions (Fig. 4A). The uptake of [^3H]glutamine in the presence of external Na^+ into the proteoliposomes containing internal glutamine, increased as function of the time up to 90 min i.e., when the radioactivity equilibrium was reached; if Na^+ was present also inside the proteoliposomes a stimulation of the uptake was observed. On the contrary, no [^3H]glutamine uptake was detected in the absence of external Na^+ even in the presence of internal Na^+ . Moreover, nearly no [^3H]glutamine uptake could be detected into vesicles without internal substrate or with lower internal glutamine concentration (50 μM) even in the presence of internal Na^+ (Fig. 4A). No transport was observed in proteoliposomes reconstituted with boiled protein, demonstrating that glutamine antiport was mediated by the hASCT2 protein. The experimental data fitted a first order rate equation from which a rate constant, k , of 0.039 min^{-1} and a transport rate (the product of k and the transport at equilibrium) of $4.67 \text{ nmol} \cdot \text{min}^{-1} \cdot \text{mg protein}^{-1}$ were calculated in the absence of internal Na^+ ; in its presence a rate constant, k , of 0.0279 min^{-1}

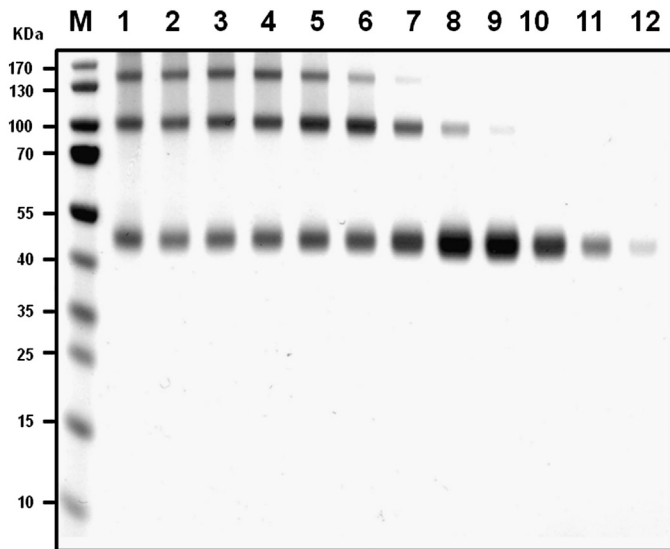


Fig. 3. SDS-PAGE analysis of (Opt)hASCT2 size exclusion chromatography. A total of 250 μL of desalted purified hASCT2 was loaded onto a Superdex 200 size exclusion column and eluted with 20 mM Tris pH 7.4, 100 mM NaCl, 10% glycerol, 6 mM β -mercaptoethanol and 0.03% C_{12}E_8 . Fractions of 0.5 mL were collected and analyzed by SDS-PAGE (4–12%). M: protein markers; lanes 1–12 protein fractions from 8 mL to 14 mL volume column. Fractions 8–11 correspond to a molecular mass of about 150 kDa according to standard calibration of the column manufacturer.

and a transport rate of $5.0 \text{ nmol} \cdot \text{min}^{-1} \cdot \text{mg protein}^{-1}$ were calculated. Fig. 4B shows the effects of different concentrations of intraliposomal Na^+ . The stimulation of transport was maximal at 20 mM (40 mOsm) internal Na^+ and did not increase at higher concentration. No stimulation was observed if Na^+ was substituted by K^+ or by sucrose, indicating that the observed effect was specifically exerted by Na^+ . The dependence of the glutamine antiport on the pH has been studied (Fig. 5). Maximal transport activity was observed at pH 7.0. At more acidic or alkaline pH the activity drastically decreased.

3.4. Amino acid and inhibitor specificity

The effect of externally added amino acids on the glutamine antiport was analyzed (Fig. 6). Cysteine, threonine, serine, alanine, and asparagine, were the most efficient in inhibiting the transport with more than 80% inhibition at amino acid concentration of 1 mM. Inhibition between 70 and 40% was exerted by methionine, valine and leucine. The extent of inhibition decreased to less than 40% for tyrosine and less than 20%, or insignificant, for the other amino acids. The amino acid analog MeAIB and BCH did not inhibit at all the transporter (Fig. 6). The sensitivity to chemical compounds known to interact with specific amino acid residues of proteins was also investigated (Fig. 7). The SH reagents HgCl_2 , mersalyl and pOHMB were the most potent inhibitors, followed by methanethiosulfonates, while maleimides (NEM, PEM) and the NH_2 reagent PLP had lower inhibitory effects. The histidine reagent DEPC did not exert any inhibitory effect on ^3H glutamine uptake. To establish which of the amino acids could be transported by the antiport reaction catalysed by the reconstituted hASCT2, the experiments of Fig. 8 have been performed. ^3H glutamine uptake was measured in proteoliposomes containing different amino acids as counter substrates. Serine, asparagine and threonine efficiently stimulated ^3H glutamine uptake, i.e., were transported by ASCT2 as efflux substrates from the intraliposomal compartment. Surprisingly, alanine and cysteine, even though revealed to be good inhibitors of ^3H glutamine uptake, could not be transported (Fig. 8A), as well as valine, methionine, histidine, glutamate and arginine, tested among the non-inhibiting amino acids; the same results were obtained when 20 mM internal Na^+ was present (not shown). Alternatively, ^3H glutamine efflux from pre-labeled proteoliposomes was measured in the

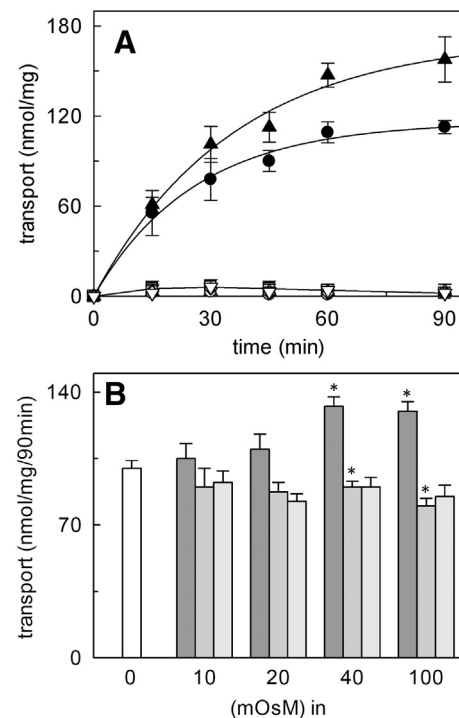


Fig. 4. ^3H glutamine uptake by hASCT2 reconstituted in proteoliposomes: effects of external and internal Na^+ . (A) The reconstitution was performed as described in Materials and methods. Transport was started by adding 50 μM ^3H glutamine at time zero to proteoliposomes reconstituted with hASCT2 (●, □, Δ) or with protein treated for 20 min at 100 °C (○), in the absence (□, ◇) or presence (●, ○, ▲, ◇) of 50 mM external Na-gluconate; 10 mM glutamine (●, ○, □, ▲, ◇), 50 μM glutamine (◇) or no internal substrate (Δ) was present inside the proteoliposomes. In (◇, ◇) 20 mM internal Na-gluconate was present. The transport reaction was stopped at the indicated times, as described in Materials and methods. Results are means \pm S.D. from three experiments. (B) The reconstitution was performed as described in the Materials and methods except that Na^+ -gluconate (dark bars), and K⁺-gluconate (gray bars) were added into proteoliposomes at the concentrations: 5, 10, 20 and 50 mM; light gray bars indicates intraliposomal sucrose at concentrations: 10, 20, 40, 100 mM; white bar, no additions. Transport was started by adding 50 μM ^3H glutamine at time zero to proteoliposomes together with extraliposomal 50 mM Na^+ -Gluconate. The transport reaction was stopped at 90 min, as described in Materials and methods. Results are means \pm S.D. from three experiments. *Significantly different from sample without added inhibitor as estimated by Student's *t* test ($P < 0.05$).

presence of externally added amino acids (Fig. 8B). Serine, asparagine, threonine, alanine and cysteine revealed to strongly stimulate efflux of ^3H glutamine, i.e. could be inwardly transported in antiport with glutamine. Valine and methionine were also inwardly transported

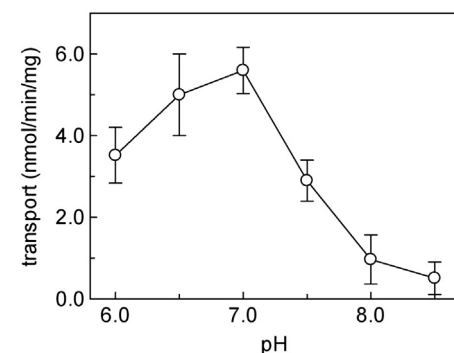


Fig. 5. Effect of pH on hASCT2 transport activity. The reconstitution was performed as described in Materials and methods except that 20 mM Tris/HCl at the indicated pH was used. Transport was started by adding 50 μM ^3H glutamine in 20 mM Tris/HCl at the indicated pH to proteoliposomes containing 10 mM glutamine, in the presence of 50 mM external Na-gluconate. Results are means \pm S.D. from three experiments.

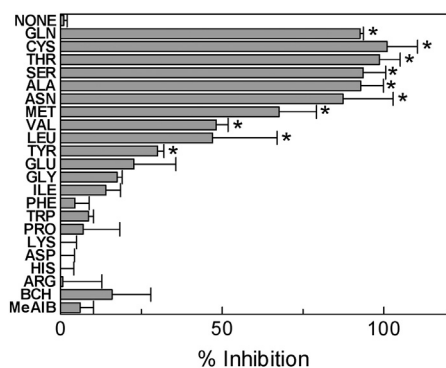


Fig. 6. Effect amino acids and substrate analogs on hASCT2 transport activity. The reconstitution was performed as described in [Materials and methods](#). Transport was started by adding 50 μM [^3H]glutamine to proteoliposomes containing 10 mM internal glutamine, in the presence of 50 mM external Na-gluconate. The molecules were added 1 min before the labeled substrate at the concentration 1 mM. Percentage of inhibition was calculated for each experiment with respect to the sample without added inhibitor. Results are means \pm S.D. from three experiments. *Significantly different from sample without added inhibitor as estimated by Student's *t* test ($P < 0.05$).

even though less efficiently while, histidine, glutamate and arginine were not transported.

3.5. Kinetics of ASCT2 mediated transport

The dependence of the transport rate on the glutamine concentration was studied. The initial rate of glutamine antiport ([Fig. 9A](#)) showed a dependence on the external glutamine concentration fitting the Michaelis–Menten equation, from which half-saturation constant (K_m) of 0.097 ± 0.019 mM and a V_{max} of 13.3 ± 1.9 $\text{nmol} \cdot \text{min}^{-1} \cdot \text{mg protein}^{-1}$ (from three different experiments) were derived. A similar experiment was performed to obtain information on the intraliposomal K_m , which resulted to be much higher than the external one ([Fig. 9B](#)). The measured value was $1.8 \text{ mM} \pm 0.52$ (from three different experiments). The calculated V_{max} (12.0 ± 1.5 $\text{nmol} \cdot \text{min}^{-1} \cdot \text{mg protein}^{-1}$) was similar to that measured in the experiment of [Fig. 9A](#).

The dependence of the transport on the concentration of external cations, as gluconate salts, was studied. The data of [Fig. 9C](#) shows that the transport rate of glutamine antiport, starting from zero was strongly stimulated by external Na^+ . The data could be fitted in the Michaelis–Menten equation from which a V_{max} of 11.5 ± 0.57 $\text{nmol} \cdot \text{min}^{-1} \cdot \text{mg protein}^{-1}$ and a K_m of 32 ± 4.7 mM were calculated. The presence of Li^+ or K^+ in the extraliposomal compartment was not able to stimulate the glutamine transport.

4. Discussion

One of the major challenges concerning the study of mammalian and especially human transporters is to obtain sufficient amount of purified proteins for both structural and functional characterization. Moreover, the availability of suitable methods for transport assay is essential to characterize recombinant proteins obtained by heterologous production. Only in recent years, the number of successful over-production trials of mammalian and human transporters is slightly increasing. Over-production has been achieved using *Escherichia coli* as host, both as entire organism [[31,32](#)] or in cell free systems [[33](#)]. However, in several cases it was not possible to obtain significant levels of human proteins in bacteria, thus suggesting another host for production. This was the case for hASCT2 which was toxic to several bacterial strains screened for expression trials (data not shown). Using the yeast *P. pastoris* we succeeded in obtaining high levels of recombinant hASCT2, similar to the recently expressed hLAT2 transporter [[34](#)]. hLAT2 and hASCT2 represent the only mammalian amino acid transporters produced in yeast, so far. hASCT2 is structurally unrelated to hLAT2, but presents significant homology to glutamate

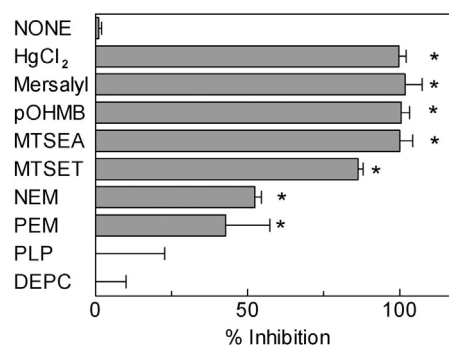


Fig. 7. Effect of protein specific reagents on hASCT2. The reconstitution was performed as described in [Materials and methods](#). Transport was started by adding 50 μM [^3H]glutamine to proteoliposomes containing 10 mM internal glutamine, in the presence of 50 mM external Na-gluconate. The molecules were added 1 min before the labeled substrate at the following concentrations: 0.02 mM HgCl_2 , mersalyl, p-OHMB; 1 mM MTSEA, MTSET, NEM or PEM; 10 mM PLP; 4 mM DEPC. Percentage of inhibition was calculated with respect to the sample without added inhibitor. Results are means \pm S.D. from three experiments. *Significantly different from sample without added inhibitor as estimated by Student's *t* test ($P < 0.05$).

transporters [[6,9](#)]. An important step for increasing the yield of recombinant hASCT2 protein was the optimization of the codons of the yeast translation machinery. Similarly, bacterial over-production of a different transporter, OCTN2, was obtained only after codon bias [[35](#)]. Noteworthy, the over-produced hASCT2 was associated to the yeast membrane

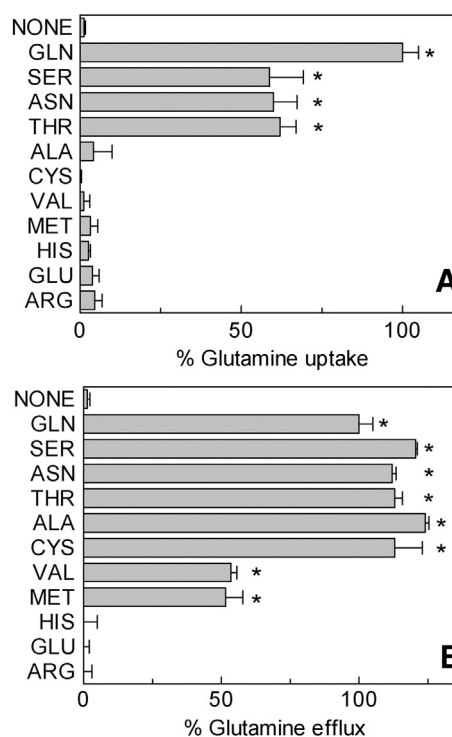


Fig. 8. Amino acids as counter substrates for hASCT2. The reconstitution was performed as described in [Materials and methods](#). (A) The indicated substrates (10 mM) were present in the intraliposomal space (included in the reconstitution mixture). Transport was started by adding 50 μM [^3H]glutamine to the proteoliposomes in the presence of 50 mM external Na-gluconate. Percentage glutamine uptake was calculated for each experiment with respect to proteoliposomes containing 10 mM internal glutamine (100%). (B) Proteoliposomes were preloaded with 50 μM [^3H]glutamine and its efflux was measured in the presence of 10 mM of the indicated external amino acid. The efflux experiment was performed as described in [Materials and methods](#) and percentage glutamine efflux was calculated for each experiment with respect to proteoliposomes with externally added glutamine (100%). Results are means \pm S.D. of the percentage of three experiments. *Significantly different from samples without internal or external substrate as estimated by Student's *t* test ($P < 0.05$).

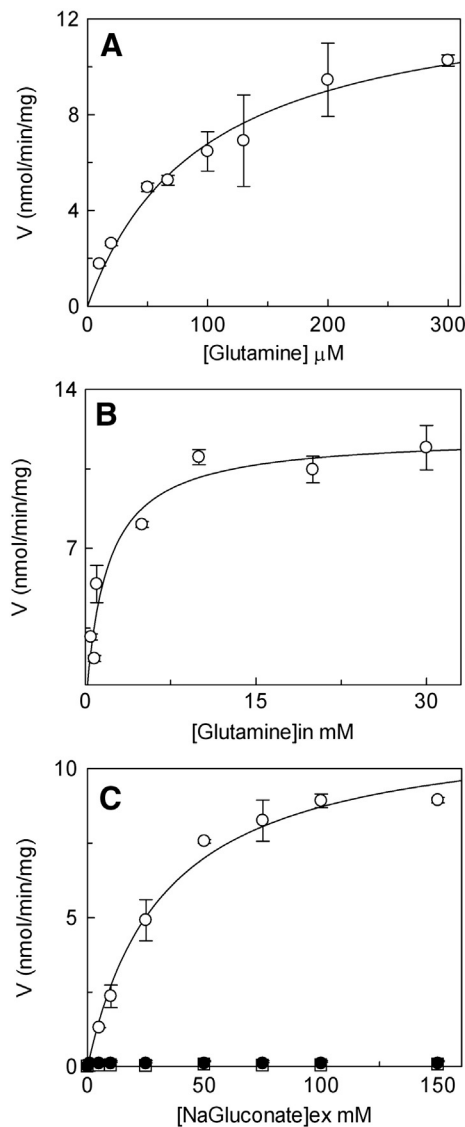


Fig. 9. Dependence of substrate concentration and the rate of glutamine antiport. The transport rate was measured adding [3 H]glutamine at the indicated concentration to proteoliposomes containing 10 mM internal glutamine (A) or 200 μ M [3 H]glutamine to proteoliposomes containing internal glutamine at the indicated concentrations (B), in the presence of 50 mM external Na-gluconate in 10 min; in (C) transport rate was measured adding 50 μ M [3 H]glutamine to proteoliposomes containing 10 mM glutamine in the presence of the indicated concentrations of Na-gluconate (\circ), K-gluconate (\bullet) or Li-acetate (\square) in 10 min. Data were plotted according to Michaelis–Menten equation. Results are means \pm S.D. of three experiments.

fraction indicating proper folding of recombinant hASCT2. The preferred detergent for solubilization, C₁₂E₈, was proven by the functional characterization and correlated well with previous studies conducted on the rASCT2 solubilized in its active form from rat kidney membranes [17]. Moreover, the purified hASCT2 was eluted from Superdex 200 chromatography as a 150 kDa oligomeric form suggesting that the protein tends to form trimers. This observation is in agreement with the data obtained on the GltPh transporter of *P. horikoshii* [6] and to the homology structural model of rASCT2 [9].

To obtain functional information on the recombinant hASCT2 we have performed reconstitution into proteoliposomes which gives the possibility, as above mentioned, to better control several experimental conditions. Indeed, virtually all the reconstituted transporter molecules are inserted in the lipid bilayer of the liposomes with the same orientation of the native membrane (right-side-out) as suggested by the essential requirement of external Na⁺ for transport (Fig. 9C), which

correlates with the presence of Na⁺ in the extracellular compartment; accordingly, single K_m values are observed both outside and inside. Similar orientation was previously found for other reconstituted transporters [4,17,26,36]. However, definitive proofs of protein orientation will be given by structure/function relationship studies. The unidirectional insertion of transport proteins in the membrane is probably guaranteed by the slow process of proteoliposome formation starting from mixed micelles or destabilized liposomes. The insertion of the protein into the bilayer is also influenced by the asymmetrical structure of the protein itself together with the small radius of the starting micelles.

The basic functional properties of the reconstituted transporter, i.e., the Na⁺-dependence, intolerance for substitution of Na⁺ with Li⁺ and K⁺, the specificity for neutral amino acids, and the lack of inhibition by the amino acid analogs MeAIB and BCH, correspond to those described in cell systems so far [3,12]. On the other hand, some important novel information on the hASCT2 has been obtained in the study presented here. In particular, besides the already documented specificity for glutamine, alanine, serine, threonine and cysteine, an asymmetric behavior with respect to the transported amino acids has been highlighted. In particular, specific amino acids such as cysteine, alanine, valine and methionine can be translocated from outside to inside of proteoliposomes, but not vice-versa. This finding suggests that hASCT2 provides cells with these amino acids exporting glutamine, threonine, serine or asparagine on the basis of metabolic needs of cells or the amino acid concentrations. At the same time, the bi-directional transport of glutamine is in agreement with the role proposed for ASCT2 in astrocytes and as a general mechanism of small amino acid reabsorption [1,14,37,38]. Also serine, asparagine and threonine are bi-directionally translocated in line with the role designed for ASCT2, together with LAT1 in the mTOR pathway which controls several cell functions [2]. It has been found that Na⁺ stimulates the glutamine antiport also from the internal side to some extent, even though at a concentration higher than the intracellular Na⁺ concentration. This may be explained either by sodium counter-transport, as previously found for ASCT1 [39] or by allosteric mechanism. In this work the external K_m for glutamine of hASCT2 has been measured and found to be in the same range as that measured in cell systems [2,12]. Moreover, by using the proteoliposome assay, the internal K_m for glutamine, so far unknown, has been determined to be twenty times higher than the external one. This reflects the difference between the extra- and intracellular concentration of glutamine and other amino acids [40]. Moreover, the difference between the external and internal K_m values is in favor of the functional asymmetry of the transporter and is in agreement with the structural asymmetry of the hASCT2 protein (Fig. 10), which shows a cone-shaped form enlarged towards the extracellular side. The proteoliposome method allowed further insights in the structure–function relationship. Indeed, the reconstituted transporter, has been shown to be strongly inhibited by hydrophilic thiol specific reagents, but much less by hydrophobic ones or by the amino specific reagent PLP. These data indicates that the Cys residues involved in the observed inhibition should be located in a hydrophilic environment accessible from the extracellular space. On the basis of the homology model, Cys395 is the only Cys residue exposed towards the extracellular environment (Fig. 10), thus, it might be involved in the interaction with the hydrophilic SH reagents and inactivation of the transporter. Even though this is a speculative consideration, it correlates well with the location of Cys395 in the middle of two helical hairpins (Fig. 10 dark gray structure) whose homologues in the GltPh have been recognized as a mobile structure involved in the conformational changes allowing substrate transport [41].

By comparison with the rASCT2 some differences arose such as the K_m values which are lower for hASCT2 than those of the rat counterpart, as well as the sensitivity to DEPC that inhibits rASCT2 but not the human counterpart. Moreover the hASCT2 is not regulated by intracellular ATP as observed for the rat protein. This can be explained by the

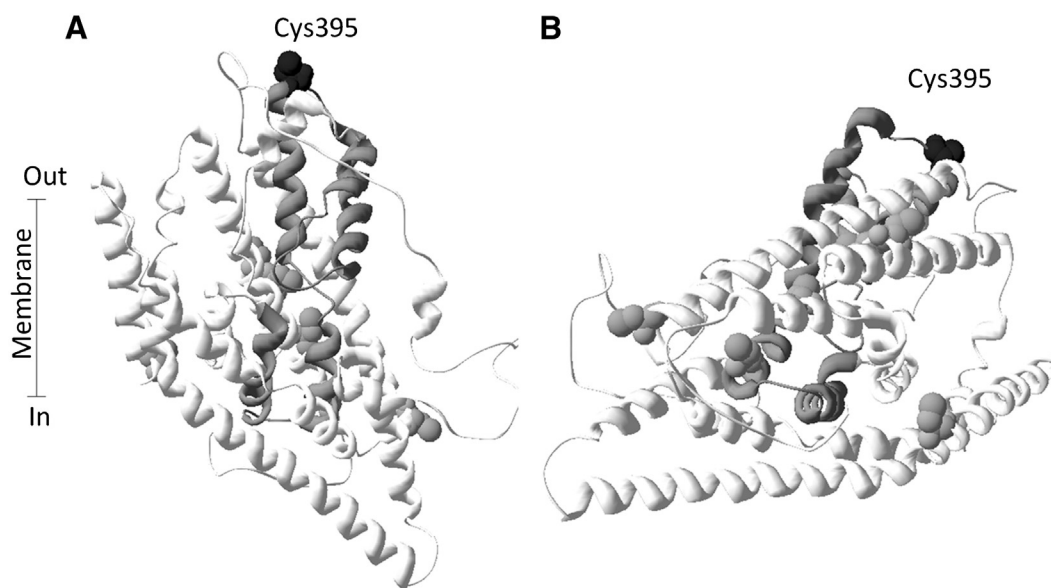


Fig. 10. Homology structural model of hASCT2. Ribbon diagram viewing the transporter from the lateral side (A) or by the intracellular side (B); Cys395 is highlighted in black. The structure homologous to the sequence segment from HP (helical hairpin) 1 to HP2 of GltPh [6,40] is highlighted in dark gray. The homology model has been represented using the molecular program SpdbViewer 4.01.

different structural properties of the human protein in comparison with the homologue protein from rat. In fact, the N-terminal sequence of the rat protein, which contains a nucleotide binding motif [17] presents some differences with respect to the human protein. Regulation of hASCT2 has been described in cell systems but no evidence of direct effectors on the activity of the transport proteins is so far presented [42–44]. Noteworthy, ASCT2 represents a potential target for cancer therapy (see Introduction). ASCT2 over-expression has been linked to the tumor suppressor pRb/E2F pathway [45]. In this context, and in line with the molecular screening on the rat isoform [19], the reconstituted hASCT2 will be very helpful for testing drugs and xenobiotics of relevance for human health. This could allow the identification of possible specific inhibitors of hASCT2 activity, in order to elicit apoptosis in cancer cells. The availability of recombinant proteins also allows site-directed mutagenesis on the human ASCT2. Applying such methods will shed further light on the involvement of hASCT2 in pathophysiology as well as in defining molecular mechanisms of transport and structural details such as the actual oligomeric form of the protein. However, only X-ray diffraction analysis of hASCT2 crystals could definitively give information on the three-dimensional structure of the transporter. The high level of production of the functional protein in a homogeneous purified fraction allows crystallographic screening for this purpose. The homology structure and, when available, the high-resolution structure will in addition be used in docking strategies for fast analysis of transporter-inhibitor interactions, which could be validated in proteoliposomes.

Acknowledgements

This work was supported by funds from: Programma Operativo Nazionale PON-ricerca e competitività 2007–2013 [PON 01_00937] “Modelli sperimentali Biotecnologici integrati per lo sviluppo e la selezione di molecole di interesse per la salute dell'uomo”, Ministero Istruzione Università e Ricerca (MIUR); European Commission, FSE funds and Calabria Region.

References

- [1] M. Palacin, R. Estevez, J. Bertran, A. Zorzano, Molecular biology of mammalian plasma membrane amino acid transporters, *Physiol. Rev.* 78 (1998) 969–1054.
- [2] B.C. Fuchs, B.P. Bode, Amino acid transporters ASCT2 and LAT1 in cancer: partners in crime? *Semin. Cancer Biol.* 15 (2005) 254–266.
- [3] S. Broer, M. Palacin, The role of amino acid transporters in inherited and acquired diseases, *Biochem. J.* 436 (2011) 193–211.
- [4] L. Pochini, F. Oppedisano, C. Indiveri, Reconstitution into liposomes and functional characterization of the carnitine transporter from renal cell plasma membrane, *Biochim. Biophys. Acta* 1661 (2004) 78–86.
- [5] C. Indiveri, Studying amino acid transport using liposomes, *Methods Mol. Biol.* 606 (2010) 55–68.
- [6] D. Yernool, O. Boudker, Y. Jin, E. Gouaux, Structure of a glutamate transporter homologue from *Pyrococcus horikoshii*, *Nature* 431 (2004) 811–818.
- [7] L.R. Forrest, R. Kramer, C. Ziegler, The structural basis of secondary active transport mechanisms, *Biochim. Biophys. Acta* 1807 (2011) 167–188.
- [8] S. Broer, Apical transporters for neutral amino acids: physiology and pathophysiology, *Physiology* (Bethesda) 23 (2008) 95–103.
- [9] F. Oppedisano, M. Galluccio, C. Indiveri, Inactivation by Hg²⁺ and methylmercury of the glutamine/amino acid transporter (ASCT2) reconstituted in liposomes: prediction of the involvement of a CXXC motif by homology modelling, *Biochem. Pharmacol.* 80 (2010) 1266–1273.
- [10] F. Oppedisano, L. Pochini, S. Broer, C. Indiveri, The BOAT1 amino acid transporter from rat kidney reconstituted in liposomes: kinetics and inactivation by methylmercury, *Biochim. Biophys. Acta* 1808 (2011) 2551–2558.
- [11] V. Ganapathy, M. Thangaraju, P.D. Prasad, Nutrient transporters in cancer: relevance to Warburg hypothesis and beyond, *Pharmacol. Ther.* 121 (2009) 29–40.
- [12] V. Torres-Zamorano, F.H. Leibach, V. Ganapathy, Sodium-dependent homo- and hetero-exchange of neutral amino acids mediated by the amino acid transporter ATBO, *Biochem. Biophys. Res. Commun.* 245 (1998) 824–829.
- [13] N. Utsunomiya-Tate, H. Endou, Y. Kanai, Cloning and functional characterization of a system ASC-like Na⁺-dependent neutral amino acid transporter, *J. Biol. Chem.* 271 (1996) 14883–14890.
- [14] A. Broer, N. Brookes, V. Ganapathy, K.S. Dimmer, C.A. Wagner, F. Lang, S. Broer, The astroglial ASCT2 amino acid transporter as a mediator of glutamine efflux, *J. Neurochem.* 73 (1999) 2184–2194.
- [15] M. Pollard, D. Meredith, J.D. McGivan, Identification of a plasma membrane glutamine transporter from the rat hepatoma cell line H4-IIE-C3, *Biochem. J.* 368 (2002) 371–375.
- [16] M. Dolinska, B. Zablocka, U. Sonnewald, J. Albrecht, Glutamine uptake and expression of mRNA's of glutamine transporting proteins in mouse cerebellar and cerebral cortical astrocytes and neurons, *Neurochem. Int.* 44 (2004) 75–81.
- [17] F. Oppedisano, L. Pochini, M. Galluccio, M. Cavarelli, C. Indiveri, Reconstitution into liposomes of the glutamine/amino acid transporter from renal cell plasma membrane: functional characterization, kinetics and activation by nucleotides, *Biochim. Biophys. Acta* 1667 (2004) 122–131.
- [18] F. Oppedisano, L. Pochini, M. Galluccio, C. Indiveri, The glutamine/amino acid transporter (ASCT2) reconstituted in liposomes: transport mechanism, regulation by ATP and characterization of the glutamine/glutamate antiport, *Biochim. Biophys. Acta* 1768 (2007) 291–298.
- [19] F. Oppedisano, M. Catto, P.A. Koutentis, O. Nicolotti, L. Pochini, M. Koyioni, A. Introcaso, S.S. Michaelidou, A. Carotti, C. Indiveri, Inactivation of the glutamine/amino acid transporter ASCT2 by 1,2,3-dithiazoles: proteoliposomes as a tool to gain insights in the molecular mechanism of action and of antitumor activity, *Toxicol. Appl. Pharmacol.* 265 (2012) 93–102.
- [20] P.M. Sharp, W.H. Li, The codon adaptation Index—a measure of directional synonymous codon usage bias, and its potential applications, *Nucleic Acids Res.* 15 (1987) 1281–1295.

- [21] F. Oberg, J. Sjöhamn, M.T. Conner, R.M. Bill, K. Hedfalk, Improving recombinant eukaryotic membrane protein yields in *Pichia pastoris*: the importance of codon optimization and clone selection, *Mol. Membr. Biol.* 28 (2011) 398–411.
- [22] M. Nyblom, F. Oberg, K. Lindkvist-Petersson, K. Hallgren, H. Findlay, J. Wikström, A. Karlsson, O. Hansson, P.J. Booth, R.M. Bill, R. Neutze, K. Hedfalk, Exceptional overproduction of a functional human membrane protein, *Protein Expr. Purif.* 56 (2007) 110–120.
- [23] J. Stratton, V. Chiruvolu, M. Meagher, High cell-density fermentation, *Methods Mol. Biol.* 103 (1998) 107–120.
- [24] M.E. Bushell, M. Rowe, C.A. Avignone-Rossa, J.N. Wardell, Cyclic fed-batch culture for production of human serum albumin in *Pichia pastoris*, *Biotechnol. Bioeng.* 82 (2003) 678–683.
- [25] F. Oberg, J. Sjöhamn, G. Fischer, A. Moberg, A. Pedersen, R. Neutze, K. Hedfalk, Glycosylation increases the thermostability of human aquaporin 10 protein, *J. Biol. Chem.* 286 (2011) 31915–31923.
- [26] L. Pochini, M. Scalise, M. Galluccio, L. Amelio, C. Indiveri, Reconstitution in liposomes of the functionally active human OCTN1 (SLC22A4) transporter overexpressed in *Escherichia coli*, *Biochem. J.* 439 (2011) 227–233.
- [27] A. Tonazzi, C. Indiveri, Effects of heavy metal cations on the mitochondrial ornithine/citrulline transporter reconstituted in liposomes, *Biometals* 24 (2011) 1205–1215.
- [28] F. Palmieri, C. Indiveri, F. Bisaccia, V. Iacobazzi, Mitochondrial metabolite carrier proteins: purification, reconstitution, and transport studies, *Methods Enzymol.* 260 (1995) 349–369.
- [29] M. Galluccio, C. Brizio, E.M. Torchetti, P. Ferranti, E. Gianazza, C. Indiveri, M. Barile, Over-expression in *Escherichia coli*, purification and characterization of isoform 2 of human FAD synthetase, *Protein Expr. Purif.* 52 (2007) 175–181.
- [30] A. Sali, T.L. Blundell, Comparative protein modelling by satisfaction of spatial restraints, *J. Mol. Biol.* 234 (1993) 779–815.
- [31] M. Quick, E.M. Wright, Employing *Escherichia coli* to functionally express, purify, and characterize a human transporter, *Proc. Natl. Acad. Sci. U. S. A.* 99 (2002) 8597–8601.
- [32] C. Indiveri, M. Galluccio, M. Scalise, L. Pochini, Strategies of bacterial over expression of membrane transporters relevant in human health: the successful case of the three members of OCTN subfamily, *Mol. Biotechnol.* 54 (2012) 724–736.
- [33] T. Keller, D. Schwarz, F. Bernhard, V. Dotsch, C. Hunte, V. Gorboulev, H. Koepsell, Cell free expression and functional reconstitution of eukaryotic drug transporters, *Biochemistry* 47 (2008) 4552–4564.
- [34] M. Costa, A. Rosell, E. Alvarez-Marimon, A. Zorzano, D. Fotiadis, M. Palacin, Expression of human heteromeric amino acid transporters in the yeast *Pichia pastoris*, *Protein Expr. Purif.* 87 (2013) 35–40.
- [35] M. Galluccio, L. Amelio, M. Scalise, L. Pochini, E. Boles, C. Indiveri, Over-expression in *E. coli* and purification of the human OCTN2 transport protein, *Mol. Biotechnol.* 50 (2012) 1–7.
- [36] M. Scalise, M. Galluccio, L. Pochini, C. Indiveri, Over-expression in *Escherichia coli*, purification and reconstitution in liposomes of the third member of the OCTN sub-family: the mouse carnitine transporter OCTN3, *Biochem. Biophys. Res. Commun.* 422 (2012) 59–63.
- [37] J.W. Deitmer, A. Broer, S. Broer, Glutamine efflux from astrocytes is mediated by multiple pathways, *J. Neurochem.* 87 (2003) 127–135.
- [38] S. Broer, N. Brookes, Transfer of glutamine between astrocytes and neurons, *J. Neurochem.* 77 (2001) 705–719.
- [39] N. Zerangue, M.P. Kavanaugh, ASCT-1 is a neutral amino acid exchanger with chloride channel activity, *J. Biol. Chem.* 271 (1996) 27991–27994.
- [40] L.A. Cynober, Plasma amino acid levels with a note on membrane transport: characteristics, regulation, and metabolic significance, *Nutrition* 18 (2002) 761–766.
- [41] N. Reyes, C. Ginter, O. Boudker, Transport mechanism of a bacterial homologue of glutamate transporters, *Nature* 462 (2009) 880–885.
- [42] C.I. Bungard, J.D. McGivan, Identification of the promoter elements involved in the stimulation of ASCT2 expression by glutamine availability in HepG2 cells and the probable involvement of FXR/RXR dimers, *Arch. Biochem. Biophys.* 443 (2005) 53–59.
- [43] J.S. Amaral, M.J. Pinho, P. Soares-da-Silva, Genomic regulation of intestinal amino acid transporters by aldosterone, *Mol. Cell. Biochem.* 313 (2008) 1–10.
- [44] N.E. Avissar, H.C. Sax, L. Toia, In human enterocytes, GLN transport and ASCT2 surface expression induced by short-term EGF are MAPK, PI3K, and Rho-dependent, *Dig. Dis. Sci.* 53 (2008) 2113–2125.
- [45] M.R. Reynolds, A.N. Lane, B. Robertson, S. Kemp, Y. Liu, B.G. Hill, D.C. Dean, B.F. Clem, Control of glutamine metabolism by the tumor suppressor Rb, *Oncogene* (2013), <http://dx.doi.org/10.1038/onc.2012.635>.

Cloning, Large Scale Over-Expression in *E. coli* and Purification of the Components of the Human LAT 1 (SLC7A5) Amino Acid Transporter

Michele Galluccio · Piero Pingitore ·
Mariafrancesca Scalise · Cesare Indiveri

Published online: 3 August 2013
© Springer Science+Business Media New York 2013

Abstract The high yield expression of the human LAT1 transporter has been obtained for the first time using *E. coli*. The hLAT1 cDNA was amplified from HEK293 cells and cloned in pH6EX3 vector. The construct pH6EX3-6His-hLAT1 was used to express the 6His-hLAT1 protein in the Rosetta(DE3)pLysS strain of *E. coli*. The highest level of expression was detected 8 h after induction by IPTG at 28 °C. The expressed protein was collected in the insoluble fraction of cell lysate. On SDS-PAGE the apparent molecular mass of the polypeptide was 40 kDa. After solubilization with sarkosyl and denaturation with urea the protein carrying a 6His N-terminal tag was purified by Ni²⁺-chelating affinity chromatography and identified by anti-His antibody. The yield of the over-expressed protein after purification was 3.5 mg/L (cell culture). The human CD98 cDNA amplified from Image plasmid was cloned in pGEX-4T1. The construct pGEX-4T1-hCD98 was used to express the GST-hCD98 protein in the Rosetta(DE3)pLysS strain of *E. coli*. The highest level of expression was detected in this case 4 h after induction by IPTG at 28 °C. The expressed protein was accumulated in the soluble fraction of cell lysate. The molecular mass was determined on the basis of marker proteins on SDS-PAGE; it was about 110 kDa. GST was cleaved from the protein construct by incubation with thrombin for 12 h and the hCD98 was separated by Sephadex G-200 chromatography (size exclusion). hCD98 showed a 62 kDa

apparent molecular mass, as determined on the basis of molecular mass markers using SDS-PAGE. The yield of CD98 was 2 mg/L of cell culture.

Keywords Amino acid · Transport · *E. coli* · LAT1 · CD98 · Over-expression

Abbreviations

GST	Glutathione- <i>S</i> -transferase
IPTG	Isopropyl-β-D-thiogalactopyranoside
BCH	2-Aminobicyclo-(2,2,1)-heptane-2-carboxylic acid
PMSF	Phenylmethylsulfonyl fluoride
DTE	1,4-Dithioerythritol
C ₁₂ E ₈	Octaethylene glycol monododecyl ether

1 Introduction

LAT1 (SLC7A5) belongs to the amino acid transporter group called system L, which is responsible of providing cells with aromatic and branched chain neutral amino acids [2]. Several authors have found this transporter highly expressed in many tumors [10, 11]. Indeed, intracellular amino acid availability is a key factor for tumor progression and survival [10, 11, 14] since, in addition to source of nitrogen for the synthesis of endogenous compounds, amino acids are largely used in tumors as oxidative fuel for ATP production. Accordingly, LAT1 which mediates absorption of amino acids, plays an important role in tumor cells. The LAT1 transporter forms a heterodimer with CD98 (SLC3A2). The LAT1 subunit in humans is a 507 amino acid long polypeptide with a theoretical molecular mass of 55.0 kDa. The protein is hydrophobic and is predicted to be constituted by 12 transmembrane segments [3, 5, 18, 20, 21]. The CD98

Michele Galluccio and Piero Pingitore contributed equally to this work.

M. Galluccio · P. Pingitore · M. Scalise · C. Indiveri (✉)
Unit of Biochemistry and Molecular Biotechnology, Department
BEST (Biologia, Ecologia, Scienze della Terra), University of
Calabria, Via P. Bucci 4c, 87036 Arcavacata di Rende, Italy
e-mail: cesare.indiveri@unical.it

subunit, is constituted by 630 amino acids. Its theoretical mass is 68.0 kDa. This subunit has only one transmembrane segment and, hence, is much more hydrophilic with respect to LAT1. The function of the LAT1/CD98 heterodimer has been investigated in intact cells. It catalyses Na⁺-independent transport of amino acids by an antiport mode. Glutamine, methionine, valine, leucine, isoleucine, tryptophan, phenylalanine and histidine are efficiently transported by LAT1 [17]. A distinctive feature of LAT1 is the sensitivity to the inhibitor BCH. Structural data on this transporter are available nor on the LAT1 subunit neither on the CD98 one. As suggested by the high level of expression in tumors with respect to normal cells, the LAT1 transporter is a suitable target for anticancer therapy. Indeed inhibitors of its activity might be potential anticancer drugs [1, 15, 23]. Moreover, LAT1 seems to be also involved in pharmacokinetics of several drugs [8, 24]. However, systematic screenings of molecules which could interact with the transporter and affect its activity are not yet available. To perform such studies, resolution of the structure is necessary, which needs large scale purified transport proteins. However, heterologous over-expression of human proteins is still at the beginning with few cases of success [16]. In particular, over-expression of amino acid transporters has never been obtained in bacteria. Very recently the amino acid transporter hLAT2 together with the counterpart hCD98 have been over-expressed in *P. pastoris* [7]. In the present work the over-expression of the human LAT1 and its counterpart CD98 has been achieved using *E. coli*. To our knowledge the present study represents the first case of over-expression of the human LAT1 transporter at a large scale and is the first step towards the structure–function relationships of the transporter.

2 Materials and Methods

2.1 Materials

Chemicals used for experiments, protease inhibitor cocktail (P8849), Nickel Affinity Gel (HIS-Select[®]—P6611) and the Monoclonal Anti-polyHistidine-Peroxidase antibody (A7058) were from Sigma-Aldrich; plasmids (pET vectors) and cell strains from Novagen; restriction endonucleases and specific reagents for cloning from Fermentas; Glutathione Sepharose 4B from GE Healthcare; thrombin and Amicon Ultra centrifugal filters 2 mL 50 K were from EMD Millipore.

2.2 hLAT1 cDNA Cloning

The hLAT1 cDNA (1,521 bp) (GenBank NM_003486, SLC7A5) was amplified from total reverse-transcribed

mRNA extracted from HEK293 cells. Primers used for amplification were 5'-ATGGCGGGTGCGGGCCCCGAAGCGGCGCGCTAGC-3' (forward) and 5'-TGTCTCCTGGGGACCACCTGCATGAGCTTCTGAC-3' (reverse). The sequence of the cDNA was analysed by an automated sequencer (ABI 310 Applied Biosystems) and corresponded to the hLAT1 coding sequence in three different determinations. The hLAT1 cDNA was then amplified using the primers 5'-CGCGGATCCATGGCGGGTGCGGGCCCCGAAG-3' (forward) and 5'-CCGCTCGAGCTATGTCTCTCTGGGGGACCAC-3' (reverse). Each primer carries the recognition sites of *Bam*HI and *Xho*I restriction enzymes. The cDNA containing the restriction sites was cloned in the pH6EX3 [4] and pET-41a(+) expression vectors. The resulting recombinant plasmids, defined pH6EX3-hLAT1 and pET-41a(+)-hLAT1, encoded the hLAT1 protein carrying the extra N-terminal 6His tag or a GST tag, plus a S tag, respectively.

2.3 Cloning of cDNA Coding for hCD98 Cell-Surface Antigen Heavy Chain (SLC3A2 or 4F2)

The 1,890 bp cDNA encoding for SLC3A2, acquired from LifeSciences (IRAU969D0814D), was amplified by 5'-CCGGAATCCATGGAGCTACAGCCTCTCTGA-3' (forward) and 5'-CCGCTCGAGTCAGGCCGCGTAGGGGAAGC-3' (reverse) primers, then sub-cloned in the pH6EX3 or pGEX-4T1 vectors. The recombinant plasmids pH6EX3-hCD98 or pGEX-4T1-hCD98, code for fusion proteins corresponding to the mature form of hCD98 carrying the N-terminal amino acid sequence M-S-P-I-H-H-H-H-H-H-L-V-P-R-G-S-E-A-S-N-S- or the glutathione-S-transferase, respectively.

2.4 Expression of Recombinant GST-hLAT1 Protein

To produce the GST-hLAT1 recombinant protein, *E. coli* Rosetta(DE3)pLysS cells, treated with calcium chloride, were transformed with the pET-41a(+)-hLAT1 [6]. Selection of transformed colonies was performed on LB-agar plates in which 30 µg/mL kanamycin plus 34 µg/mL chloramphenicol were present. Colonies were inoculated in 100 mL of a medium (2× YT at pH 7.0) containing Bacto peptone (1.6 %), Bacto yeast extract (1 %) and NaCl (0.5 %). Also this medium contained kanamycin and chloramphenicol at the same concentrations as above. Cell cultures were grown overnight (37 °C) under rotary shaking (about 200 rpm). Fifty mL aliquot of the cell culture was transferred to 0.5 L of a medium (2× YT) prepared with the components above described. When the optical density of the cell cultures, measured at 600 nm wavelength, was 0.5–0.7, different IPTG concentrations (from 0.1 to 1 mM) were tested for inducing the expression of the protein coded by the cDNA inserted in the recombinant plasmid. Two 0.25 L

aliquots of the cell suspension were differently treated: one aliquot was grown at 28 °C while the other at 37 °C. Every 2 h, 50 mL from each aliquot were collected and centrifuged (3,000g, 4 °C, 10 min); pellets (aliquots of 0.2 g wet weight) were stored at -20 °C. A bacterial pellet aliquot, after thawing was dissolved in 2 mL medium (20 mM hepes/tris pH 7.5 plus 20 µL of protease inhibitor cocktail and 0.5 mM PMSF). The suspension was treated by sonication (10 min/1 s sonication/1 s intermission, 4 °C; SONICS sonifier, Vibracell VCX-130). The insoluble cell fraction was separated by centrifugation (12,000g, 4 °C, 30 min). Proteins were separated on SDS-PAGE.

2.5 6His-hLAT1 Expression

pH6EX3-hLAT1 was used to transform *E. coli* Rosetta (DE3)pLysS. Transformed colonies were selected, inoculated and induced as above described (Sect. 2.4). After IPTG addition 0.25 L of cell aliquots were grown at 28 °C or 37 °C. Fifty mL cell fractions were harvested every 2 h, centrifuged (3,000g, 4 °C, 10 min). Pellet storing, cell sonication and protein separation were performed as described above (Sect. 2.4).

2.6 6His-CD98 Expression

pH6EX3-hCD98 was used for transforming *E. coli* Rosetta(DE3)pLysS. Expression, pellet storing, cell sonication and protein separation were performed as above described (Sects. 2.4, 2.5).

2.7 GST-hCD98 Expression

pGEX4T1-hCD98 was used for transforming *E. coli* Rosetta(DE3)pLysS. Expression, pellet storing, cell sonication and protein separation were performed as above described (Sects. 2.4, 2.5).

2.8 hLAT1 Purification

In order to purify 6His-LAT1 protein the pellet was used. After washing by 0.1 M tris/HCl pH 8.0, the pellet was dissolved in 100 mM DTE, 0.8 % sarkosyl, 3.5 M urea, 10 % glycerol, 200 mM NaCl and buffered at pH 8.0 with 10 mM tris/HCl. After centrifugation (12,000g, 10 min, 4 °C) the supernatant was recovered and applied on a His select Ni²⁺ affinity gel column (0.5 × 2.5 cm) equilibrated with 8 mL buffer (0.1 % sarkosyl, 10 % glycerol, 200 mM NaCl, 10 mM tris/HCl pH 8.0). 5 mL washing buffer (0.1 % Triton X-100/200 mM NaCl/10 % glycerol/5 mM DTE/10 mM tris/HCl pH 8.4), 3 mL washing buffer plus 10 mM imidazole, 3 mL washing buffer plus 50 mM imidazole were

used for eluting proteins in 12 fractions (1 mL). Purified hLAT1 (about 120 µg) was present in the tenth fraction.

2.9 GST-hCD98 Purification

To purify the GST-hCD98 protein, the soluble fraction obtained as described above was used. 1.5 mL was mixed with 500 µL of glutathione Sepharose 4B preconditioned with PBS buffer at pH 7.4 and kept for 30 min in a Stuart agitator. After 120 min the resin was washed three times with the buffer PBS pH 7.4 and, then added with 1.5 mL of 10 mM GSH/20 mM TrisHCl pH 8.2. After 2 min the suspension was subjected to short spin centrifugation and the supernatant was collected (1.5 mL containing 400 µg of purified GST-hCD98).

2.10 Thrombin Treatment and Separation of hCD98

The purified hCD98 obtained as described in 2.9 was concentrated in Amicon centrifugal filters to a volume of 200 µL and incubated 12 h at 25 °C, 500 rpm with 1.5 unit of thrombin and, then, loaded on G-200 chromatography column (0.7 cm diameter, 15 cm height) preconditioned with PBS pH 7.4 and eluted with the same buffer. Purified hCD98 was collected in fraction three (80 µg protein in 500 µL) and GST in fractions 6–7 (60 µg 1,000 µL).

2.11 Other Methods

Measurement of protein concentration and protein separation in SDS-PAGE were performed according to refs. [9] and [19] under the specific conditions described in Ref. [12]. Evaluation of protein concentration was also performed on Coomassie-stained protein bands using the Chemidoc imaging system (Bio-Rad).

3 Results

3.1 Expression of hLAT1

The 1,521 bp hLAT1 cDNA was amplified from HEK 293 cells using primers constructed on hLAT1 cDNA ends (NM_003486 of GenBank). The cDNA apparent size was about 1,500 bp estimated on agarose gel. The amplified cDNA did not contain mutations with respect to the hLAT1 coding sequence (GeneBank, not shown). Different vectors were employed to express hLAT1. To improve the solubility of the hydrophobic hLAT1 protein, the cDNA was firstly cloned in the vector pET41-a(+) containing a N-terminal GST-tag. The construct pET41-a(+)-hLAT1 was then used to transfect *E. coli* Rosetta(DE3)pLysS cells. As shown in Fig. 1 the GST-hLAT1 construct was

efficiently expressed after 2–8 h of IPTG induction (Fig. 1 lanes 3–5). However, the protein was collected only in the insoluble fractions of cell lysate. Thus, plasmids without GST or other tags were also employed to test the expression of hLAT1, such as pET-28a(+), pMWT7, pH6EX3 and pET-21a(+). All the constructs were used to transfect *E. coli* Rosetta(DE3)pLysS cells. Only in the case of pH6EX3-hLAT1 a significant amount of over-expressed protein was revealed in cell lysate insoluble fractions. On the basis of previous experience with membrane transporter expression [12, 16, 22] the growth temperature was kept at 28 °C. Figure 2 shows the protein patterns of cell lysates at increasing time after induction with IPTG. A protein (Fig. 2 lanes 2–5), with apparent molecular mass of about 40 kDa was present after induction by 0.4 mM IPTG, which was absent in the non induced cell lysate (Fig. 2 lane 1). This protein band was accompanied by a second protein with slightly lower (39 kDa) apparent molecular mass. The amount of the 40 kDa protein increased with the time with optimal conditions at 8 h after 0.4 mM IPTG induction (Fig. 2 lane 5). The effect of changing the growth temperature was investigated. After 8 h of induction, the amount of over-expressed protein at 37 °C (Fig. 3 lane 3) was comparable to that obtained at 28 °C (Fig. 3 lane 6). On the contrary, even after overnight growth, at 20 °C the expression of hLAT1 protein (Fig. 3 lane 8) was much lower than at 28 °C. The hLAT1 obtained using the pH6EX3 vector contained an N-terminus 6His-tag which was useful to purify the protein under denaturing condition on Ni²⁺-chelating affinity resin.

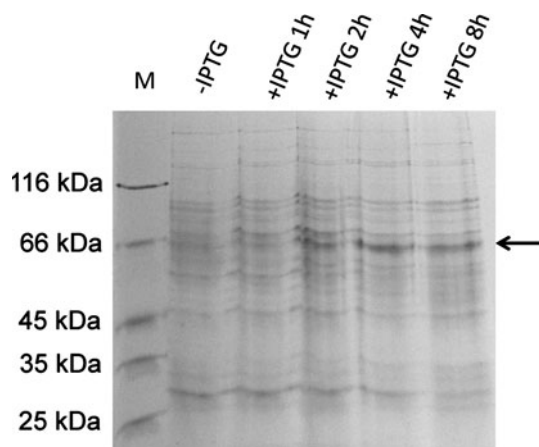


Fig. 1 Recombinant GST-hLAT1 expression. Proteins were separated by SDS-PAGE and stained as described in Sect. 2.11. Lane M: molecular mass standards: 116 kDa (β -galactosidase), 66 kDa (BSA), 45 kDa (ovalbumin), 35 kDa (lactate dehydrogenase), 25 kDa (REase BSP98I); lane – IPTG, uninduced cell lysate (80 μ g), lanes + IPTG: pellets of the insoluble fraction of cell lysate (80 μ g), after 1, 2, 4 and 8 h of IPTG-induction, respectively. The arrow indicates the over-expressed protein

3.2 Purification of the Expressed 6His-hLAT1

Deoxycholate, and the non ionic Triton X-100, C₁₂E₈ or *n*-dodecyl- β -D-maltoside at concentrations up to 5 % were not suitable for solubilising hLAT1 (not shown). Only sodium dodecylsulphate and sarkosyl were effective in solubilising the expressed protein. Therefore, as done for OCTN1, OCTN2 and OCTN3 [16], hLAT1 was solubilized in sarkosyl, which is a milder ionic detergent than sodium dodecylsulphate. A concentration of 0.8 % was enough to solubilize the expressed protein. Sarkosyl was used to solubilize the protein pellet (Fig. 2 lane 5) together with

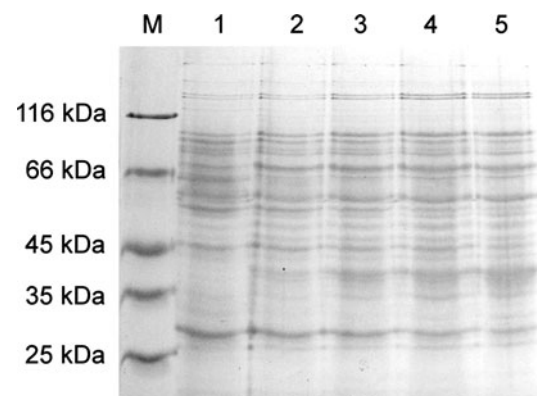


Fig. 2 Recombinant 6His-hLAT1 expression. Proteins were separated by SDS-PAGE and stained as described in Sect. 2.11. Lane M: molecular mass standards (see Fig. 1); lane 1, uninduced cell lysate (80 μ g), lanes 2–5: pellets of the insoluble fraction of cell lysate (80 μ g), after 1, 2, 4 and 8 h of IPTG-induction, respectively

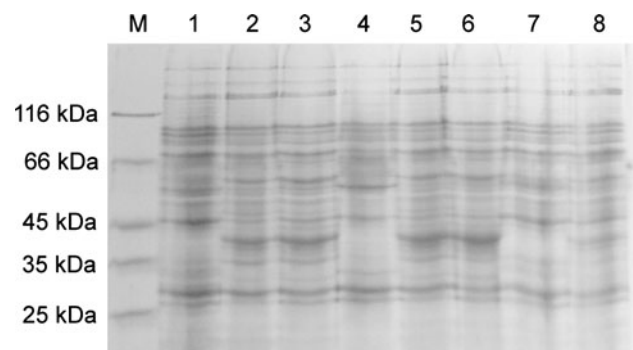


Fig. 3 Effect of temperature on the expression of recombinant pH6EX3-hLAT1 in *E. coli* Rosetta(DE3)pLysS. Proteins were separated by SDS-PAGE and stained as described in Sect. 2.11. Lane M: molecular mass standards (see Fig. 1); lane 1, uninduced cell lysate (80 μ g) cultured at 37 °C, lanes 2, 3: pellets of the insoluble fraction of cell lysate (80 μ g), cultured at 37 °C after 4 and 8 h of IPTG-induction, respectively; lane 4, uninduced cell lysate (80 μ g) cultured at 28 °C, lanes 5, 6 pellets of the insoluble fraction of cell lysate (80 μ g), cultured at 28 °C after 4 and 8 h of IPTG-induction, respectively; lane 7, uninduced cell lysate (80 μ g) cultured at 20 °C, lane 8, pellet of induced cell lysate (80 μ g), cultured over night at 20 °C

3.5 M urea and 5 mM DTE (see Sect. 2.8). A Ni^{2+} -chelating column was then used for purification of recombinant hLAT1. After loading the solubilized protein on the column, most of the contaminating proteins were eluted by the washing buffer (not shown). The 6His-hLAT1 was specifically eluted in the presence of imidazole (50 mM); the corresponding eluted fraction contained a purified protein which was separated on SDS-PAGE (Fig. 4a, lane 2). The protein was enriched of about 30 folds compared to the total protein content in the bacterial lysate. The recombinant hLAT1 was identified by an anti-His antibody: an immunostained band was detected both in the bacterial lysate obtained after IPTG induction as well as in the purified protein fraction (Fig. 4b lanes 1, 2). The purification procedure led to a yield of hLAT1 protein of about 3.5 mg/L of cultured cells or 3.5 mg purified protein per 4 g cells (wet weight).

3.3 Expression of hCD98

The 1,521 bp hCD98 cDNA was amplified from Image plasmid using primers constructed on the basis of the hCD98 cDNA (BC001061.2, GenBank). The cDNA showed a 1,500 bp apparent size on agarose gel. No mutations were present in the cDNA with respect to the hCD98 sequence (GeneBank, not shown). The pH6EX3 vector was firstly used for hCD98. However, a low amount of soluble protein was obtained with this plasmid in Rosetta(DE3)pLysS and other *E. coli* strains (not shown). Thus, to increase the efficiency of expression the use of a tag was adopted. The hCD98 cDNA was cloned in pGEX-

4T1 carrying an N-terminal GST-tag. *E. coli* Rosetta (DE3)pLysS cells were transfected with this construct and the dependence of the expression pattern on the IPTG concentration and time of induction were tested at 28 °C. As shown in Fig. 5 an abundant protein band was detected in the soluble fractions of cell lysates under different conditions (lanes 2–10) and without detergent, indicating that the construct was soluble in agreement with the predominance of hydrophilic amino acids with respect to LAT1; this band was not present in non induced cells (lane 1). The highest amount of the construct was obtained 4 h after induction with 0.4 mM IPTG (lane 6). The molecular mass of the protein, 116 kDa, was not far from the sum of the theoretical molecular masses of hCD98 plus GST, i.e. 94.6 kDa. The construct GST-hCD98 carried a thrombin cleavage site between the two proteins. To find optimal conditions for separating the hCD98 from the GST tag, the dependence of the thrombin cleavage on the time of incubation was studied in the soluble fraction of cell lysate. After 12 h of incubation virtually all the protein construct had been cleaved with appearance of two protein bands with apparent molecular masses of 62 and 27 kDa, close to the molecular mass of hCD98 and GST, respectively, (not shown). The entire protein construct was subjected to purification on a GST-Sepharose resin prior to thrombin treatment according to the optimal conditions found. After 12 h of thrombin treatment the construct was completely hydrolyzed in the two fragments, i.e., the GST and the hCD98 (Fig. 6 lane 2). After the cleavage the two proteins were separated by Sephadex G-200 chromatography and the hCD98 was obtained in a 99 % pure form

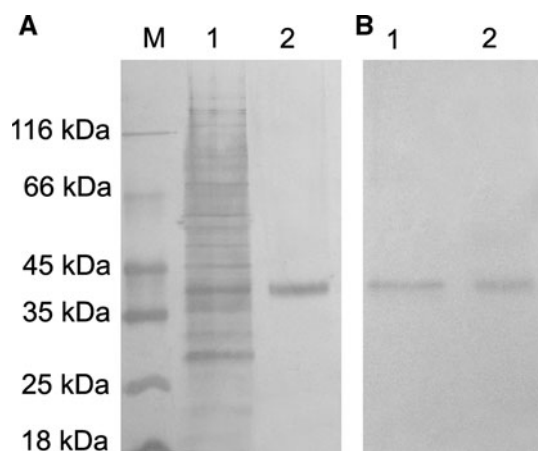


Fig. 4 hLAT1 purification. Proteins were separated by SDS-PAGE and stained (see Sect. 2.11). Lane M molecular mass standards (see Fig. 1). Lane 1 pellet of the insoluble fraction of cell lysate (80 μg), cultured at 28 °C after 8 h of IPTG-induction, lane 2 purified hLAT1 protein (2.5 μg). **b** Immunodecorated proteins recognized by anti-His antiserum (1:1,000) after Western blotting on PVDF membrane. 3,3'-diaminobenzidine staining of the same protein fractions of lanes 1 and 2 of (a)

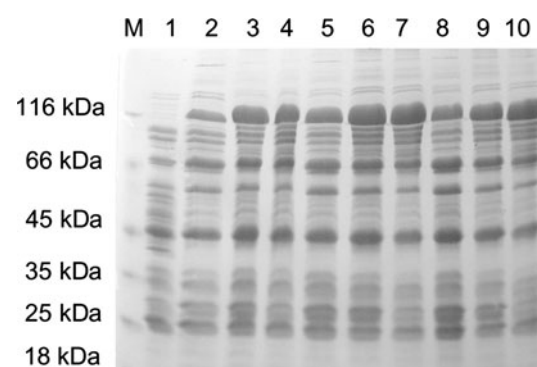


Fig. 5 Expression of recombinant pGEX-4T1-hCD98 in *E. coli* Rosetta(DE3)pLysS. Proteins were separated by SDS-PAGE and stained as described in Sect. 2.11. Lane M molecular mass standards (see Fig. 1); lane 1 uninduced cell lysate (80 μg), lanes 2–4 soluble fraction of cell lysate (90 μg), after 2 h of 0.1, 0.4, 1 mM IPTG-induction, respectively; lanes 5–7 soluble fraction of cell lysate (110 μg), after 4 h of 0.1, 0.4, 1 mM IPTG-induction, respectively; lanes 8–10 soluble fraction of cell lysate (110 μg), after 6 h of 0.1, 0.4, 1 mM IPTG-induction, respectively

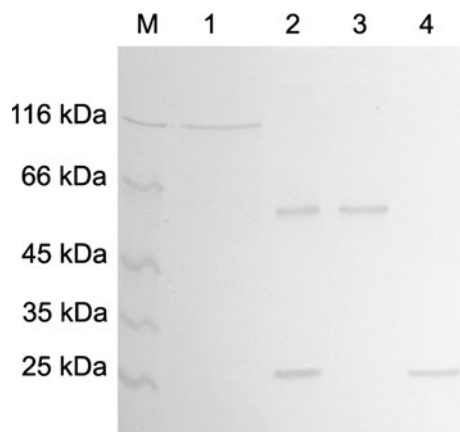


Fig. 6 CD98 purification. Proteins were separated by SDS-PAGE and stained as described in Sect. 2.11. Lane M molecular mass markers as in Fig. 1; lane 1 purified GST-hCD98 (10 μ g); lane 2 protein of lane 1 after 12 h of thrombin treatment; lane 3 purified hCD98 after G-200 gel filtration chromatography (2.5 μ g); lane 4 purified GST after G-200 gel filtration chromatography (2 μ g)

(Fig. 6 lane 3). The apparent molecular mass of hCD98, 62 kDa fitted with the theoretical mass of the protein, 68 kDa. The yield of the purification was about 2 mg/L of cell culture.

4 Discussion

This work describes the first case, to our knowledge, of high level expression of the human amino acid transporter LAT1 in *E. coli*. This transporter belongs to the same family of LAT2 which was previously over-expressed in *P. pastoris* [7]. Both transporters, are L-type amino acid transporters showing wide specificity towards large and small neutral amino acids [21]. These transporters form heterodimers with CD98 protein. While hLAT2 and hCD98 have been over-expressed in the yeast *P. pastoris*, in the present work hLAT1 and hCD98 have been obtained at high expression level in the bacteria *E. coli* and then purified with no (hCD98) or a small 6His tag (hLAT1). Thus, the main novelty of this work consists, besides in obtaining over-expressed hLAT1, also in the successful use of bacterial system for over-expression of two human plasma membrane transporters of aminoacids. Indeed, this system revealed suitable for the expression of hLAT1, which was not expressed in appreciable amount by *P. pastoris*. Several plasmids and *E. coli* strains have been tested to achieve appreciable expression of the protein. The over-expressed cell lysate contained an abundant protein band accompanied by a faint band with a slightly lower apparent molecular mass; these proteins were not present in the cell lysate obtained in absence of IPTG induction. The slightly higher electrophoretic mobility of the lower band was probably

due to a more compact form of the protein induced by partial oxidation and formation of disulphides among some of the 12 Cys in hLAT1 amino acidic sequence. The concentration of the lower band decreased, respect to the main band, with increasing the time of induction and was virtually absent in the purified fraction. Probably the presence of DTE in the purification buffer prevented the formation of the oxidized form of the protein. While hLAT1 was obtained in high yield in pH6EX3 plasmid, in the case of hCD98 a GST tag at the N-terminus of the protein had to be introduced for expression the hCD98 at appreciable level, as it was previously found for the over-expression of another human plasma membrane transporter [12]. After thrombin treatment, GST and hCD98 were efficiently separated by size exclusion chromatography with a high yield of purified protein. Further important advances of this methodology is the availability of hLAT1 purified protein, highly hydrophobic, in a soluble state in non-ionic detergent. This protein, indeed, was not solubilized from the cell lysate using non-ionic detergents while it became soluble after the Ni^{2+} -affinity chromatography procedure. This was due to a slow process of on-column substitution of the ionic detergent with the non ionic Triton X-100. The electrophoretic mobility of the protein was higher than expected, i.e., the apparent molecular mass was lower than the theoretical mass, 55,010 Da, as calculated using Compute pI/Mw tool available at http://web.expasy.org/compute_pi/. This discrepancy was observed for several transport proteins [13, 16, 21] and is due to the higher degree of hydrophobicity of the membrane proteins respect to the molecular mass markers.

5 Conclusion

The availability of the hLAT1 protein in a soluble state is of great importance for further structural analysis, since the protein in this form can be treated by chromatography and concentrative steps previous to crystallization. The importance of the study of hLAT1 resides in the finding that the expression of this transporter is increased in several human cancers [14]. In this respect, the over-expression of hLAT1 in *E. coli* and its purification in a soluble form in non-ionic detergent, will allow functional and kinetic characterization by mean of proteoliposome reconstitution, as already performed for other plasma membrane transporters [16]. Therefore, the results described in this work constitutes the basis for in vitro screening of molecules, including drugs and biologically active compounds, which specifically interact with the transporter inhibiting its function. This has a great impact in human health offering important perspectives in cancer therapy, as previously

postulated on the basis of studies performed with intact cells [10].

Acknowledgments This work was supported by funds from PON-ricerca e competitività 2007–2013 (PON project 01_00937: “Modelli sperimentali biotecnologici integrati per la produzione ed il monitoraggio di biomolecole di interesse per la salute dell’uomo”) MIUR (Ministry for Instruction University and Research) and European Commission, FSE fund and Calabria Region.

Conflict of interest The authors declare no conflict of interest.

Ethical standards The experiments comply with the current Italian laws.

References

- Baniasadi S, Chairoungdua A, Iribe Y, Kanai Y, Endou H, Aisaki K, Igarashi K, Kanno J (2007) *Arch Pharm Res* 30:444–452
- Barker GA, Ellory JC (1990) *Exp Physiol* 75:3–26
- Bode BP (2001) *J Nutr* 131:2475S–2485S Discussion 2486S–2477S
- Brizio C, Galluccio M, Wait R, Torchetti EM, Bafunno V, Accardi R, Gianazza E, Indiveri C, Barile M (2006) *Biochem Biophys Res Commun* 344:1008–1016
- Broer S (2002) *Pflugers Arch* 444:457–466
- Cohen SN, Chang AC, Hsu L (1972) *Proc Natl Acad Sci USA* 69:2110–2114
- Costa M, Rosell A, Alvarez-Marimon E, Zorzano A, Fotiadis D, Palacin M (2013) *Protein Exp Purif* 87:35–40
- del Amo EM, Urtti A, Yliperttula M (2008) *Eur J Pharm Sci* 35:161–174
- Dulley JR, Grieve PA (1975) *Anal Biochem* 64:136–141
- Fan X, Ross DD, Arakawa H, Ganapathy V, Tamai I, Nakanishi T (2010) *Biochem Pharmacol* 80:811–818
- Fuchs BC, Bode BP (2005) *Semin Cancer Biol* 15:254–266
- Galluccio M, Amelio L, Scalise M, Pochini L, Boles E, Indiveri C (2012) *Mol Biotechnol* 50:1–7
- Galluccio M, Pochini L, Amelio L, Accardi R, Tommasino M, Indiveri C (2009) *Protein Exp Purif* 68:215–220
- Ganapathy V, Thangaraju M, Prasad PD (2009) *Pharmacol Ther* 121:29–40
- Geier EG, Schlessinger A, Fan H, Gable JE, Irwin JJ, Sali A, Giacomini KM (2013) *Proc Natl Acad Sci USA* 110:5480–5485
- Indiveri C, Galluccio M, Scalise M, Pochini L (2013) *Mol Biotechnol* 54:724–736
- Kanai Y, Endou H (2003) *J Toxicol Sci* 28:1–17
- Kanai Y, Hediger MA (2004) *Pflugers Arch* 447:469–479
- Laemmli UK (1970) *Nature* 227:680–685
- Palacin M, Estevez R, Bertran J, Zorzano A (1998) *Physiol Rev* 78:969–1054
- Palacin M, Nunes V, Font-Llitjos M, Jimenez-Vidal M, Fort J, Gasol E, Pineda M, Feliubadalo L, Chillaron J, Zorzano A (2005) *Physiology (Bethesda)* 20:112–124
- Scalise M, Galluccio M, Pochini L, Indiveri C (2012) *Biochem Biophys Res Commun* 422:59–63
- Shennan DB, Thomson J (2008) *Oncol Rep* 20:885–889
- Wempe MF, Rice PJ, Lightner JW, Jutabha P, Hayashi M, Anzai N, Wakui S, Kusuhara H, Sugiyama Y, Endou H (2012) *Drug Metab Pharmacokinet* 27:155–161